Copyright is owned by the Author of the thesis. Permission is given for a copy to be downloaded by an individual for the purpose of research and private study only. The thesis may not be reproduced elsewhere without the permission of the Author.

Biosensors for fertility and pregnancy in cattle

A thesis presented

in partial fulfilment of the requirements

for the degree of

Doctor of Philosophy in Chemistry

at Massey University, Palmerston North,

New Zealand

Yu-ting Hsu

2013

Acknowledgements

First and foremost I would like to thank my supervisors Associate Professor Eric Ainscough and Associate Professor Ashton Partridge who were friendly and supportive throughout my study. Additionally, I would like to thank Professor Bernd Rehm and the Polybatics group for providing the polyhydroxyalkanoate granules and valuable information and advice towards the research and development of a surface plasmon resonance sensor.

I would like to acknowledge the MacDiarmid Institute for providing financial support.

I wish to thank Dr Wayne Campbell and Dr Krishanthi Jayasundera for the synthesised progesterone ligands. I would like to thank Associate Professor Len Blackwell and Dr Jenness Guthrie for advice and information on the lateral flow immunoassay development.

Finally, I wish to thank my family and Ross for supporting my efforts to pursue a PhD.

Abstract

This project is focused on progesterone sensing, using both surface plasmon resonance (SPR) and lateral flow immunoassay (LFIA) methods with a new progesterone (P4) sensing material to develop cost effective assays for progesterone sensing in bovine serum and milk samples.

P4-PEG-OVA was synthesised, characterised and used for P4 detection. The P4-PEG-OVA sensor surface showed an improvement in surface response compared with two shorter ligand 4TP-P4-OVA and 4TPH-P4-OVA in SPR studies.

An analysis method has been developed and modified for bovine serum and milk analyses. The results indicated the P4-PEG-OVA ligand allowed sensitive P4 detection in SPR sensing and allowed bovine P4 cycle profiling. The SPR analysed data was compatible with the ECLIA and ELISA independent analyses and the P4 cycle of each of the three bovine milk samples showed a very similar trend and the extraction level was also consistent.

The P4-PEG-OVA ligand was used to develop a LFIA sensor strip, and the inhibition assay for bovine serum and milk analyses established. The results indicated that, after appropriate sample pre-treatment, the bovine estrous cycle profile could be detected. The LFIA method can be a potentially quick, easy and cost effective semi-quantitative P4 analysis for serum and milk samples.

A new material, polyhydroxyalkanoate (PHA) granules has been investigated for the possibility of developing a new surface biosensor. From the surface studies, the results indicated that the 3GNZZPhaC beads have the potential to become an alternative binding material for SPR sensing due to its unique gold binding property. A flow cell was designed, constructed, and tested on 3GNZZPhaC beads prior the preliminary SPR investigations.

The ZZPhaC beads also showed the gold binding property and ZZPhaC beads were used for SPR studies. The results suggested a possible application for them as a new SPR binding material for antibody detection.

Contents

List of figures, tables and reaction schemes

Chapter 1

Chapter 2

Chapter 3

Chapter 4

Abbreviations

4TP-P4	3-(pregn-4-ene-3,20-dione-4-yl)thiopropanoic acid
4TPH-P4	6-[3-[(pregn-4-ene-3,20-dione-4-yl)thiopropano-yl] amino]hexanoic acid
AFM	atomic force microscopy
Anti-P4	progesterone antibody
AuNPs	gold nanoparticles
BSA	bovine serum albumin
C	control line
CBG	corticosteroid binding globulin
CM5	carboxymethylate dextran
CL	corpus luteum
DCC	1,3-dicyclohexylcarbodiimide
DMF	dimethylformamide
DNA	deoxyribonucleic acid
dpm	disintegration per minute
EC20	the lowest concentration that can be distinguished from the background noise
EC50	the half maximal effect concentration
EC80	the highest concentration that can be distinguished from the background noise
ECLIA	electrochemiluminescence immunoassay
EDC	1-ethyl-3(-3-dimethylaminopropyl)carbodiimide
EDTA	ethylenediaminetetraacetic acid
EIAs	enzyme immunoassays
ELISA	enzyme-linked immunosorbent assay
FC1	flow cell one

FC2	flow cell two
FSH	follicular stimulating hormone
GC-MS	gas chromatography–mass spectrometry
GEPIs	genetically engineered polypeptides for inorganics
HBS-EP$^+$	SPR buffer contained 0.1 M HEPES, 1.5 M NaCl, 30 mM EDTA and 0.5% v/v Surfactant P20
hCG	gonadotropin
HEPES	4-(2-hydroxyethyl)-1-piperazineethanesulfonic acid
HPLC	high performance liquid chromatography
IFC	integrated micro fluidic cartridge
IgG	immunoglobulin G
kDa	kilodalton
LC-MS	liquid chromatography–mass spectrometry
LFDs	lateral flow devices
LFIA	lateral flow immunoassay
LH	luteinising hormones
LOD	limit of detection
NHS	N-hydroxysuccinimide
NZVP	New Zealand Veterinary Pathology Limited
P4	progesterone
P4-PEG	*N*-(13-(carbonylamino)-4,7,10-trioxatridecanyl)- 3-(pregn-4-ene-3,20-dione-4-yl)thiopropanamide
PHA	polyhydroxyalkanoate
PHB	polyhydroxybutyrate
PHBA	poly(3-hydroxybutyrate-co-3-hydroxyvalerate)
pI	isoelectric point
pK	disassociate constant

OVA	ovalbumin
RIAs	radioimmunoassays
RU	response unit
SEM	scanning electron microscopy
SPR	surface plasmon resonance
SPRI	surface plasmon resonance imaging
T	test line
THF	tetrahydrofuran
TIR	total internal reflection
ZZ domain	antibody binding domain of protein A
θ_{SPR}	surface plasmon resonance angle
$\boldsymbol{\lambda_{max}}$	lambda(max)

Chapter 1

Introduction

1.1 Dairy farming in New Zealand

Dairy farming in New Zealand makes a major contribution to the economy, the dairy sector generated more than 2.8% of gross domestic product in 2010 (GDP) and 26% of exports.[1,2] There is no doubt that dairy farming is the backbone of the national economy. In 2011/12, the total dairy cow population was 4.6 million and the dairy companies processed 19.1 billion litres of milk. There is a continuous drive to improve and enhance dairy productivity to meet the demands. Hence it is crucial to achieve a good level of reproductive performance in a dairy herd. The desire reproductive level can be maintained by having regular reproductive cycles.

The reproductive cycles of cows can be monitored by following the estrous cycle which is described in following section (section 1.2).

1.2 Mammalian/bovine progesterone (P4) cycle

A mammalian species such as a cow is polyestrous and can go into heat several times a year, the estrous cycle re-occurring on average every 21 days. Bovine estrus lasts a short period of time (approximately 15 to 18 hours), and ovulation occurs about 15 hours after the end of estrus. The estrous cycle can be divided into stages including pro-estrus, metestrus and diestrus. The follicular growth and regression of the corpus luteum (CL) increases in the pro-estrus stage and the genital system ceases to be under the domination of progesterone. Metestrus is the stage after the end of estrus, when the follicle matures, ovulates and the CL starts to develop. The diestrus is the stage between two estrous cycles where the CL produces progesterone (P4) and the uterus is prepared for fertilisation of an ovum.

The ovarian function is controlled mainly by the secretion of the hormones follicle stimulating hormone (FSH) and luteinising hormones (LH). FSH is responsible for stimulating the early growth of follicles and LH causes final maturation and ovulation as well as stimulates the formation of the CL. The CL is formed from the luteinised granulosa and thecal cells which produce progesterone. The P4 concentration starts to increase 3-4 days

after estrus and reaches a maximum concentration at roughly 8 days and continues till 16 or 17 days. The P4 level declines and reaches a basal level at the time of next estrus (Figure 1.1). P4 prepares the uterus for entry of the fertilised egg as well as maintains any pregnancy that occurs. The level of P4 remains high during diestrus and pregnancy, this inhibits the effect of estrogen to prevent estrus behaviour. Hence P4 plays an important role in controlling ovarian cyclical activity in a cow.

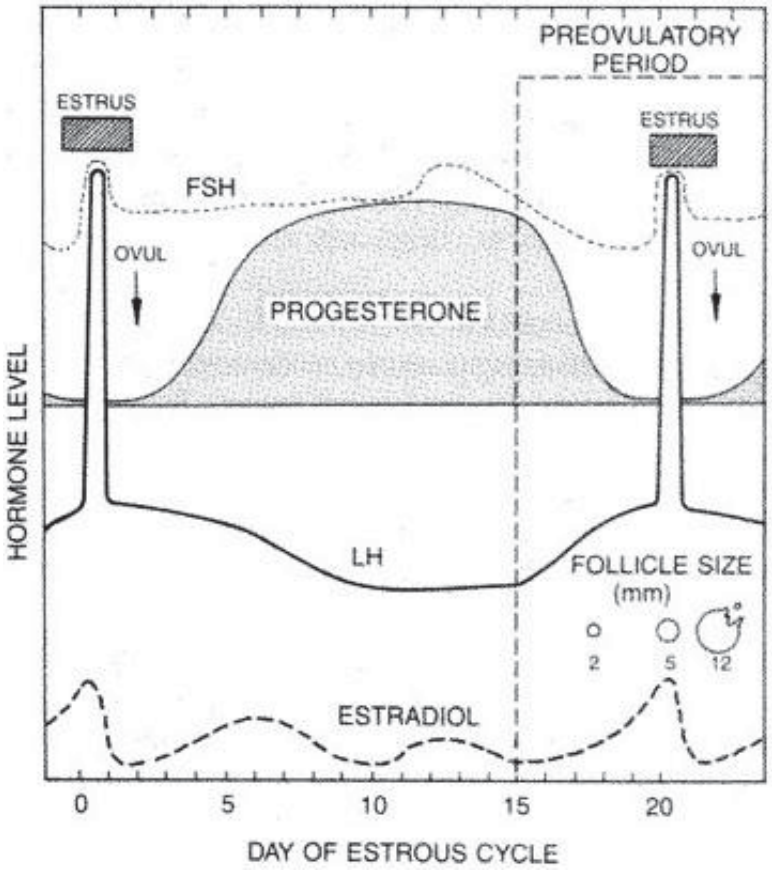

Figure 1.1 A bovine estrous cycle can be monitored by measuring the P4 concentration in both serum and milk samples. The duration of a typical bovine estrous cycle is approximately 21 days.[3]

The estrous detection methods include elevation in body/milk temperature, observation of animal behaviour, electrical impedence and hormonal assay (P4 assay). When the efficiency and accuracy and the running costs are taken under consideration there are advantages and disadvantages in each method.[4]

The P4 assay has been used widely in research and applied in the dairy industry including milk, serum and urine samples. It is the best method for detecting estrous detection errors by other methods.[5] (More assay details are described in section 1.6.2)

The P4 concentration in blood and milk are closely correlated but as P4 has a high affinity for fat the concentration of progesterone in milk is somewhat higher than the concentration of progesterone in the blood, but the relative relationship between the milk and blood level is the same (the general profile of the cycle should match). Hence the P4 level in either blood or milk is a good indication of a regular reproductive cycle.

1.3 Biosensors

A biosensor is an analytical device, which enables the detection of the analyte in solution, then converts the bio-recognition event into a measurable electrical signal. It consists of: the capture agent, the detector (e.g. physicochemical, optical, piezoelectric and electrochemical) and the electronics or signal processor to display the results (Figure 1.2).

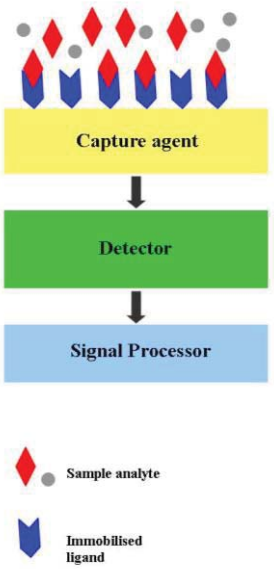

Figure 1.2 A typical biosensor comprises a capture agent unit which consists of a biological element such as an enzyme, immunoagents, or microorganisms.

There are two types of capture agents which are the catalytic capture agent and affinity capture agent. Capture agents are usually selective biological elements such as enzymes, antibodies or nucleic acids, etc. The transducer/detector transforms the signals resulting from the interaction between the target analyte with the capture agent which can be measured and quantified piezoelectrically, calorimetrically, optically or electrochemically.

A piezoelectric device can use gold to detect the specific angle which electron waves are emitted when the substance is exposed to laser light or crystals such as quartz, which vibrate under the influence of an electric field. The change in vibration frequency is proportional to the mass of the absorbed material.[6,7]

Calorimetric sensors measure the heat from a biochemical reaction at the sensing element. For example, if an enzyme catalysed reaction is exothermic, two thermistors may be used to measure the difference in resistance between reactant and product, hence the analyte concentration can be determined.

Electrochemical sensors such as amperometric sensor are commonly based on enzymatic catalysis of a reaction which produce or consume electrons. The sensor substrate usually contains a reference electrode, active electrode, and sink electrode. Alternatively in a potentiometric sensor, the target analyte is involved in the reaction which takes place on the active electrode surface and the ions produced create a potential which is subtracted from the reference electrode to give a signal. It measures either current at fixed potential or measures the potential at zero current.

Optical biosensors are divided into two major categories: colorimetic and photometric. Colorimetric sensors measure the change in light absorption and photometric sensors detect and measure the photon output for luminescent or fluorescent process using photomultiplier systems. Surface Plasmon resonance based sensor is one of the common optical sensors; it operates using a sensor chip which consists of a plastic cassette to support a gold coated glass plate with a specific binding material and immobilised ligand which will be discussed in section 1.2.

A successful biosensor should comprise the following characteristics: highly specific to the target analyte; stable under normal storage; the response should be accurate, precise, reproducible and linear within working analytical range; it should be cheap, small, portable

and user friendly (operators require minimum training). There are many potential applications of biosensors and it is widely used as an analytical tool in many different fields including: food analysis, study of biomolecules and interactions, drug development, medical diagnosis, environmental field monitoring, quality control, detection systems for biological agents, etc. The most recognised example is the blood glucose biosensor which uses the enzyme glucose oxidase to undergo redox conversion of O_2 and glucose to hydrogen peroxide and gluconolactone and detected electronically. The pregnancy test is the other well established biosensor which detects the human chorionic gonadotropin (hCG) in blood or urine using a test strip or stick.

The sensing techniques used for biosensors include: fluorescence, DNA microarray, impedance spectroscopy, scanning probe microscopy, quartz crystal microbalance, surface enhanced Raman spectroscopy, lateral flow immunoassay and the surface plasmon resonance. In this thesis, we have focused on new research of the lateral flow immunoassay and surface plasmon resonance techniques to develop new biosensors for progesterone.

1.4 Surface Plasmon Resonance (SPR)

The SPR effect, is a charge density oscillation that exists at the interface of two media with dielectric constants of opposite sign. The charge density waves are associated with the electromagnetic wave, the field vectors of which reach their maxima at the interface and decay evanescently into both media. The surface plasmon is excited at the interface between the metal film (Au coated sensor chip) and a dielectric medium, and causes a measurable change in refractive index, which can be used for sensing the analyte. The phenomenon was first observed in 1902 by Wood,[8] who observed a pattern of "anomalous" dark and light bands in reflected light when polarized light shone on a mirror with a diffraction grating on the surface. The phenomenon was not completely explained till 1968 by Otto[9] then Kretschmann and Raether.[10] SPR was first applied as a biosensing technique by Liedberg in 1983[11] and since then the user friendly SPR technology has been applied to several practical applications including chemical and biosensing, and SPR Imaging (SPRI).

There are several configurations of SPR instruments that are capable of generating and measuring an SPR signal, and three different optical systems used to include surface plasmons: prisms, gratings and optical waveguides.

The modern SPR sensing system (Figure 1.3) based on Kretschmann configuration[10], where the metal film is evaporated onto a glass slide. Polarised light is directed through the prism onto the glass gold interface, resulting in plasmon ripples. The capture agent Y is immobilised onto the dextran surface and is followed by the injection of the aqueous solution of target analyte ▲ through the continuous flow cell resulting in an optical response.

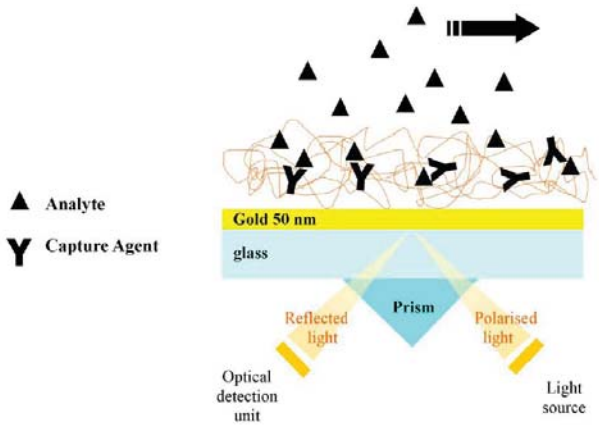

Figure 1.3 A modern SPR sensing system based on the Kretschmann configuration.

Changes in reflection angle of the polarised light are measured, and result from changes in the refractive index of the solution within ~300 nm of the sensor surface, and correlates directly with the binding of ligands to the capture agents. The result then can be plotted as responses (or resonance units, RUs) versus time, which is called a sensorgram (Figure 1.4).

The background response will be generated and subtracted from the sensorgram in order to obtain the actual binding response. One RU corresponds to approximately 1 pg target analyte/mm^2.[12]

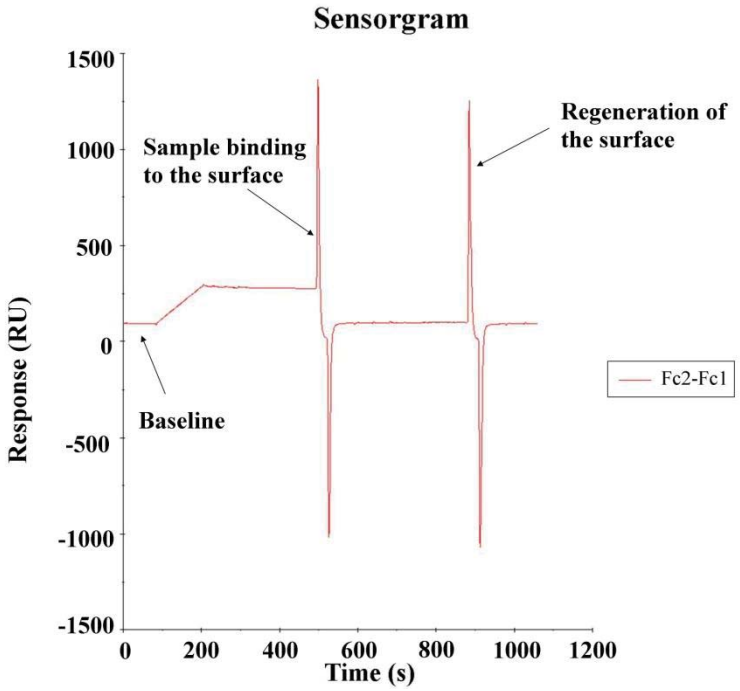

Figure 1.4 Sensorgram showing the steps of an analysis cycle. The progesterone standard was injected at 30 µL/min for 120 s and this was followed by a regeneration step of injection of NaOH solution (10 mM) for 30 s which regenerates the surface. The analyte flows through flow cell one (FC1) and flow cell two (FC2) sequentially; the response was measured by subtracting the reference response of FC1 from the binding response of FC2.

SPR is a powerful tool for real time analysis of biomolecular interactions.[13] The earlier applications of SPR sensing were focused on antigen-antibody interactions.[14] Since then many examples of biomolecular interactions have been studied using SPR including antibody-antigen interactions,[15,16] DNA hybridization,[17] immunoreactivity of antibody conjugates[18] and quantitative immune assays.[19-21]

1.4.1 SPR-based applications

The SPR phenomenon has been applied to the development of a number of sophisticated measurement technologies including: fluorescence, Raman scattering and second harmonic generation. However, modern day instrumentation has made SPR a relatively straight forward method.

The method of SPR is based on either direct or indirect SPR measurements (competitive measurement). SPR is excellent for evaluation of macromolecules such as recombinant

protein to natural ligands and monoclonal antibodies, equilibrium analysis and kinetic studies. Several biosensors and immunoassays have been developed using the SPR sensing system. Many studies have shown the enhancement of SPR sensitivity when combining colloidal gold particles with the metal layer.[22,23] In one study, it has also been incorporated with colloidal gold particles as the substrate instead of the gold metal layer.[24]

1.4.2 The Biacore X100 system

The Biacore SPR biosensor consists of three key components which enable the observation of the SPR phenomenon and adapts it to useful application. The three components are the cold sensor chip, the microfluidic sample handling system, and the SPR detector. The system enables real time observation for interactions between ligands and analytes, and enables studies of a wide range of molecules in different sample environments. The kinetics, affinity, specificity and concentration analysis can all be done with one system (Figure 1.5).

Figure 1.5 The Biacore X100 system. To study the interaction between the capture agent and the analyte, the sensor chip requires surface immobilisation with the capture agent which is then inserted into the sensor chip holder. The continuous flow micro-fluid channel enables analyte flow at the chosen condition and enables real time observation of the capture agent and the analyte.

1.4.2.1 The microfluidic system

The interactions between analyte and the surface occurs in the flow cells. The flow cells are formed when the sensor chip is docked in the system as the microfluidic cartridge is pressed against a sensor surface (Figure 1.6). In the Biacore X100 system, there are two channels, flow cell one (FC1) and flow cell two (FC2). The channels can be opened and closed by a system of valves. The specific ligand-protein conjugate is commonly immobilised on FC2 sensor surface to interact with target analyte as it passes through the flow cell. FC1 is used as on-line reference cell, and it is immobilised with the same linking protein as in flow cell two. The response unit from FC2 was then subtracted by FC1, the reference cell, and the blank subtracted data are presented directly on the screen during analysis.

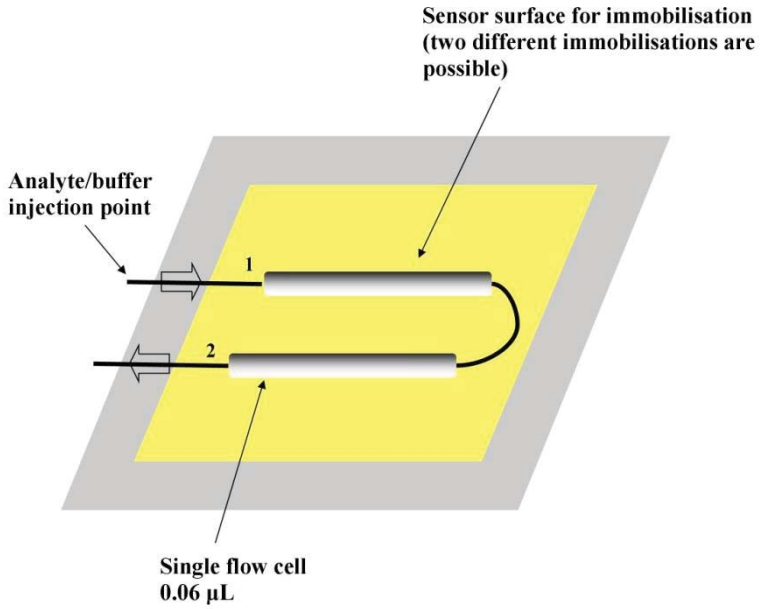

Figure 1.6 The microfluidic system and flow cell of a Biacore X100. Two flow cells, FC1 and FC2 are formed over one sensor surface when the sensor chip is docked in the instrument, and the flow cells can be used in series or individually. The automatic in-line reference substation was done by using FC2 minus FC1 from same sample injection.

1.4.2.2 Biacore sensing chips

The SPR sensor chips enable quantitative measurement of the binding interaction between one or more molecules, and they are dependent on the immobilisation of the target molecules to the sensor chip surface. A typical sensor chip comprises a glass layer, a gold layer and coupling layer (surface) for coupling the capture agent to the gold layer (50 nm, Biacore sensor chip). Table 1.1 lists the various types of Biacore sensing chips available. CM5 is used most commonly and the coupling layer consists of a carboxymethylated dextran (Figure 1.7).

Table 1.1 To study an interaction, it is important to select the most suitable sensor chip for individual studies. There is a range of sensor chips available commercially for specific requirements.[25]

Sensor chip	Surface	Properties
CM5	The matrix consists of carboxymethylated dextran.	Most versatile chip.
CM4	The matrix is similar to CM5 but with a lower degree of carboxymethylation which can improve sensitivity for certain interactions.	May help reducing non specific binding e.g. in crude sample environment.
CM3	The matrix is also similar to CM5 but with shorter dextran chains.	For low immobilisation levels and work with cells and viruses.
C1	Carboxymethylated, matrix free surface.	For work with cells and particles when dextran matrix is not required.
SA	Carboxymethylated dextran matrix with pre-immobilised streptavidin.	For capture biotinylated ligands.
NTA	A carboxymethylated dextran surface with immobilised NTA	For capture His-tagged ligands.
HPA	A flat hydrophobic surface consisting of long-chain alkanethiol molecules is directing attached to the gold surface.	For observation of lipid monolayers interacting with membrane binding biomolecules.
L1	The matrix consists carboxymethylated dextran with lipophilic modification	For capture of liposomes with retained lipid bilayer structure.
Au	Untreated gold surface	Plain gold layer for immobilisation of desire ligands.

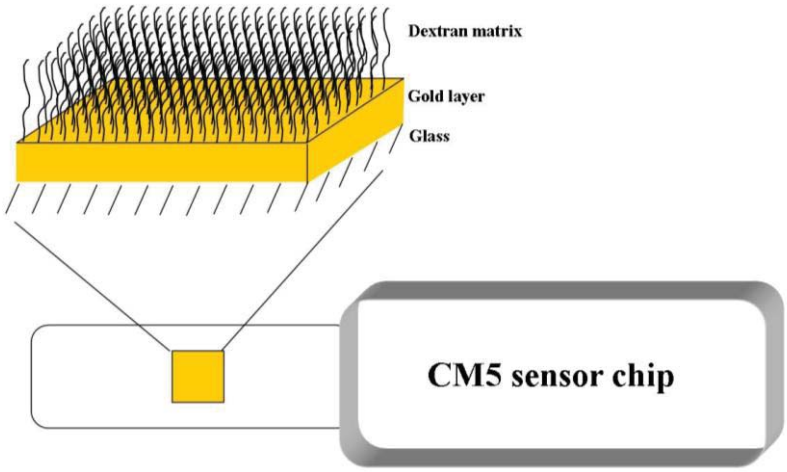

Figure 1.7 Each sensor chip consists of a gold coated surface with a different matrix. The CM5 chip is the most versatile and this has a carboxymethylated dextran matrix as a coupling layer.

1.4.2.3 Surface immobilisation

Surface immobilisation of the capture agent by the coupling layer is an important step for SPR analysis. The immobilisation techniques are varied depending on the type of capture agent (protein, e.g. ovalbumin, sugar, DNA, low molecular weight substance) and analyte (small or large molecular weight) depending on the purpose of the study e.g. one that relates to specificity, concentration, affinity or kinetics. The commonly used immobilisation techniques are: covalent coupling chemistries and unidirectional immobilisation.

Covalent coupling is stable and in general requires no modification of the capture agent; the immobilisation level is easily controlled and ligand consumption is low. The capture agents are immobilised by reacting with the functional groups such as amine ($-NH_2$), thiol (-SH), and aldehyde (-CHO).

The covalent immobilisation techniques often result in a heterogeneous alignment of the capture agent to the dextran surface. The unidirectional immobilisation can be used to reduce or eliminate induced heterogeneity. Biotinylation of the ligand allows unidirectional immobilisation as biotin is coupled with the NHS-SS-biotin to free amino groups such as N-terminus and lysine residues. Another technique commonly carried out is the use of capturing antibodies in the affinity capturing system. The unidirectional method is, in general,

applicable but the capture agent may require further modification. However, the capture agent consumption is high and attachment is not always stable. The advantages of unidirectional capturing immobilisations are that the capture agent orientation is specific, and always has a fresh surface.

The immobilisation level of the capture agent depends on the purpose of the study which is relative to the total response and can be calculated using the equations below.

$$Rmax = \left(\frac{MWA}{MWL}\right) \times RL \times Sm$$

$$RL = Rmax\left(\frac{1}{Sm}\right)\left(\frac{MWL}{MWA}\right)$$

$$MWA = Molecular\ weight\ of\ analyte$$

$$MWL = Molecular\ weight\ of\ ligand$$

$$RL = Response\ due\ to\ the\ ligand$$

$$Sm = Amount\ of\ binding\ sites$$

$$Rmax = Response\ due\ to\ injecting\ the\ analyte$$

This allows estimation of the quantity of the capture material and target analyte needed to get a statistically significant response. Therefore, the cost of the experiment can be minimised.

1.5 The Lateral Flow Immunoassay (LFIA)

The technology for the rapid immunochromatographic test strip also known as lateral flow immunoassay was developed in 1970s, and it became a popular platform for rapid immunoassays in 1980s. The LFIA technology has been employed to develop a wide range of applications in various fields including clinical, veterinary, agricultural, food and environmental applications.[26,27]

The development of LFIA has been under especially intense investigation due to its desired properties such as easy one step application and rapid and low cost analysis and LFIA has been widely used as a convenient assay system.

There are many advantages of the LFIA system, including: it is an established mature technology; relatively easy to manufacture and scalable to high volume production; relatively stable with reasonable shelf-lives; rapid and easy to use; can be specific and sensitive; and it is relatively low cost. The LFIA system requires no specially trained personnel or specialised apparatus; hence it is very suitable for applications outside of the laboratory. LFIA also provides a quick binary (yes/no) response. The current LFIA system is based on the movement of aqueous samples that migrate through the detection region where specific molecules are attached to interact with analyte. The detection region of a LFIA system comprises a test line and control line. A test line is sprayed with the specific antibody/antigen which is used to capture the target analyte. A secondary antibody is typically used for the control line to check and confirm the flow of the test strip.

There are two types of LFIA systems, the sandwich format also known as positive assay (Figure 1.8) and the competitive assay format also known as negative assay (Figure 1.9). The sandwich format is designed for an analyte that has more than one epitopes, the part of an antigen that is recognised by the immune system. One analyte-specific antibody is usually used as test line material hence the intensity of the test line is directly proportional to the concentration of the analyte in the sample.

The competitive assay system is designed for analytes with molecular weight lower than 1000 Da and only one epitope. Anti-analyte antibody or analyte-protein conjugate is commonly used as the test line in competitive assay system, the intensity of the test line is inverse proportional to the analyte concentration.

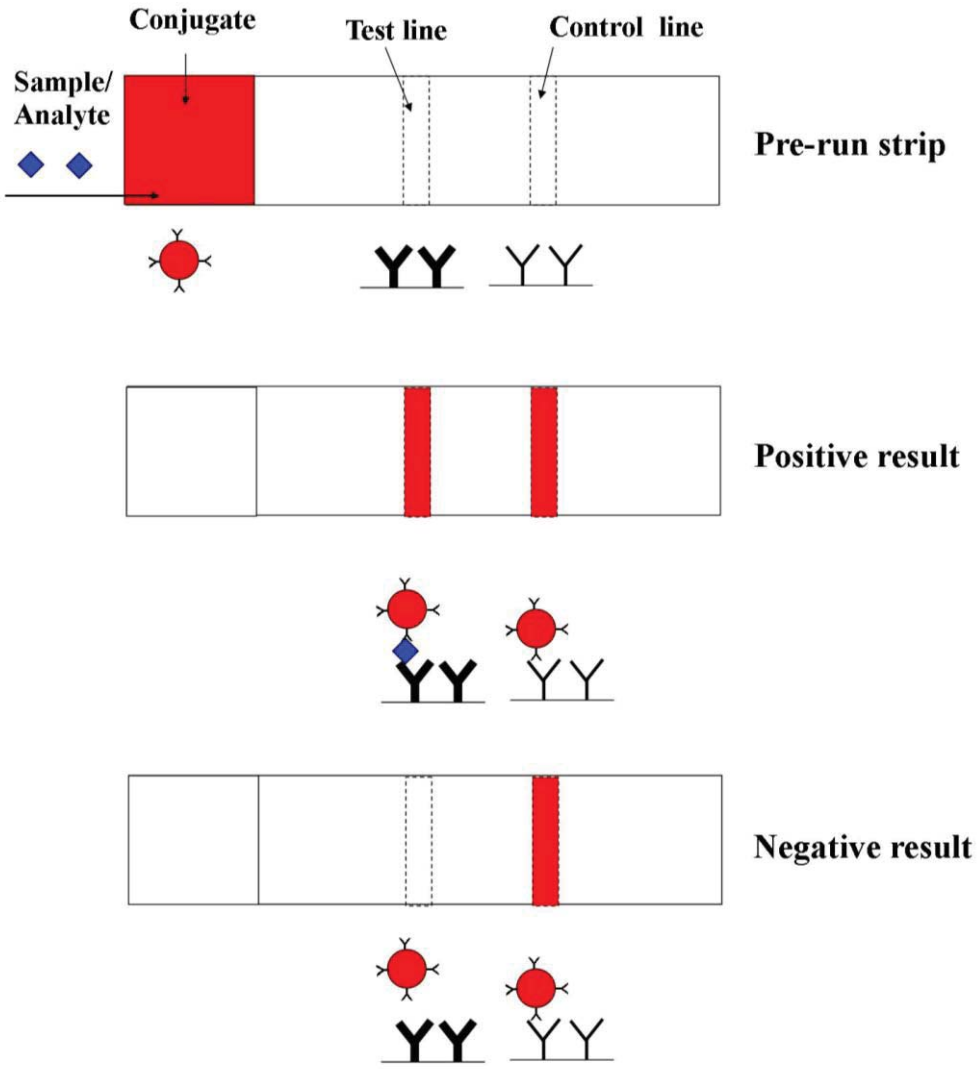

Figure 1.8 The sandwich format also known as positive assay. The assay usually consists of nanoparticles such as gold in either a sample solution or conjugate pad to give signals when it binds to the test and control lines. The sandwich assay gives a signal in the presence of sample/analyte, and the signal is increased as the concentration of target sample/analyte is increased.

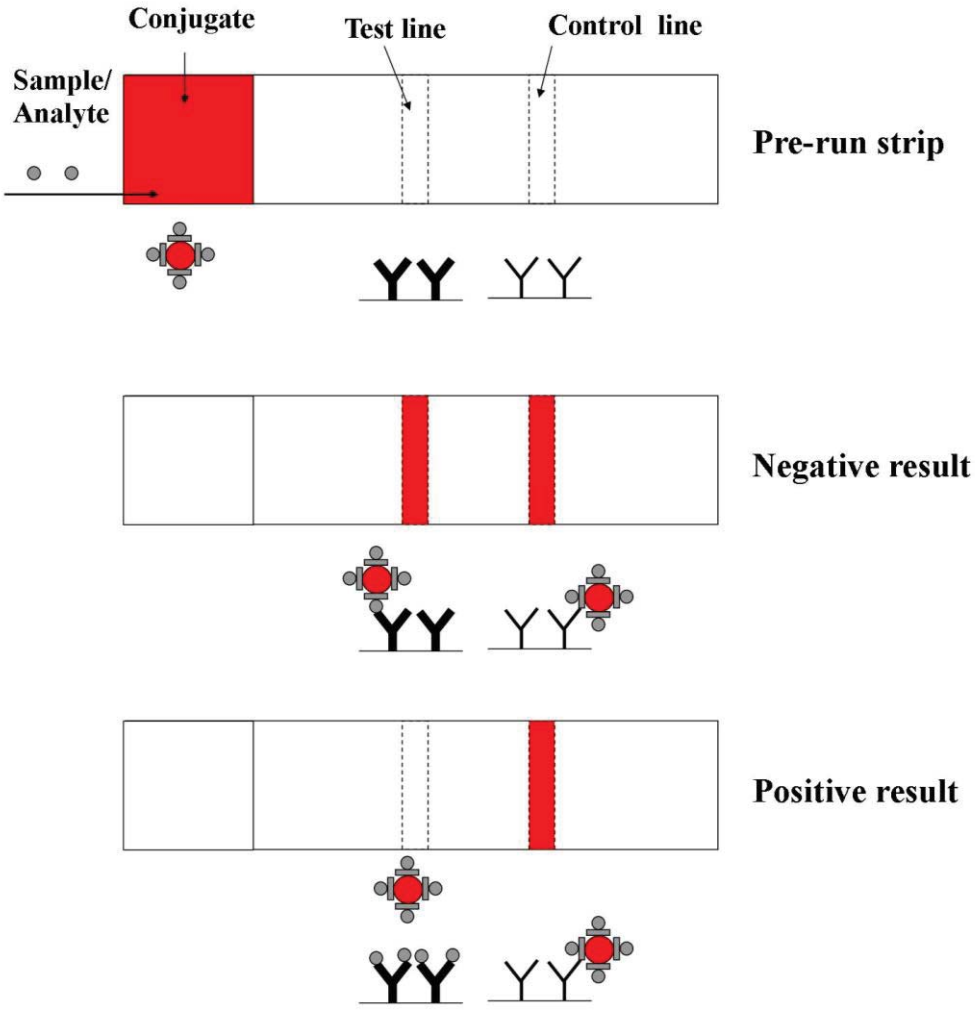

Figure 1.9 The competitive format also known as negative assay. The analyte specific antibody is usually conjugated with nanoparticles to give signals when it binds to the test line. Anti-analyte antibody or analyte-protein conjugate is commonly used as the test line. As the concentration of the target sample/analyte increases, the analyte binds to the test line. This results in the occupancy of the binding sites of the test line decreasing. Hence, the competitive assay gives decreasing signals as the concentration of the target sample/analyte increased. Further details are given in section 1.3.1.

1.5.1 Structure of a lateral flow immunoassay strip

The typical configuration of a lateral flow immunoassay strip includes a backing card, membrane, sample pad, absorbent pad and conjugate pad (Figure 1.10).

The sample pad is attached to the bottom of the membrane and also in contact with conjugate pad. The analytical region consists of test line/lines and a control line sprayed and dried onto the membrane. The absorbing pad is attached to the top end of the membrane.

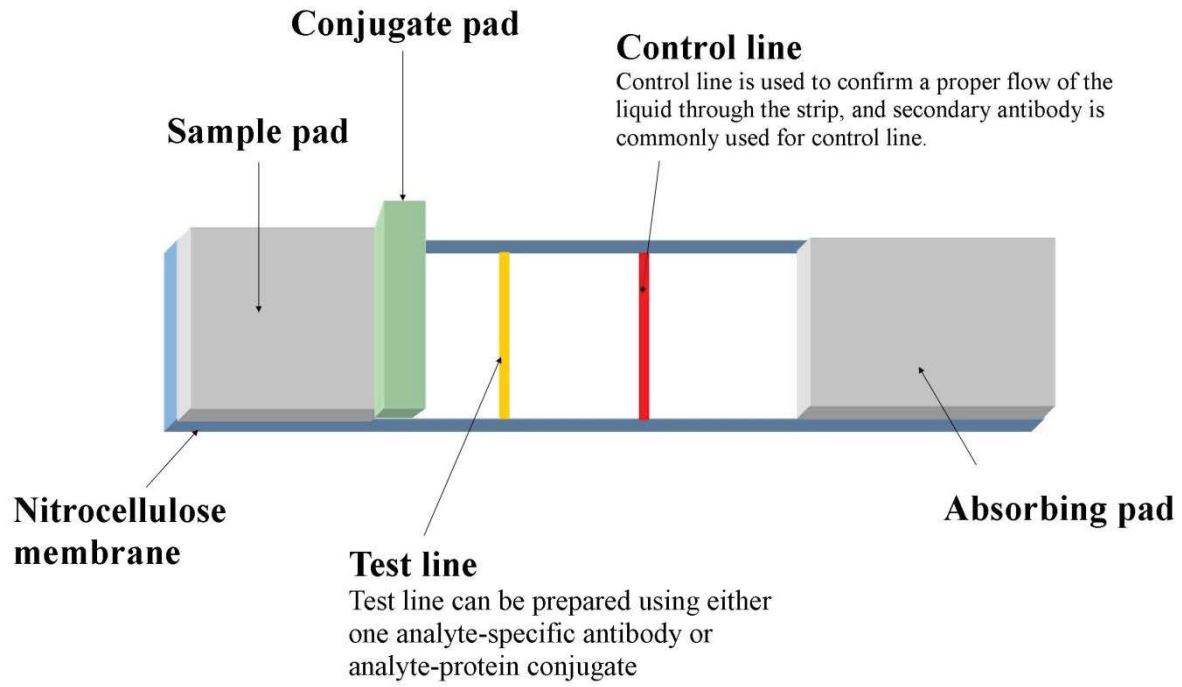

Figure 1.10 Schematic diagram of a lateral flow immunoassay strip. The strip consists of a sample pad, conjugate release pad, a membrane where the test and control lines are sprayed and a absorbent pad.

A sample such as serum, urine or milk contains target analyte and is added to the sample pad or in a Microtiter plate which is commonly used for assay development (Figure 1.11) and the analyte migrates through the conjugate pad where the analyte conjugates with particles such as gold nanoparticles or fluorescent particles as a colour indicator. The conjugated analyte then migrates through the reaction region by capillary force, and binds to the test line and the control line (Figure 1.12). For multiple analytes, more than one test line can be applied. The results are interpreted on the reaction mixture as the presence or absence of lines of capture conjugate and read either by eye or using a reader.

The properties and sensitivity of a LFIA strip can be influenced by the components of the strip. The role of each component will be described in the following section.

Figure 1.11 Microtiter plate for assay development.

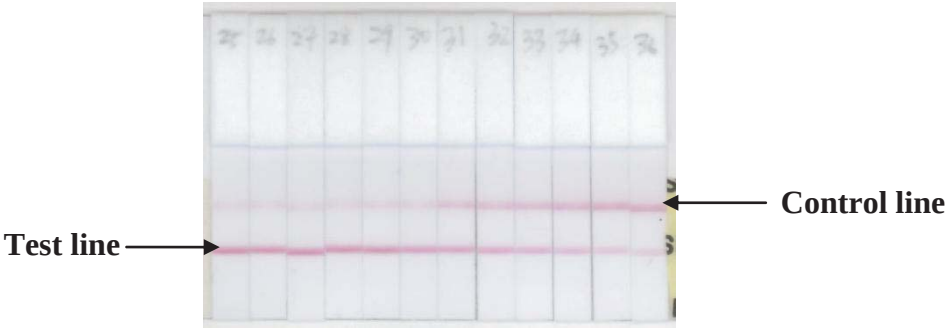

Figure 1.12 Strip tests using a series of standard solutions, gold nanoparticles are commonly used as a indicator and are pink coloured. The image was obtained using a photoscanner then subjected to quantitative analysis. The intensity of the test line is inverse proportional to the concentration of the target analyte.

1.5.1.1 Backing card

The backing card is used to laminate the LFIA components into one unit which gives structural support; the materials are typically polystyrene or other plastic materials.

1.5.1.2 Membrane materials

The membrane is the single most important material used in a LFIA strip. The capillary flow properties including: reagent deposition, assay sensitivity, assay specificity and test line

consistency are related to the physical and chemical characteristics of the membrane. The capture material for the test and control line must bind to the membrane irreversibly, and the polymer used as membrane material determines most of its binding characteristics. The few membrane materials include nitrocellulose, nylon, polyvinylidene fluoride, and polyethersulfone. Nitrocellulose is the most commonly used membrane material because of its many advantages such as relatively low costs, true capillary flow characteristics, and high protein binding. It binds to the protein for the test or control line via electrostatic interactions (Figure 1.13). The pore size of nitrocellulose ranges from 0.05 to 1.2 μm, and the unit of capillary flow rate is s/cm.

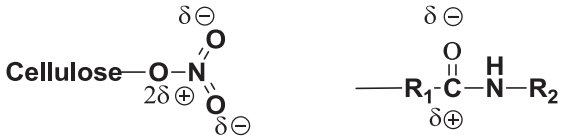

Figure 1.13 Structure of nitrocellulose ester and protein dipoles. Nitrocellulose membranes bind to protein electrostatically through interaction between the dipole of the nitro ester and the dipole of the peptide bonds of the protein.

1.5.1.3 Sample pad

The role of a sample pad is to accept a sample when placed onto a sample pad at one end of the strip, then release the analyte with high efficiency. The materials used as the sample pad can vary depending on the requirements of the application. Nitrocellulose, glass fibre, rayon, and other filtration median are typically used as sample pads.

1.5.1.4 Absorbing pad

The absorbing pad is also known as the wick. The absorbing pad is designed to pull up all the fluid added to the strip (or in the solution well) for the duration of the assay and finally stops the flow; it is commonly made of cellulose filters.

1.5.1.5 Conjugate pad

The conjugate pad is also known as a reagent pad, which contains antibodies specific to the target analyte conjugated to coloured particles such as colloidal gold. The conjugate pad accepts the conjugate and allows sufficient and consistent release of the conjugate when running the assay.

1.5.1.6 Labelling material

Colloidal particles such as colloidal gold, latexes, selenium, carbon or liposomes and magnetic particles have been used as labelling materials for the LFIA system on the conjugate pad with gold and latex particles the most commonly used.

1.5.2 Capillary flow rate

Capillary flow rate is crucial factor in LFIA analysis, and it is highly influenced by the properties of the membrane including the pore size of the membrane, pore size distribution and porosity. The capillary flow rate is the speed at which a sample front migrates along a membrane strip when liquid is introduced at the end. It is difficult to determine the flow rate as the rate decays exponentially as the liquid moves further along the membrane. Hence the capillary flow time is used as a measurement parameter, which is the time required for a liquid to move along and fill a strip of defined length; it is typically expressed as s/cm which is inversely related to flow rate. Capillary flow rate is important because the effective concentration of analyte in the sample is inversely proportional to the square of the change in flow rate.

1.6 Immunoassay

The immunoassay is a technique which incorporates the binding reaction of a target analyte (antigen) with an antibody. All immunoassay techniques can be categorised into two basic types: competitive assay and non competitive assay.

Immunoassay detects and measures the antigen or antibody present in the sample, and either the antigen or the antibody will be labelled with a radioactive isotope which can cause radioactive decay, hence the results can be quantified. The other routinely performed quantitative method is to label the antibody/antigen with enzymes which cause a colour change or produce light.

Competitive immunoassays are related to the phenomenon of the competition for the antibody between analyte and labelled analyte or the antibody present in the sample and the measurement indicates the amount of target analyte present in the sample. Non competitive immunoassay is also known as sandwich immunoassay or two site immunoassay. The measurement is based on the interaction between the sample and the excess labelled antibody which adsorbs onto the solid phase, another labelled antibody is then introduced to bind to the target analyte which results in a sandwich format of the antibodies and target analyte, hence the target analyte present in the sample can be quantified. The most important difference between a competitive and a non competitive assay is the detection of antibody occupancy.[28] In a competitive immunoassay, the labelled antigen is used to detect the antibody-binding sites which are not occupied by the analyte in the standard or sample. However, in a noncompetitive immunoassay the labelled antibody is used to detect the presence of captured analyte, hence the noncompetitive assay method is primarily detecting the antibody occupancy.

1.6.1 Immunoassay of steroids

The sensitivities of steroid analysis were at nanomolar and picomolar concentration range in the 1960s. Technologies used included gas-liquid chromatography,[29] double isotope derivatization,[30,31] spectrophotometry and fluorometry.[32]The competitive binding assay method was not used till the 1970s, and it uses a specific binding protein to measure/detect the steroids, such as serum binding protein.[33] The development of a radioimmunoassay (RIA) in 1960s[34] enabled numerous possible techniques for assay development. The sensitivity of the assay has been increased a millionfold over previous methods because of the development

of protein and haptens assay. “Limited reagent method” and “saturation analysis” were introduced by Ekins in 1960s[35] and these showed that the concentration of the binding protein was insufficient to bind to all the radioactive analyte.

1.6.2 Progesterone sensing

Progesterone, 4-pregene-3,20-dione also known as P4 is a steroid hormone. It was first discovered in 1920s by Corner and Allen in 1929[36] and its structure was determined in 1934.[37,38] Progesterone is secreted by the ovarian granulose cell before ovulation under the influence of a luteinising hormone released from the anterior pituitary.

The corpus luteum plays an important role in providing progesterone to maintain early pregnancy[39] and continues to produce progesterone throughout pregnancy.[40] Studies have shown that progesterone plays a role in regulating the sequence of the ovulatory cycle by controlling other hormones. Therefore measurement of progesterone is an ideal candidate as a marker for monitoring ovary functions.

Progesterone measurements are used routinely to monitor that ovulation has occurred and the corpus luteum is functioning normally. A rise in plasma progesterone over 30 $nmolL^{-1}$ for a mid-luteal sample indicates that ovulation has occurred.

The initial methods for progesterone detection were based on thin layer chromatography and gas chromatography,[41] and the introduction of isotope dilution as well as mass spectrometry improved the sensitivity and accuracy. Prior to the 1960s, no method had sufficient sensitivity to measure progesterone in serum. During the 1960s methods such as bioassay, gas chromatography and isotope dilution analysis were developed and used for serum progesterone measurement. The detection limit lies within the pg range.[42] Methods such as high performance liquid chromatography (HPLC) allowed progesterone analysis for bovine liver, kidney, kidney fat and milk.[43] The gas chromatography–mass spectrometry (GC-MS) method was able to achieve a detection limit of 5 μgL^{-1}, and when the liquid chromatography–mass spectrometry (LC-MS) was used progesterone was detected in the range 0.4-20 μgL^{-1}. [44] Although such methods as GC-MS and LC-MS are suitable for low P4 detection, the techniques are still too expensive for routine analysis.

The earliest measurement of free progesterone in serum was done by Yannone et al. in 1969 using the principle of equilibrium dialysis.[45] The percentage of the bound steroid can be calculated using following formula:

$$\%\, Steroid\ Bound = 100\left[1 - \left(\frac{dpm\ outside}{dpm\ inside} \times \frac{volume\ inside}{volume\ outside}\right)\right]$$

$$dpm = disintegration\ per\ minute$$

The radioactivity of the sample was measured for both inside and outside of the dialysis bag then used to calculate the percentage of the bound steroid. However, the early methods for determining the free progesterone in plasma have been confirmed to be inaccurate because there was no correction made for the plasma sample dilution and the effects of dialysis against a hypotonic solution were not accounted for in such methods.

Current methods for progesterone detection in a laboratory are based on immunochemical methods, which focus on the reaction between analyte and analyte specific antibody, hence is highly specific and sensitive. Techniques such as radioimmunoassays (RIAs), enzyme immunoassays (EIAs) required labelled analyte or antibody. EIA test kits[46] have been developed for onsite progesterone analysis and are also commercially available. The major disadvantage of the onsite EIA test kit is the number of tests available per kit and the costs are relatively high for daily application.

The alternative possible technique for progesterone analysis is LFIA, and it has been suggested that the most crucial parameter in the development of an LFIA for progesterone was the buffer.[47] In the literature, it has been reported that the LFIA method has been used to quantify progesterone in bovine milk.[48,49]

The progesterone concentration in blood and milk are closely correlated; progesterone is a steroid hormone which has an affinity for fat; thus the concentration of progesterone in milk is somewhat higher than the concentration of progesterone in the blood. However the relative relationship between milk and blood level is the same.

Biacore systems have been used for the non-labelled SPR assay of bovine milk progesterone analysis from 0.4 to 0.6 μgL^{-1} and 35 to 60 ngL^{-1} in a buffer solution.[50] A grating coupler transducer was also used for whole blood progesterone analysis which is comparable to the SPR method and the detection limit was approximately 1 ngL^{-1}.[51] The total internal reflection fluorescence methods are also used for progesterone analysis with a detection limit of 0.04 μgL^{-1} in 5 minutes.[52] There are many advantages of using evanescent wave technology including rapid real time analysis, high sensitivity, and the sensor chip can be regenerated and used many times.

1.7 Progesterone sensing and the present study

This project is focused on progesterone (P4) sensing, using both SPR and LFIA methods with a new progesterone sensing material to develop cost effective assays for progesterone sensing in bovine serum and milk samples.

Chapter 2 is concerned with the development of a new P4 linker for a P4 inhibition assay in a SPR-based sensor. The developed inhibition assay was used to perform bovine serum and milk P4 analyses.

Chapter 3 is concerned with the incorporation of one of the new P4 linkers labelled as P4-PEG-OVA into LFIA studies to develop an inhibition assay to carry out bovine serum and milk P4 analyses.

Chapter 4 is concerned with some research and development of naturally occurring polyhydroxyalkanoate granules as an alternative sensing material in both the SPR and LFIA methods.

Chapter 5 summarises the thesis conclusions and offers future research directions. All the experimental procedures, methods, and instruments used are placed in the Appendix.

References

(1) *Ministry for Primary Industries: Agriculture and the New Zealand economy*; **2013**.http://www.mpi.govt.nz/agriculture/pastoral/dairy.aspx

(2) *Dairy's role in sustaining New Zealand - the sector's contribution to the economy*; **2010**.http://www.fonterra.com/wps/wcm/connect/fcf7000044f43b8bb2b2fbac5c5d2692/NZIER+economic+report+to+Fonterra+and+DNZ+2010.pdf?MOD=AJPERES&CACHEID=fcf7000044f43b8bb2b2fbac5c5d2692

(3) Noakes, D. E. *Fertility and obstetrics in cattle*; 2 ed.; Blackwell Science: Oxford, **1997**.

(4) *Factors affecting Calf Crop: Biotechnology of Reproduction*; 1 ed.; Fields, M. J.; Sand, R. S.; Yelich, J. Y., Eds.; CRC Press: New York, **2002**.

(5) Lehrer, A. R.; Lewis, G. S.; Aizinbud, E. *Animal Reproduction Science* **1992**, *28*, 355-362.

(6) Shin, S.; Kim, J. P.; Sim, S. J.; Lee, J. *Applied Physics Letters* **2008**, *93*, 102902/102901-102902/102903.

(7) Xiao, Y.; Liu, Y.; Borg, G.; Li, C. M. *Materials Science & Engineering, C: Materials for Biological Applications* **2011**, *31*, 95-98.

(8) Wood, R. *Philosophical Magazine* **1902**, *4*, 396-402.

(9) Otto, A. *Zeitschrift Fuer Physik* **1968**, *216*, 398-410.

(10) Kretschmann, E. *Zeitschrift fuer Physik* **1971**, *241*, 313-324.

(11) Liedberg, B.; Nylander, C.; Lunstrom, I. *Sensors and Actuators* **1983**, *4*, 299-304.

(12) Stenberg, E.; Persson, B.; Roos, H.; Urbaniczky, C. *Journal of Colloid and Interface Science* **1991**, *143*, 513-526.

(13) Phizicky, E. M.; Fields, S. *Microbiological Reviews* **1995**, *59*, 94–123.

(14) Luo, J.; Zhuo, J.; Zou, W.; Shen, P. *Journal of Biochemistry* **2001**, *130*, 553–559.

(15) Kaganer, E.; Pogreb, R.; Davidov, D.; Willner, I. *Langmuir* **1999**, *15*, 3920-3923.

(16) Lipschultz, C. A.; Li, Y.; Smith-Gill, S. *Methods (Orlando, Florida)* **2000**, *20*, 310-318.

(17) Thiel, A. J.; Frutos, A. G.; Jordan, C. E.; Corn, R. M.; Smith, L. M. *Analytical Chemistry* **1997**, *69*, 4948-4956.

(18) Adamczyk, M.; Mattingly, P. G.; Shreder, K.; Yu, S. *Bioconjugate Chemistry* **1999**, *10*, 1032-1037.

(19) Laricchia-Robbio, L.; Balzan, S.; Ghione, S.; Montali, U.; Revoltella, R. P. *Biosensors & Bioelectronics* **1998**, *13*, 1055-1060.

(20) Mullett, W.; Lai, E. P.; Yeung, J. M. *Analytical Biochemistry* **1998**, *258*, 161-167.

(21) Mullett, W. M.; Lai, E. P. C.; Yeung, J. M. *Methods (Orlando, Florida)* **2000**, *22*, 77-91.

(22) Tokareva, I.; Minko, S.; Fendler, J. H.; Hutter, E. *Journal of the American Chemical Society* **2004**, *126*, 15950-15951.

(23) Pelossof, G.; Tel-Vered, R.; Liu, X.; Willner, I. *Chemistry-A European Journal* **2011**, *17*, 8904-8912.

(24) Englebienne, P. *Analyst (Cambridge, United Kingdom)* **1998**, *123*, 1599-1603.

(25) BIACORE *BIACORE Technology Handbook*; AB ed.; BIACORE, **1998**.

(26) Tanaka, R.; Yuhi, T.; Nagatani, N.; Endo, T.; Kerman, K.; Takamura, Y.; Tamiya, E. *Analytical and Bioanalytical Chemistry* **2006**, *385*, 1414-1420.

(27) Tsao, Z.; Liao, Y.; Liu, B.; Su, C.; Yu, F. *Journal of Agricultural and Food Chemistry* **2007**, *55*, 4921-4927.

(28) *Current concepts and future developments. In Complementary Immunoassays (ed) Collins WP. , pp. 219–237.*; Ekins, R., Ed.; Wiley, Chichester, **1985**.

(29) Collins, W. P.; Sisterson, J. M.; Koullapis, E. N.; Mansfield, M. D.; Sommerville, I. F. *Journal of Chromatography* **1968**, *37*, 33-45.

(30) Kliman, B.; Peterson, R. *Journal of Biological Chemistry* **1960**, *235*, 1639-1648.

(31) Gandy, H.; Peterson, R. *Journal of Clinical Endocrinology* **1968**, *28*, 949-977.

(32) Brown, J. B.; MacLeod, S. C.; Macnaughtan, C.; Smith, M.; Smyth, B. *Journal of Endocrinology* **1968**, *42*, 5-15.

(33) Mayes, D.; Nugent, C. *Steroids* **1970**, *15*, 389.

(34) Yalow, R.; Berson, S. *Journal of Clinical Investigation* **1960**, *39*, 1157-1175.

(35) Ekins, R. *Clinica Chimica Acta* **1960**, *5*, 453-459.

(36) Corner, G. W.; Allen, W. M. *American Journal of Physiology* **1929**, *88*, 326-339.

(37) Butenandt, A.; Schmidt, J. *Berichte der Deutschen Chemischen Gesellschaft [Abteilung] B: Abhandlungen* **1934**, *67B*, 2088-2091.

(38) Fernholz, E. *Berichte der Deutschen Chemischen Gesellschaft [Abteilung] B: Abhandlungen* **1934**, *67B*, 1855.

(39) Csapo, A.; Pulkkinen, M.; Wiest, W. *American Journal of Obstetrics and Gynecology* **1973**, *115*, 759-765.

(40) LeMaire, W.; Conly, P.; Moffett, A.; Spellacy, W.; Cleveland, W.; Savard, K. *American Journal of Obstetrics and Gynecology* **1971**, *110*, 612-618.

(41) Darling, J.; Laing, A.; Harkness, R. *Journal of Endocrinology* **1974**, *62*, 291-297.

(42) Siekmann, L. *Journal of Steroid Biochemistry* **1979**, *11*, 117-123.

(43) Purdy, R. H.; Durocher, C. K.; Moore, P. H. J.; Rao, P. N. *Journal of Steroid Biochemistry* **1980**, *13*, 1307-1315.

(44) Diaz-Cruz, M. S.; Lopez de Alda, M. J.; Lopez, R.; Barcelo, D. *Journal of Mass Spectrometry* **2003**, *38*, 917-923.

(45) Yannone, M.; Mueller, J.; Osborn, R. *Steroids* **1969**, *13*, 773-781.

(46) Nebel, R. L.; Altemose, D. L.; Munkittrick, T. W.; Sprecher, D. J.; McGilliard, M. L. *Theriogenology*, *31*, 753-764.

(47) Posthuma-Trumpie, G. A.; Korf, J.; Amerongen, A. *Analytical and Bioanalytical Chemistry* **2008**, *392*, 1215-1223.

(48) Laitinen, M. P. A.; Vuento, M. *Acta Chemica Scandinavica* **1996**, *50*, 141-145.

(49) Sananikone, K.; Delwiche, M. J.; BonDurant, R. H.; Munro, C. J. *Transactions of the American Society of Agricultural and Biological Engineers* **2004**, *47*, 1357-1365.

(50) Gillis, E.; Traynor, I.; Gosling, J.; Kane, M. *Journal of AOAC International* **2006**, *89*, 838-842.

(51) Ehrentreich-Forster, E.; Scheller, F.; Bier, F. *Biosensors & Bioelectronics* **2003**, *18*, 375-380.

(52) Kaeppel, N.; Proell, F.; Gauglitz, G. *Biosensors & Bioelectronics* **2007**, *22*, 2295-2300.

Chapter 2

SPR based biosensors

2.1 Introduction

An SPR biosensor is based on the binding between an antigen and its homologous antibody. The first SPR based biosensing technique was introduced by Liedberg in 1983 for antibody absorption as well as gas detection.[1] However, the technique has been studied prior to this application when organic mono- and multilayers on a metal surface.[2,3] The SPR based sensors were able to detect the interactions between the biomolecules and the surface material directly, without the need for labelling.[4-9] Hence, SPR allows real-time measurements including determining analyte concentration.[10,11]

In a direct SPR sensor (refractometric)[12-15] the characteristics of light such as the coupling angle, wavelength, intensity, phase, or polarisation are directly modulated. For example, in an affinity biosensor, the concentration of chemical or biological analyte is measured through the binding of the analyte to a biorecognition element, and then converted into a refractive index change at the sensor surface, which modulated the light wave.[16,17]

The Kretschmann configuration, one of the configurations briefly mentioned in Chapter 1, is the most common setup for a SPR prism coupler, because it provides the most efficient way for generating surface plasmons. The metal film such as gold in the Kretschmann configuration is deposited directly on top of a prism surface.[18] The angle of the light source illuminated through the prism is greater than the critical angle for the total internal reflection (TIR). The surface plasmon occurs as plane-polarised light hits a metal film under total internal reflection conditions where 100% of the light is internally reflected (Figure 2.1).

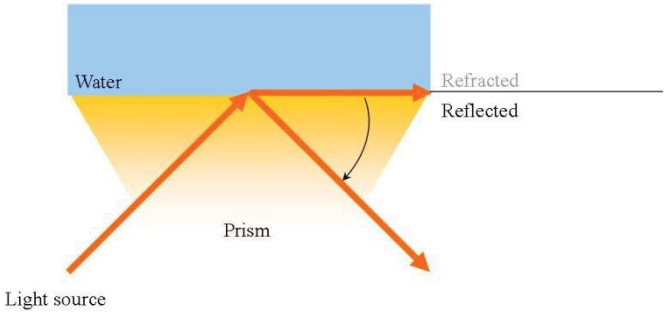

Figure 2.1 Under total internal reflection, all the incoming light is reflected within the prism.[19]

The theory, properties and the potential applications of surface plasmon can be explained by using the boundary-value problem. Surface plasmon or surface plasmon polaritrons are surface electromagnetic waves that propagate parallel to a metal/dielectric interface. In the schematic of a boundary-value problem (Figure 2.2), the plane x separates a metal with complex-value refractive index n_m from the dielectric sample with complex-value refractive index n_s. The surface plasmon propagates as an electromagnetic wave, which is parallel to the x-axis with its magnetic field parallel to the y-axis. The electromagnetic field tunnelled into the interior side of the surface forms the evanescent wave and reflection (Figure 2.3).[19,20]

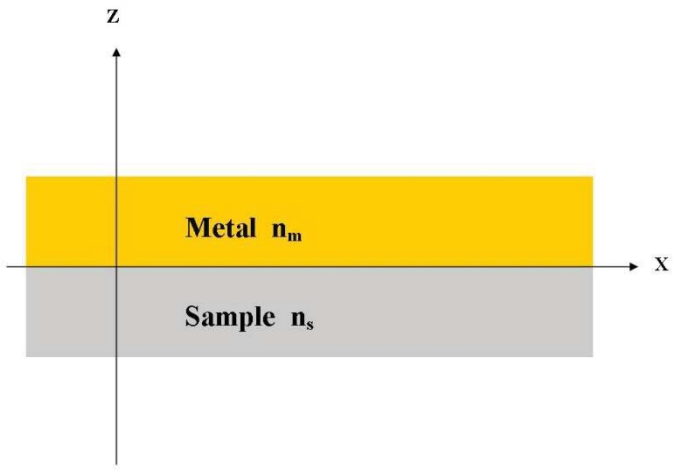

Figure 2.2 Schematic of a boundary-value problem to describe the propagation of a surface plasmon polaritron.[19]

2.1.1 The evanescent wave

Under TIR the electron field is created by the photons on the opposite site of the interface (Figure 2.3). The plasmons extended the electron field into the medium on the other side of the interface (the metal and sample interface), and the created electron field is known as an evanescent wave.

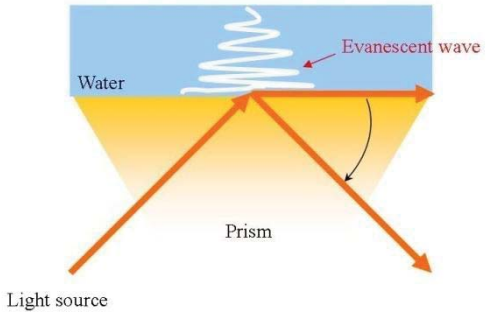

Figure 2.3 Evanescent wave generated under TIR.[19]

When the prism is in contact with a thin metal film such as gold (noble metal), the energy of that electrical field can be transferred to electrons in the metal which generate a surface plasmon oscillation. As the surface plasmon oscillation occurs, a drop in intensity of the reflected light is observed, and the angle in such a condition is called the (θ_{SPR}, Figure 2.4). The excitation of surface plasmons by light is denoted as surface plasmon resonance for a planar surface.

The amplitude of the wave decays exponentially as the distance between interface surface increases, and the decaying distance is approximately one light wavelength.[21] The depth of the evanescent wave penetrates the sample interface about 300 nm. Hence, it is practical for sample measurement with sensor surface within 300 nm. As the binding event occurs, the closer to the sensor surface results in a higher response than those further away to the sensor surface. Hence the 300 nm depth is important in SPR sensing.

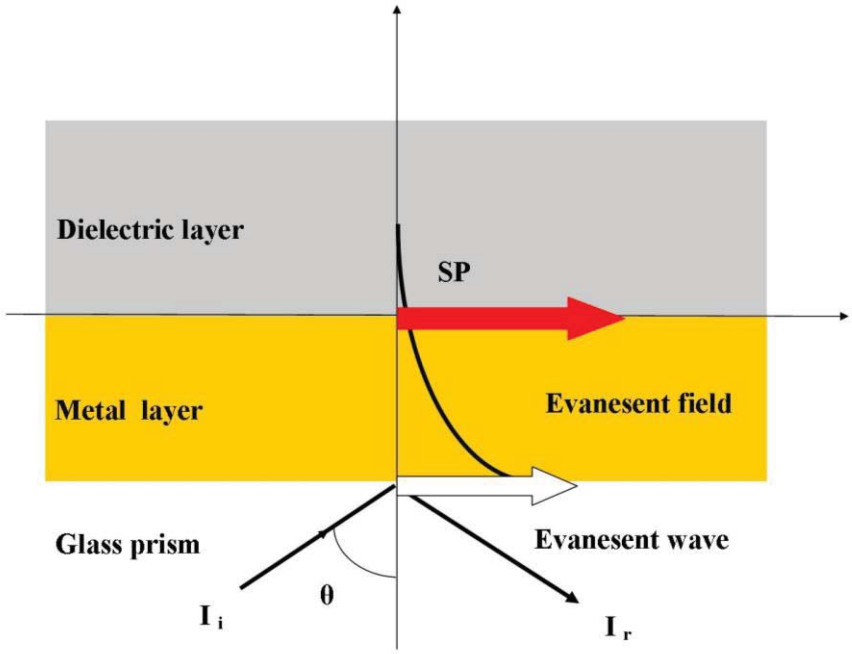

Figure 2.4 At θ_{SPR}, the reflected light intensity decreases, and this difference is measured in SPR. As the molecule interacts with the immobilised molecule on the surface, the change in refractive index results in a shift in θ_{SPR}. [19]

2.2 Development of SPR assays

There are several commonly used SPR assay formats including direct immunoassay, competition assay, inhibition assay and sandwich assay.[19,22-26]

In a direct assay, the antigen specific antibody is immobilised onto the sensor surface, and the sample solution containing the antigen is directed to the sensor surface. The response is proportional to the concentration of the antigen. A competition assay is suitable for detection of low molecular weight molecules. The antigen specific antibody is conjugated with a higher molecular weight linker in order to detect the low molecular weight antigen. A sandwich assay requires the immobilisation of antigen specific antibody onto the surface to capture the analyte, followed by binding of secondary antibody to either the antigen or the antigen bound antibody.[27,28]

This project is focused on the inhibition assay[29,30] where the target antigen progesterone (P4) is immobilised onto the surface and the sample solution containing the antigen (P4) is mixed with antigen specific antibody (Anti-P4). The antibody binds to both the antigen in the

solution as well as the antigen on the sensor surface; because the antibody has high molecular weight, the binding is directly detected. The response is approximately inversely proportional to the concentration of the antigen.

It is common to use two flow cells for SPR assay development, flow cell one (FC1) as a reference cell and flow cell two (FC2) with specific immobilised surface to interact with the analyte. FC1 is used to measure the non-specific binding of analyte to the surface (or the protein linked to the immobilised ligand). The analyte flows through both FC1 and FC2. The responses are measured by subtracting the reference response of FC1 from the binding response of FC2. Hence, the resultant response units represent only the specific binding to the immobilised ligand on the sensor surface.

The commercially available CM5 chip was used for the assay development. The dextran layer on the CM5 sensor surface is approximately 100 nm, and it was used to couple with the analyte specific ligand via carboxylic acid groups after the activation of the sensor surface. The details of the activation steps and immobilisation procedure will be described in the following section.

There are a few immobilisation techniques including covalent, capture and hydrophobic approaches to link the binding partner onto the sensor surface. The activation step allows the carbonyl functional group of the CM5 surface to couple with a NH_2 group of the ligand (e.g. ovalbumin).[22,23]

The carboxymethylate dextran (CM5) surface has carboxylic acid residues as the functional groups some of which are used for conversion to another functionality.

A direct coupling includes amine coupling, a thiol reaction, aldehyde coupling, or carboxylic acid coupling. Amine coupling (Figure 2.5) is the most versatile and widely used coupling method. The ligand couples with the reactive nucleophile functionalities attached to the carboxylic group on the sensor surface.

In step (i) (Figure 2.5) the carboxylic acid group is activated by 1-ethyl-3(-3-dimethylaminopropyl)carbodiimide-HCl (EDC-HCl) to form a covalent amide or ester bond between the carboxylic acid and the amine group (compound (a)). In step (ii) N-hydroxy succinimide (NHS) is used to convert (a) to (b) and (c). The interaction is carried out in two steps in order to avoid the carbodiimides reacting with the immobilised ligand. These

reagents are commonly used in the activation step (i) and (ii), compound (b) reacts with the ligand $-NH_2$ to give amide (d).

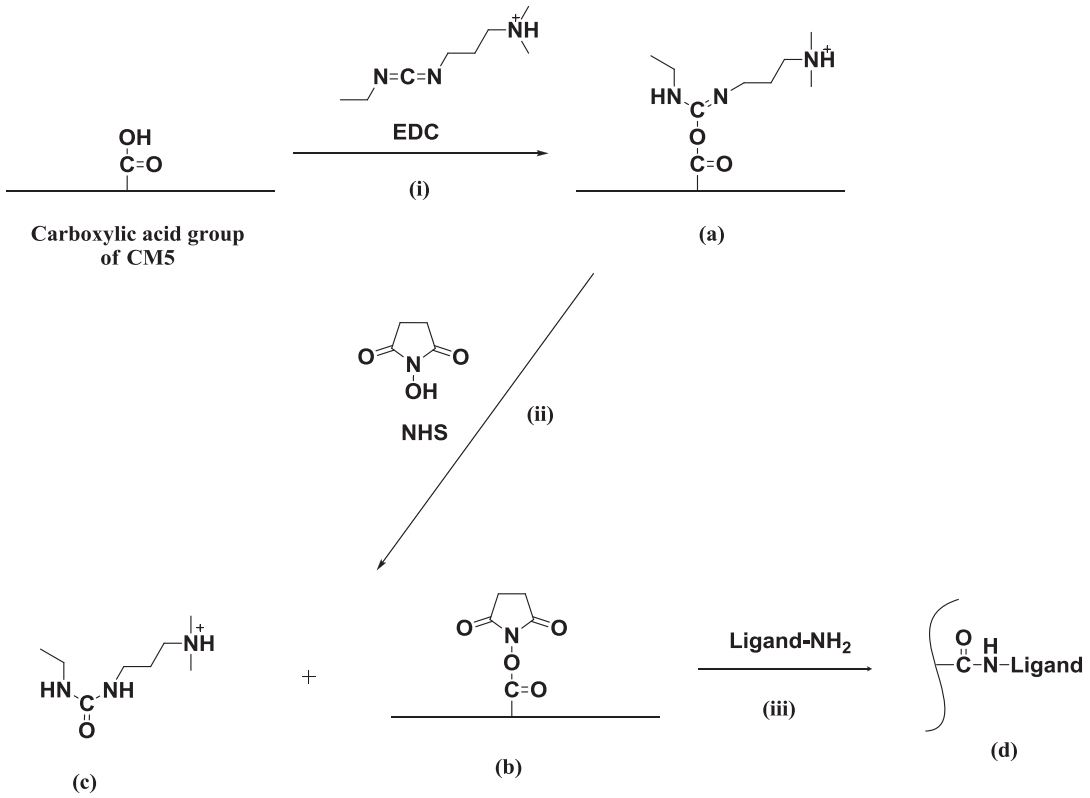

Figure 2.5 The activation steps of the carboxylic acid group of CM5 with EDC and NHS.

2.3 Progesterone (P4) derivatives

Steroids such as progesterone (P4) are too small to directly absorb onto a solid phase such as a SPR sensor surface while retaining binding to the antibody. It is common to conjugate the small steroid to a protein for surface immobilisation. This study showed that when P4 is conjugated to the ovalbumin (OVA) with different length linkers the sensitivity of the antibody binding is affected. As the linker length increased, the sensitivity of antibody binding is increased.[31] Three linkers (Figure 2.6 2.7, 2.8) were used in this project, two known linkers and one new linker in order to compare the sensitivity of P4 sensing.

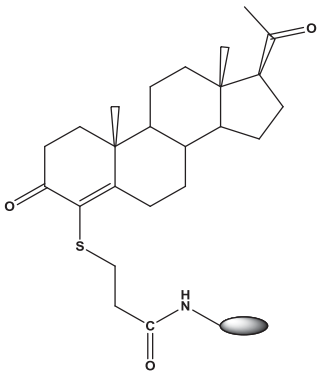

Figure 2.6 4TP-P4-OVA

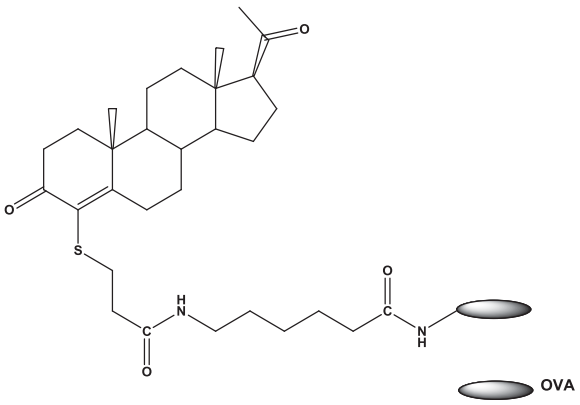

Figure 2.7 4TPH-P4-OVA

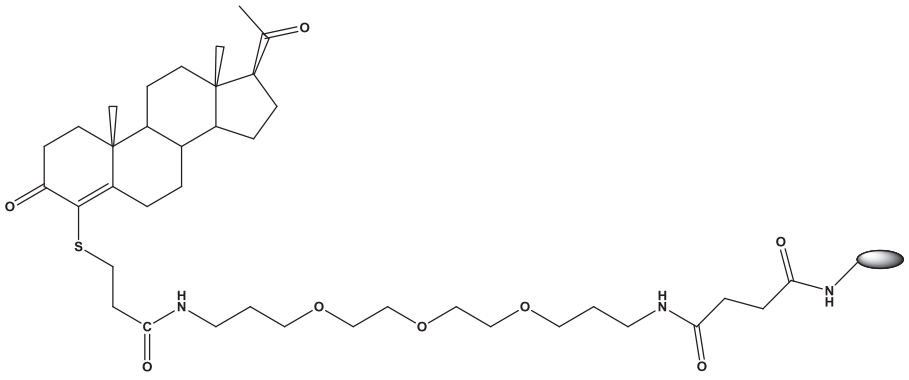

Figure 2.8 P4-PEG-OVA

2.3.1 Synthesis of P4-PEG-OVA

2.3.1.1 A brief overview of the synthesis of P4-PEG-COOH

The synthesis of P4-PEG-OVA was carried out following Scheme 2.1 and Scheme 2.2 below. Commercially available progesterone (**1**) was converted to its epoxide P4epoxide (**2**), which was converted to $P4S(CH_2)_2COOH$ (**3**), which was then sequentially converted into compounds **4**, **5** and then P4-PEG-COOH (**6**) following procedures developed for similar derivatives in the literature [32-34] and in our lab.

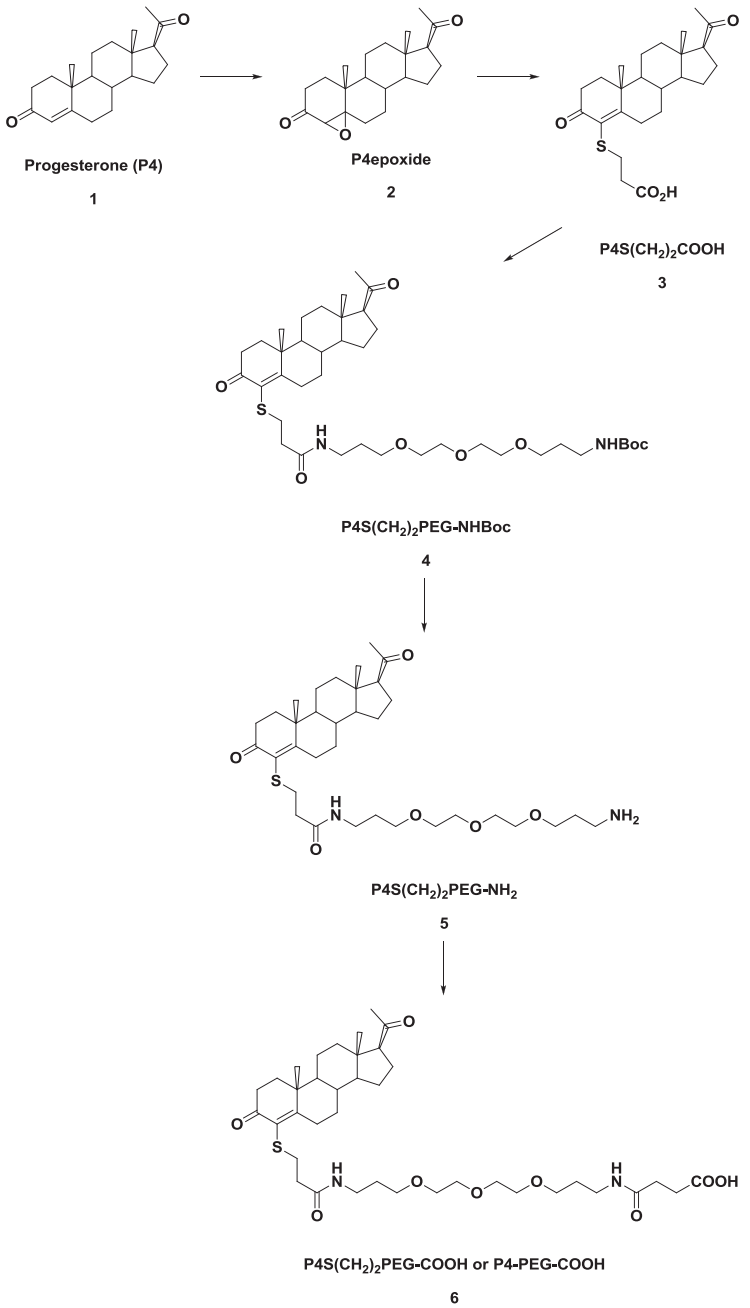

Scheme 2.1 The synthesis of the P4-PEG derivative (6) was carried out following the scheme above.

The compounds **2**, **3**, **4**, **5** and **6** have been previously synthesised in our laboratory by Dr K. Jayasundera and Dr W. Campbell from The MacDiarmid Institute, Massey University and their procedures are given in the Appendix (A.2.2.1, A.2.2.5, A.2.2.6, A.2.2.7 and A.2.2.8). They have not yet been published.

2.3.1.2 Conjugation of P4S$(CH_2)_2$PEG-COOH to ovalbumin (OVA) to give P4-PEG-OVA

A low molecular weight molecule such as P4 generates insufficient signals to be detected directly in a SPR sensing system. Hence the P4S$(CH_2)_2$PEG-COOH linker was conjugated to ovalbumin (OVA) (Scheme 2.2), then the conjugate was immobilised onto the sensor surface for further analysis (Section 2.3.1.3). The conjugation of P4S$(CH_2)_2$PEG-COOH to OVA to give P4-PEG-OVA represents new chemistry for this thesis and was effected by a standard procedure which involves activation of the carboxylic acid group with DCC and NHS and then reaction with a NH_2 group of OVA (see Appendix A.2.2.9).

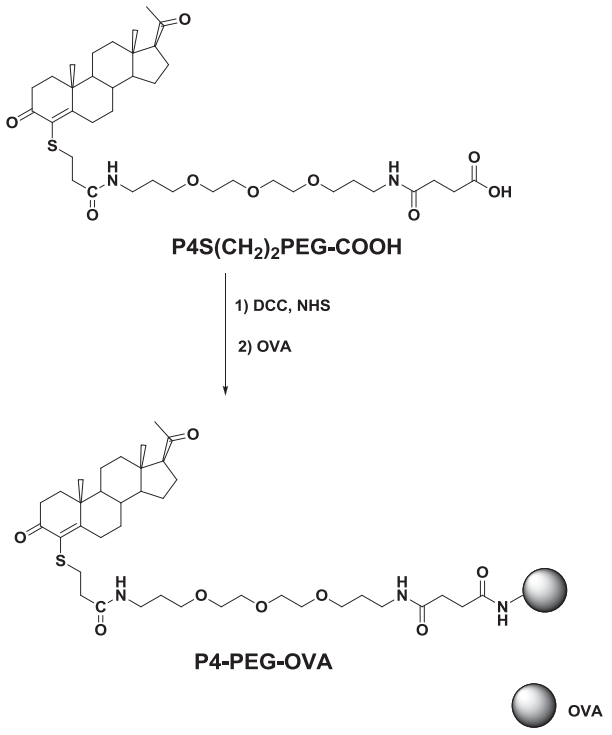

Scheme 2.2 Steps for the conjugation of P4-PEG-COOH to OVA to form P4-PEG-OVA.

2.3.1.3 Immobilisation of ligands onto the CM5 chip

The pH of the solution is crucial for the immobilisation steps. For a successful immobilisation of ligand onto a CM5 chip requires the pH of the buffer to be between the disassociation constant (pK) of the dextran and the isoelectric point (pI) of the OVA ligand. If the pH of the buffer is lower than the pK of the dextran layer, both dextran and the ligands will be positively charged, which will result in no immobilisation of ligands onto the surface. If the pH of the buffer is higher than the pI of the ligand, both dextran and ligand become negatively charged, which also results in no immobilisation of ligands onto the surface (Figure 2.9). Hence, sodium acetate buffer (10 mM, pH 4) was used as diluents to prepare all solutions for ligand immobilisation, and the sensor surface requires a pre-conditioning procedure (surface activation).

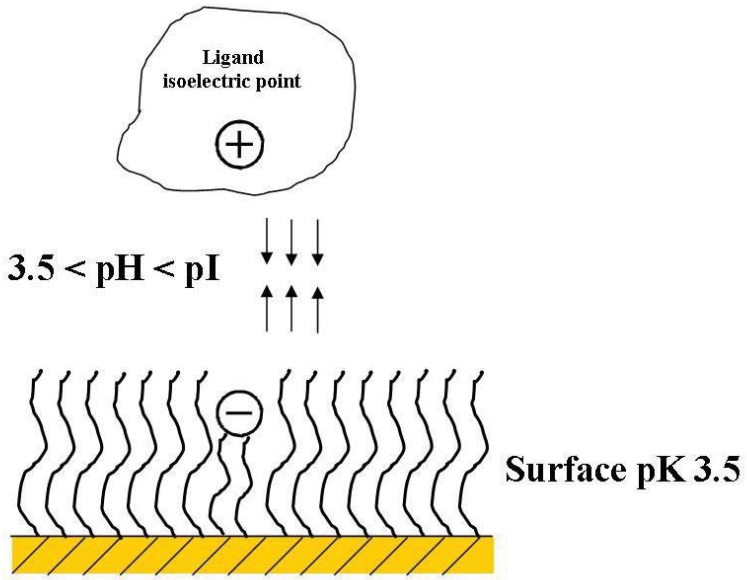

Figure 2.9 Buffer conditions for a successful immobilisation of ligands onto a CM5 sensor surface. The pH of the buffer has to be higher than the pK of the dextran layer to generate a negatively charged surface for the positively charged ligand to bind to the surface.[22]

Direct protein immobilisation is the most commonly used method for surface immobilisation, since most proteins contain potential amine groups which are readily available for the coupling reaction. The carboxylic groups on the dextran sensor surface can be activated by the activation step, which results in the formation of a covalent amide or ester between the

carboxylic acid and the amine/hydroxyl groups on the protein as has been discussed previously in Figure 2.5 and Scheme 2.2. Carbodiimide reagents are commonly used for the activation step, for example dicyclohexyl carbodiimide (DCC) is used in organic solvents, and EDC is used in aqueous solution. Ethanolamine-HCl is used as a deactivation reagent to clean and regenerate the sensor surface.

The sensorgram of FC2 (Figure 2.10) shows the process of activation of the CM5 sensor surface, immobilisation of the ligand and the deactivation/cleaning of the sensor surface. The surface was activated by injecting EDC/NHS, which was indicated by a change in the response units (154.0 RU). An extra injection of EDC/NHS was applied to ensure the activation of the sensor surface (32.5 RU). After the activation of the dextran surface, a short pulse of the ligand P4-PEG-OVA was injected to couple with the surface, giving a response of 843.0 RU indicating that the ligand has coupled with the sensor surface. The ligand was then injected with a long pulse, which gave 6938.9 RU. The desired RU for immobilisation is approximately 6000 RU; hence the immobilisation process was achieved. The deactivation step (the capping step) was carried out by injecting ethanolamine-HCl solution, to deactivate the carboxylic acid group on the sensor surface and then to clean which regenerates the sensor surface which gave a final immobilisation level of 6171.3 RU, which was the expected value.

For flow cell 1 (FC1) immobilisation, the same activation steps were carried out and OVA (50 uL, 0.05% w/v) in sodium acetate (10 mM, pH 4) was injected in short pulses to couple to the sensor surface of FC1 (Figure 2.11) until the response reached approximately 200 RU greater than the immobilisation level of FC2. After the capping step, the final response of FC1 was 6251.0 RU.

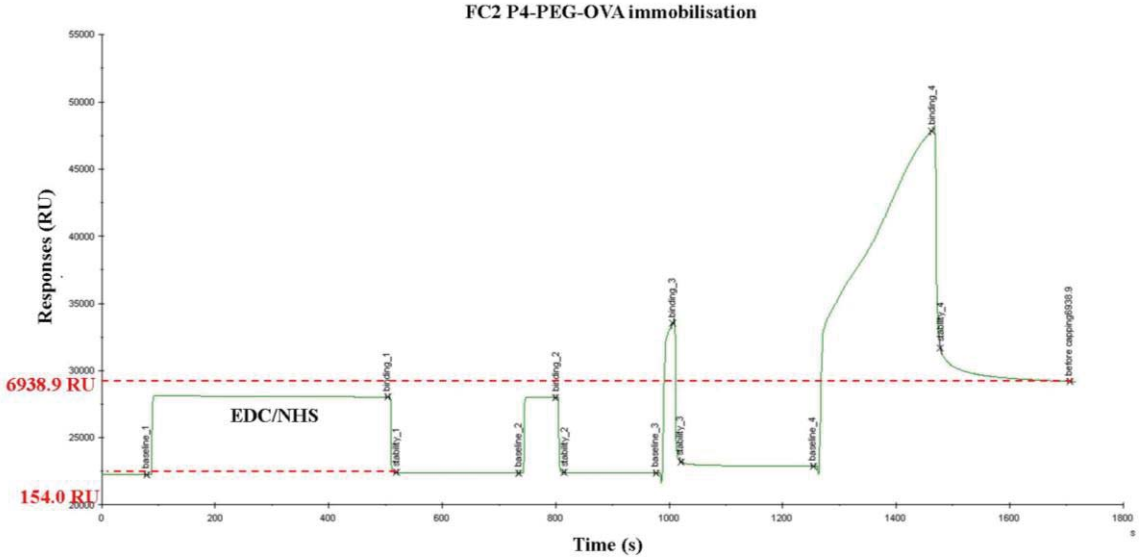

Figure 2.10 Sensorgram of flow cell two (FC2) showing the process of activation of the CM5 sensor surface, immobilisation of the P4-PEG-OVA onto a CM5 surface and the deactivation/cleaning of the sensor surface. The P4-PEG-OVA solution was injected after the surface was activated by the EDS/NHS solution. The sensor surface was regenerated/deactivated after the injection of ethanolamine-HCl solution.

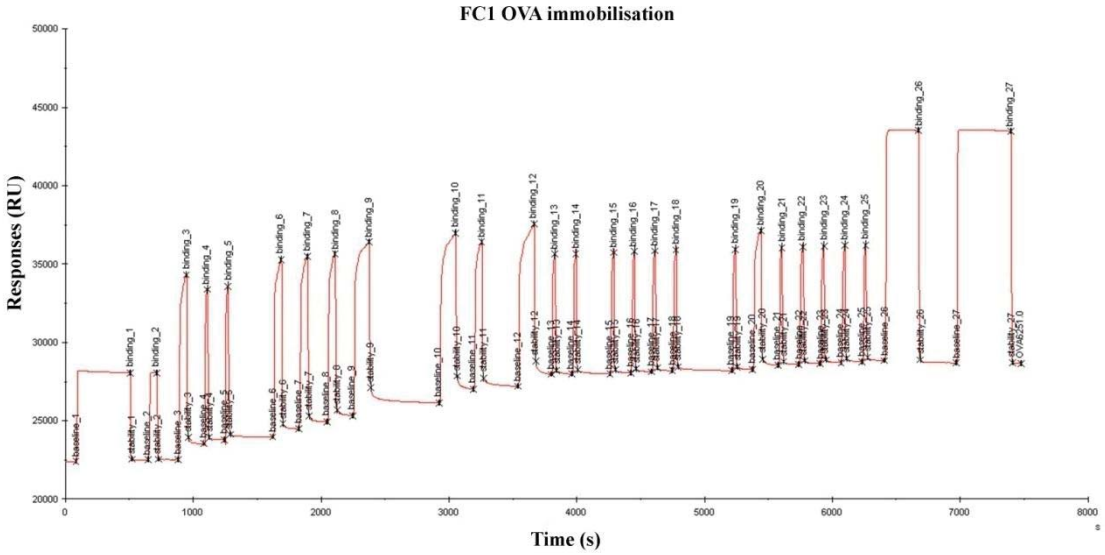

Figure 2.11 Sensorgram of flow cell one (FC1) showing the process of activation of the CM5 sensor surface, immobilisation of the OVA ligand on the CM5 and the deactivation/cleaning of the sensor surface. The OVA solution was injected in short pulses after the CM5 surface was activated by the EDS/NHS solution and this was followed by an injection of ethanolamine-HCl to regenerate the surface.

The chip was conditioned by injecting HBS-EP$^+$ buffer (10 mM, pH 7.4) at 30 µL/min for 120 s and the surface was regenerated by injecting two injections of NaOH (50 mM) at 5 µL/min for 30 s. The surface was conditioned for 5 hours (20 injections of HBS-EP$^+$ buffer).

2.3.2 Binding performance with monoclonal rat Anti-progesterone (Sigma P192)

The binding performance between anti-progesterone (Anti-P4) and progesterone-OVA (P4-OVA) conjugates was evaluated with a BIAcore X100 instrument using the progesterone-OVA conjugate surfaces as discussed in section 2.3. The binding performances of the P4-derivatives were tested with commercially available monoclonal rat Anti-P4 (Sigma, 0.1 mg/mL). The Anti-P4 solutions were prepared using HBS-EP$^+$ buffer to 7 selected concentrations. All solutions tested over the sensor surfaces consisted of the P4 derivatives (4TP-P4-OVA, 4TPH-P4-OVA, P4-PEG-OVA, see Appendix A.2.3.2.1 for details), and the calibration curve for each P4 derivative was established to determine the binding sensitivity of the monoclonal rat Anti-P4 to the sensor surface. The binding response is plotted versus the calculated Anti-P4 concentration.

2.3.2.1 4TP-P4-OVA

The calibration curve of 4TP-P4-OVA (see Figure 2.6 for structure) with rat monoclonal Anti-P4 has been established in the literature,[31] the binding responses and the performance were stable and linear.

After the injection of 1 μg/mL of antibody, the response was 9.7 RU, which indicated that the antibody was binding to the sensor surface. As the concentration of antibody increased, the response also increased. The response unit indicated that with concentration below 20 μg/mL, the binding performance is directly proportional to the concentration of the antibody (Figure 2.12).

4TP-P4-OVA has the shortest linker between the progesterone molecule and the conjugated OVA. With 20 μg/mL of antibody, the 4TP-P4-OVA surface had a response of 87.6 RU, which was not specifically sensitive. In order to achieve a sensitive assay, approximately 200 RU for primary antibody binding to the sensor surface is desired.

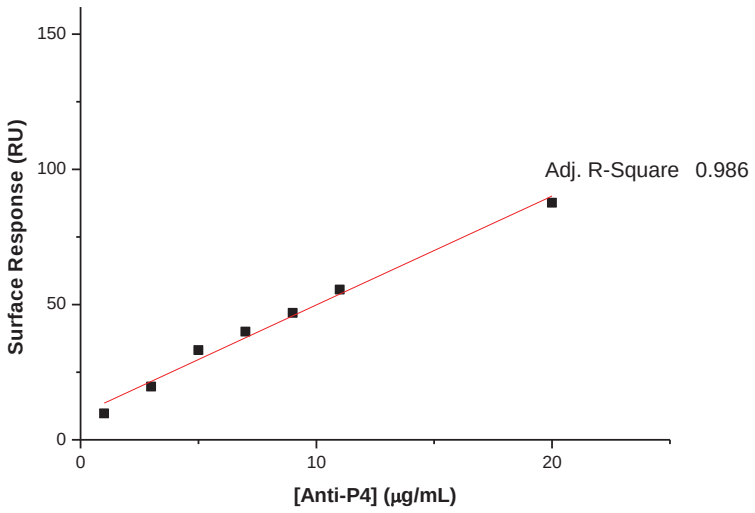

Figure 2.12 Binding curve of 4TP-P4-OVA with rat monoclonal Anti-P4.

2.3.2.2 4TPH-P4-OVA

The calibration curve of 4TPH-P4-OVA (see Figure 2.7 for structure) with rat monoclonal Anti-P4 has been established previously, and indicated that the responses are directly proportional the antibody concentrations.[31] The study also showed that increasing the linker length between the progesterone molecule and OVA, the sensitivity of the sensor surface increased.

With 20 µg/mL of antibody, the response was 145.3 RU on the 4TPH-P4-OVA sensor surface (Figure 2.13), whereas for the shorter linker 4TP-P4-OVA (discussed in section 2.3.2.1) the response was 87.6 RU. As mentioned in the previous section, the desired response for an assay should be approximately 200 RU, hence 4TPH-P4-OVA is more sensitive compared to the shorter linker ligand (4TP-P4-OVA). The extension of the linker size to 5 carbons in 4TPH-P4-OVA results in an increase in the surface response by 57.7 RU. This indicated that 4TPH-P4-OVA is more suitable for assay development than 4TP-P4-OVA.

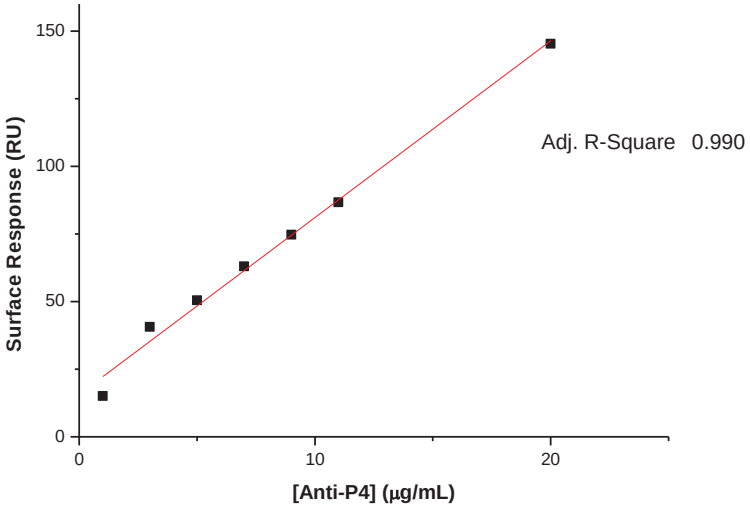

Figure 2.13 Binding curve of 4TPH-P4-OVA with rat monoclonal Anti-P4.

2.3.2.3 P4-PEG-OVA

It is established that as the linker size between the P4 molecule and OVA increases, the sensitivity of the surface response will increase. The newly synthesised P4 derivative P4-PEG-OVA (see Figure 2.8 for the structure) has a longer linker than the previous studied P4 derivatives.[31] The plot of surface responses versus antibody concentrations showed that the relationship is still directly proportional (Figure 2.14), but trailed off after 10 μg/mL. P4-PEG-OVA generated a high surface response, hence it is suitable for assay development.

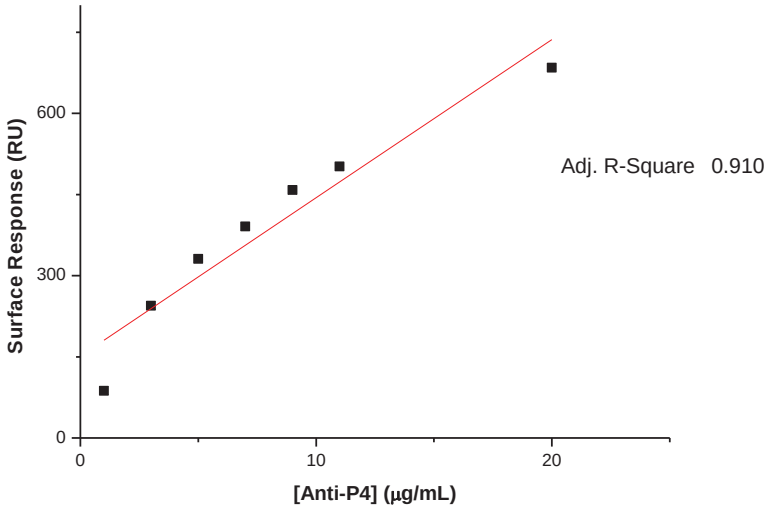

Figure 2.14 Binding curve of Anti-P4 on a P4-PEG-OVA sensor chip.

2.3.2.4 Comparison of binding performance between P4-linkers

The binding performances for P4 derivatives clearly indicated that the binding sensitivity is enhanced with increasing length of linker between the P4 molecule and OVA. The progesterone molecule is linked to the large protein (OVA) via different lengths of linker which is directly involved in the antibody binding site. Hence the effect of the length of the linker on antibody performance is clearly noticeable and the magnitude of the enhancement has not been observed in previous studies in the literature.[35]

With 20 µg/mL of the rat antibody solution, the response of 4TP-P4-OVA was 87.6 RU whereas with 4TPH-P4-OVA it was 145.3 RU, which was a 65.5% increase in surface response. P4-PEG-OVA had a response of 684.5 RU with 20 µg/mL of antibody which clearly demonstrated that with a long linker between the P4 molecule and the protein, the binding performance significantly increased (3.7 times higher than 4TPH-P4-OVA, Figure 2.15). Hence P4-PEG-OVA would be the desired conjugate to use for our sensor development.

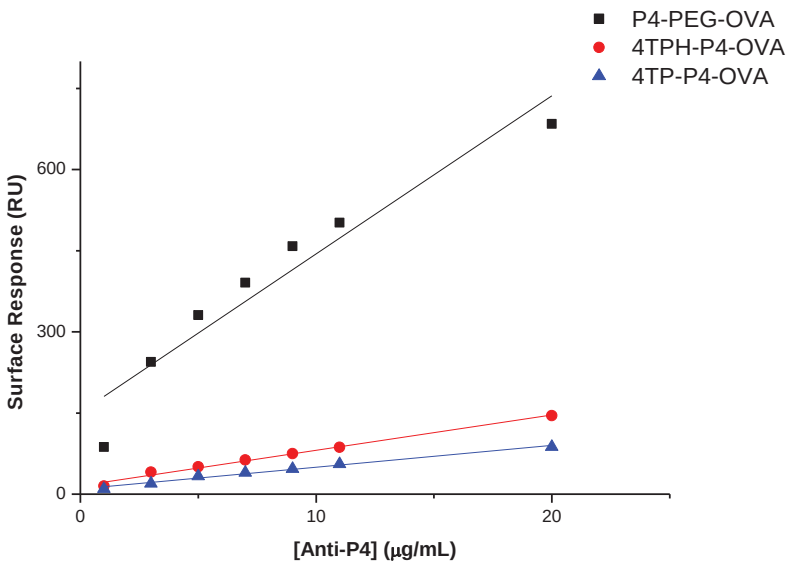

Figure 2.15 Comparison of binding curves for P4 derivatives.

2.3.3 Binding performance with monoclonal mouse Anti-P4 (Serotech)

The effect of linker length between P4 molecule and OVA has been clearly demonstrated from the rat monoclonal Anti-P4 in section 2.3.2.4. Commercially available mouse monoclonal Anti-P4 (Serotech, 1 mg/mL) was also used for binding performance studies (see Appendix A.2.3.2.2 for details) and then the results compared with those from the rat monoclonal Anti-P4.

2.3.3.1 Binding performance stability on the 4TP-P4-OVA sensor

It was originally established that the binding performance of mouse Anti-P4 varied approximately 17% from day to day (Figure 2.16). In order to determine the stability of mouse Anti-P4, the same stock mouse Anti-P4 was used in a binding study on the 4TP-P4-OVA sensor surface six months after it was first tested (Figure 2.17). By repeating the experiment 3 times the stability of the mouse Anti-P4 was verified and the results showed that the response of mouse Anti-P4 does vary slightly over time.

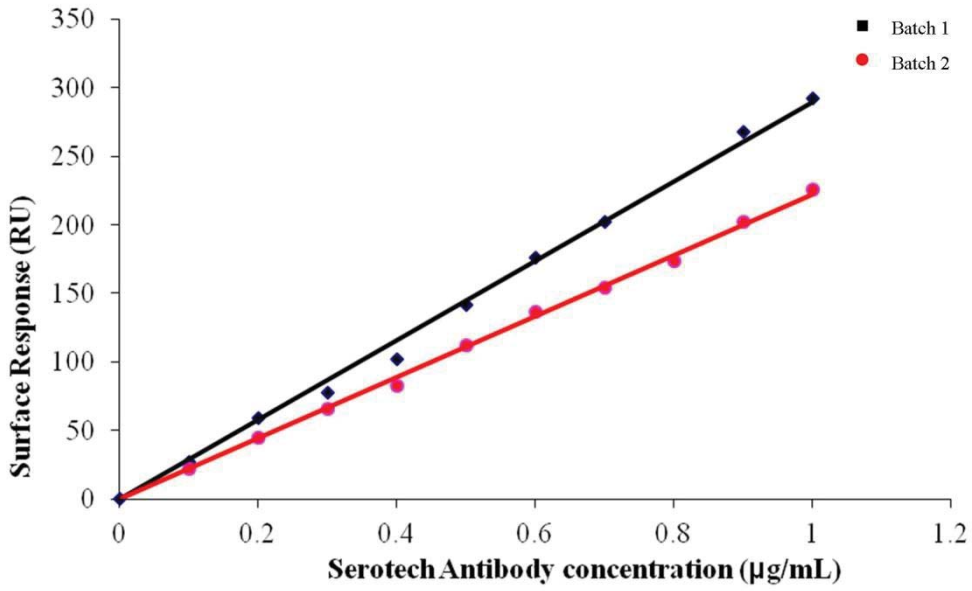

Figure 2.16 Mouse Anti-P4 surface performance varied on two different days (Batch 1 and Batch 2) with the same sensor surface (4TP-P4-OVA), but it is a significantly more sensitive antibody compared with rat Anti-P4.

The assays used a low concentration of mouse anti progesterone, the variation in surface response is most likely due to the low concentration rather than non specific binding since the monoclonal antibody is highly specific to the binding partner (the antigen).

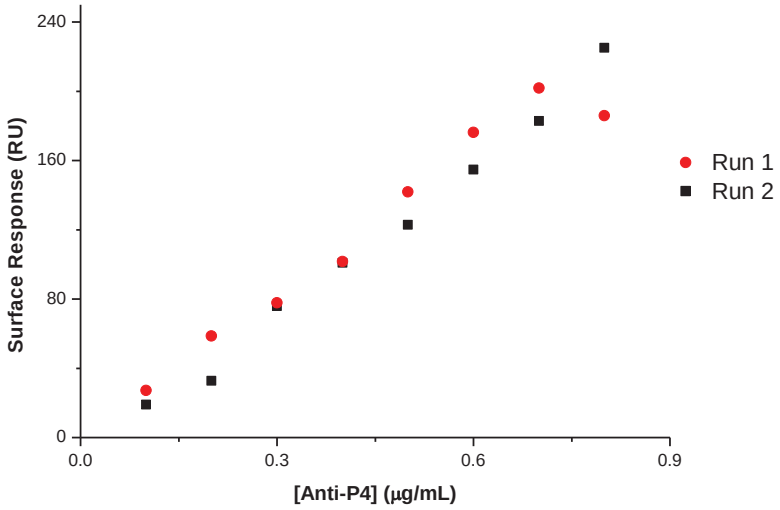

Figure 2.17 Binding performance of mouse Anti-P4 with Run 1 and Run 2 performed 6 months apart. The surface response varied over time, but still gave a relative linear response.

2.3.3.2 Comments about mouse and rat Anti-P4 binding to a 4TP-P4-OVA surface

The binding response for the mouse Anti-P4 with 4TP-P4-OVA surface is relatively high compared with rat Anti-P4 to the same sensor surface. The surface response to mouse Anti-P4 was 225.1 RU with 0.8 µg/mL (Figure 2.18), whereas with rat Anti-P4 it was 9.7 RU (see section 2.3.2.1) with 1.0 µg/mL. The surface response of mouse Anti-P4 was reasonably linear and much higher than the rat Anti-P4.

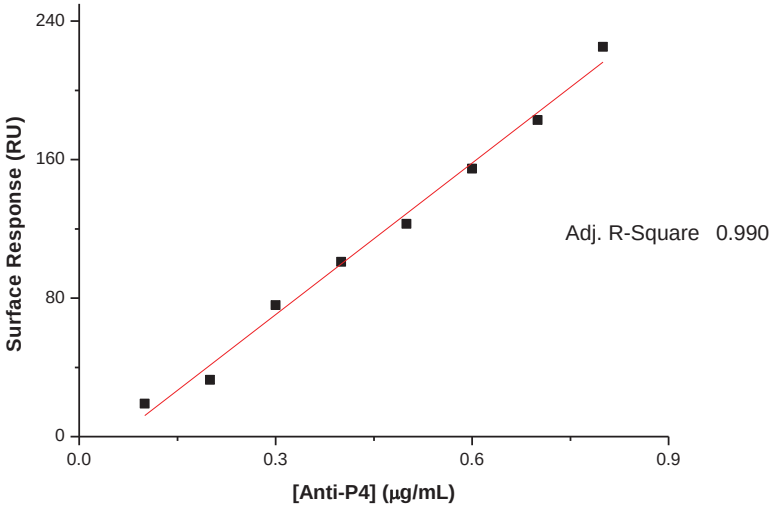

Figure 2.18 Binding curve of 4TP-P4-OVA with mouse Anti-P4.

2.3.3.3 Comments about mouse and rat Anti-P4 binding to a 4TPH-P4-OVA surface

The 4TPH-P4-OVA sensor surface generated 236.0 RU (Figure 2.19) with 0.8 µg/mL of mouse Anti-P4 which is slightly higher than the 4TP-P4-OVA sensor surface with the same mouse Anti-P4 concentration. However, the surface response was significantly higher compared with the surface response from rat Anti-P4 at 1 µg/mL (15.1 RU).

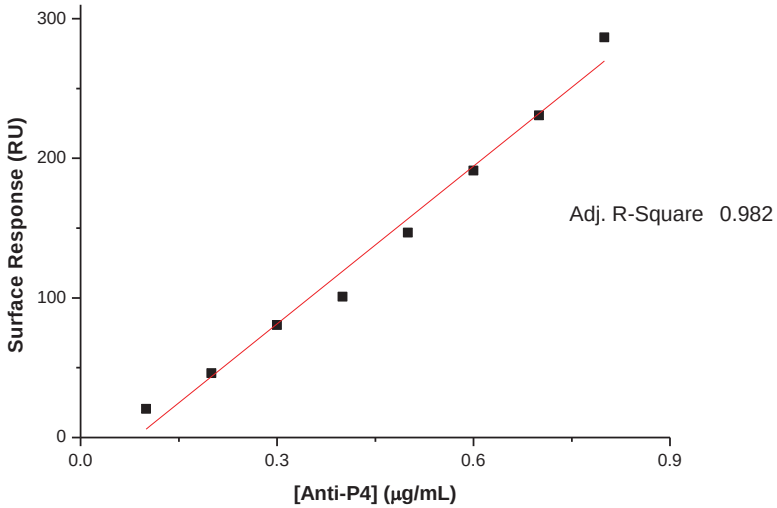

Figure 2.19 Binding curve of 4TPH-P4-OVA with mouse Anti-P4.

2.3.3.4 Comments about mouse and rat Anti-P4 binding to a P4-PEG-OVA surface

The P4-PEG-OVA sensor surface is the most sensitive sensor surface for Anti-P4 binding performance (both rat Anti-P4 and mouse Anti-P4). The plotted surface response versus mouse Anti-P4 concentration showed a relative linear relationship (Figure 2.20). With 0.1 μg/mL of mouse Anti-P4 generated 45.7 RU, which was significantly higher than 4TP-P4-OVA (19.0 RU) and 4TPH-P4-OVA (20.5 RU).

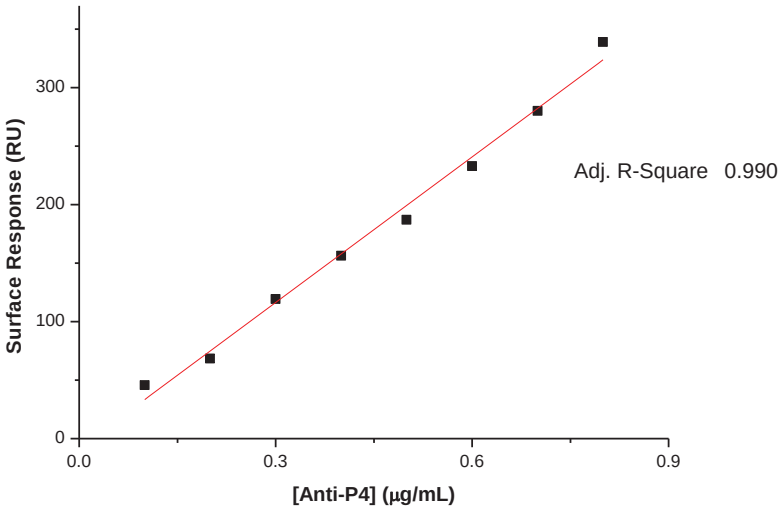

Figure 2.20 Binding curve of P4-PEG-OVA with mouse Anti-P4.

From the binding studies for both Anti-P4, it is clearly shown that the mouse Anti-P4 is more desirable for the assay development because it is more sensitive and readily available. Therefore, mouse Anti-P4 was used for the inhibition assay development.

2.3.3.5 Comparison of binding performance between P4 linkers

The surface responses from mouse Anti-P4 followed a similar trend compared with the rat Anti-P4. The 4TP-P4-OVA surface generated the lowest surface response compared with the 4TPH-P4-OVA and P4-PEG-OVA surfaces. The effect of linker length on surface response was still significant (Figure 2.21).

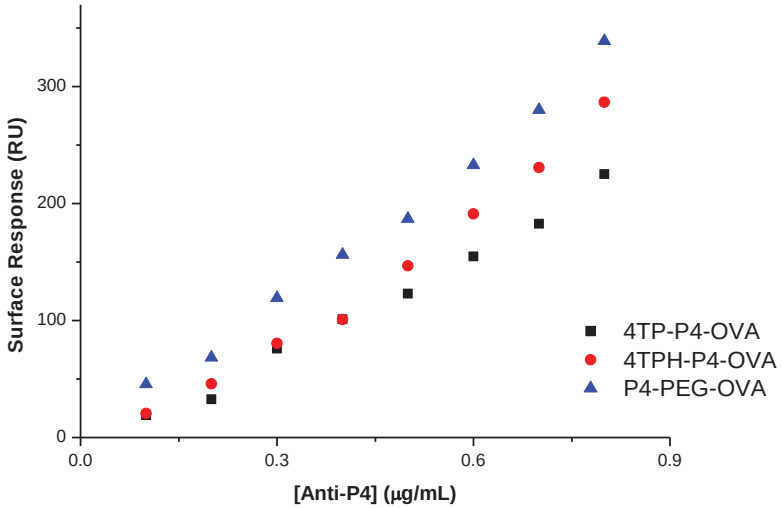

Figure 2.21 Mouse Anti-P4 binding curves of 4TP-P4-OVA, 4TPH-P4-OVA, P4-PEG-OVA conjugates.

It has been established for each Anti-P4, that as the concentration of Anti-P4 increased, the surface response increased. The relationship between the surface response and the Anti-P4 concentration (0.1 to 0.9 µg/mL) is linear.

Since mouse Anti-P4 is as sensitive as the rat Anti-P4, mouse Anti-P4 (Serotech) was used to carry out the inhibition assay scouting.

2.3.4 Inhibition assay development with mouse Anti-P4 (Serotech)

The observed binding curve for each P4 derivative was used to carry out a P4 assay development. The P4 standard curve for each P4 derivative was established using the inhibition assay method (section 2.2). The sensitivity of each sensor surface was investigated and the most sensitive surface to carry on sample analysis was determined.

The surface responses were plotted versus the standard concentrations and the dose response curve (sigmoidal fitting) was fitted. A sigmoidal fitting is commonly used to analyse dose response relationship, competitive binding assays (the competition of a ligand for receptor binding).

The half maximal effective concentration (EC50), the lowest concentration that can be distinguished from the background noise (EC20) and the highest concentration that can be distinguished from the background noise (EC80) were determined from the standard curve. The EC50 of the standard curve was used to monitor the sensitivity and indicate the most accurate working area of an assay.

The P4 inhibition assay was performed using a series of P4 standard solutions (prepared in HBS-EP$^+$ buffer). Each P4 standard solution was incubated with Anti-P4 solution (1.2 µg/mL, Serotech) at room temperature before the injection. The incubated solution was injected over each P4 sensor surface at 30 µL/min for 120 s (see Appendix A.2.3.3 for details).

2.3.4.1 Assay development with 4TP-P4-OVA

The 4TP-P4-OVA sensor surface was used as a reference sensor chip to investigate the enhancement in surface response of extending the length of the linker between the P4 molecule and OVA. The working range of a sensor surface is obtained from the EC80 and EC20 values from the standard curve (Figure 2.22). The 4TP-P4-OVA sensor surface had a working range of 0.27-2.38 ng/mL with an EC50 of 0.80 ng/mL.

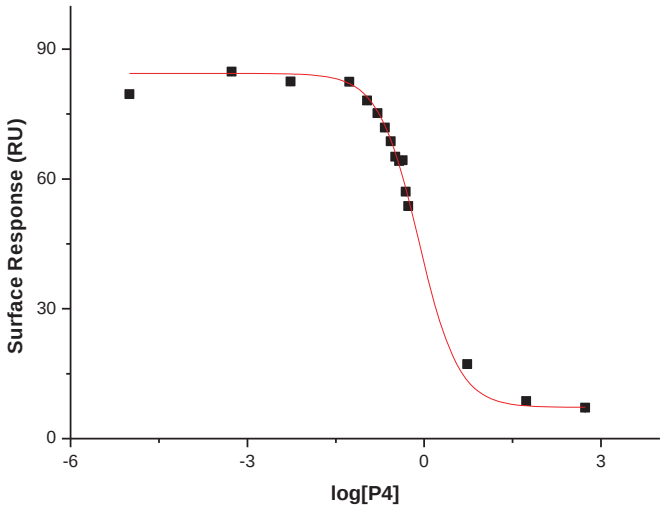

Figure 2.22 4TP-P4-OVA standard curve for P4 concentration extrapolation has a working range of 0.27-2.38 ng/mL.

2.3.4.2 Assay development with 4TPH-P4-OVA

The sensor surface of 4TPH-P4-OVA has an extended linker between the P4 molecule and OVA. It has a working range of 0.3-0.742 ng/mL with an EC50 of 0.530 ng/mL (Figure 2.23). The surface is more sensitive than the shorter linked surface 4TP-P4-OVA. However, the slope of the standard curve became steeper, thus the detection range has been decreased.

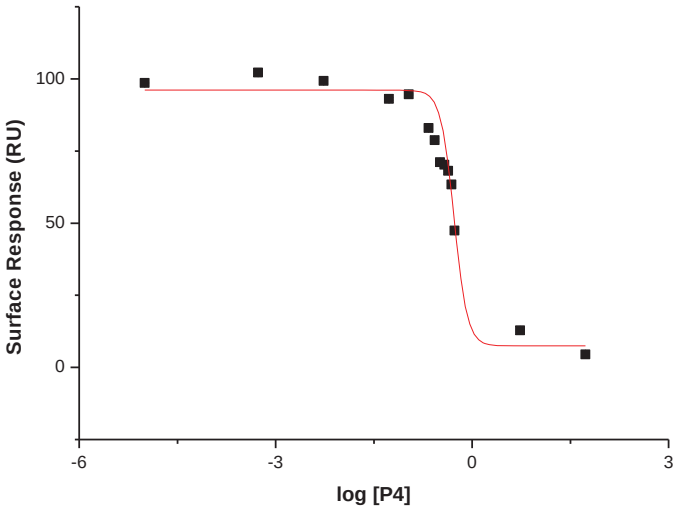

Figure 2.23 The 4TPH-P4-OVA standard curve for P4. The working range has been calculated to be 0.3-0.742 ng/mL.

2.3.4.3 P4 standard curve scouting on the P4-PEG-OVA chip

The P4-PEG-OVA chip was used to investigate the range of a P4 standard curve. The P4 standard curve scouting was carried out to determine the concentrations of P4 standard solutions as well as the slope of the standard curve (Figure 2.24). A series of standard progesterone solutions was prepared in HBS-EP$^+$ buffer, at concentrations ranging from 0 to 5060 ng/mL. The established binding curve was used to assess the concentration required for standard curve scouting. Each sample (200 µL) was mixed with an equal volume of Anti-P4 solution (Serotech, 1.2 µg/mL in HBS-EP$^+$ buffer). The solutions were individually injected over P4-PEG-OVA at 30 µL/min (2 min, 60 µL). The biosensor surface was regenerated after each run using NaOH (50 mM) at 5 µL/min (30 s).

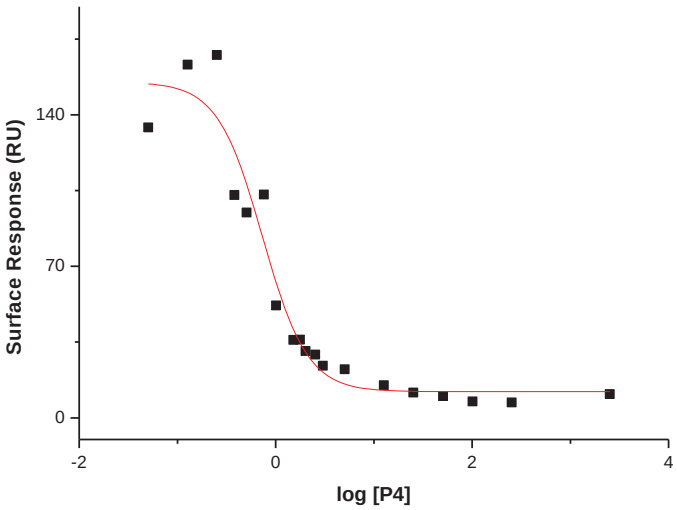

Figure 2.24 A P4 standard curve scouting on a P4-PEG-OVA sensor surface.

After completion of the scouting of the P4 standard curve, the P4 standard solutions were established and prepared to obtain the P4 standard curve on the P4-PEG-OVA sensor surface.

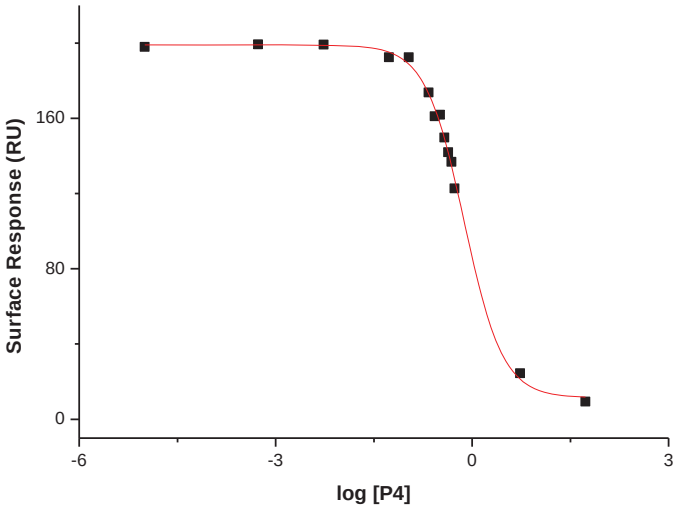

Figure 2.25 A P4-PEG-OVA standard curve for P4 concentration extrapolation has a working range of 0.294 to 1.942 ng/mL.

The P4-PEG-OVA sensor surface has an EC50 of 0.7561 ng/mL (Figure 2.25). After each inhibition assay, the sensor surface required complete surface regeneration to optimise the binding stability.

The long hydrophilic linker is prone to extend out to the solution as the assay is performed and is also suspected of being folded after a high concentration of P4 solution was injected. The surface does regenerate after 20 injections of buffer and remains stable.

The P4 standard curves for all three linkers were established with mouse Anti-P4 (Figure 2.26), and it was clear that P4-PEG-OVA gave a greater surface response range (from 0 to approximate 200 RU) when the same P4 standard solutions were used.

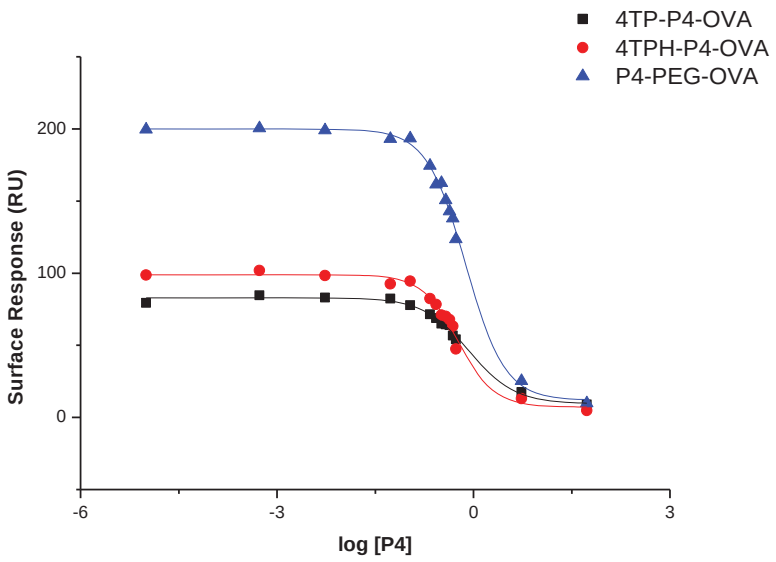

Figure 2.26 Mouse Anti-P4 standard curves of 4TP-P4-OVA, 4TPH-P4-OVA, and P4-PEG-OVA conjugates.

The lower EC50 value is desirable for the assay development. Hence, theoretically 4TPH-P4-OVA would be a better surface than P4-PEG-OVA. However, the 4TPH-P4-OVA also has a very low EC20 value (0.73 ng/mL), hence it was not suitable to compare with the other two linkers (Table 2.1). Although the P4-PEG-OVA surface has a lower EC20 value compared with the 4TP-P4-OVA surface, it has a lower EC50 value. Hence the P4-PEG-OVA linker surface was more desirable compared to the two short linker surface and was used for P4 detection in serum and milk samples.

Table 2.1

	4TP-P4-OVA	4TPH-P4-OVA	P4-PEG-OVA
EC80 (ng/mL)	0.27	0.38	0.29
EC50 (ng/mL)	0.80	0.53	0.76
EC20 (ng/mL)	2.38	0.73	1.94

2.4 Determination of P4 in bovine serum samples

All blood and milk samples (from cow 1, 2, 3 and 4; see Appendix A.2.1) were collected every 2 days for a period of 8 weeks. The details for sample collection are described in Appendix A.2.1.1 and A.2.1.2. The blood samples were spun down at 3000 rpm, and the liquid serum samples were used for analysis. The samples were independently analysed by New Zealand Veterinary Pathology Limited (NZVP) as well as the P4-PEG-OVA SPR assay.

2.4.1 Non-specific binding of P4 to corticosteroid binding globulin

Steroid hormones such as progesterone, cortisol and other corticosteroids are bound by transcortin, which is also known as corticosteroid binding globulin (CBG).

It is important to quantitatively displace the steroid binding protein before carrying out a direct assay and there are a few commonly used methods including: (i) by protein-binding agents 8-anilino-1-naphthalene sulphonic acid (ANS) and salicylate, (ii) by proteolytic enzymes, (iii) by low pH, high concentration of urea or by heat treatment. However, some of the sample treatment processes can potentially reduce the specific binding of the antibody.

Therefore, the serum samples were tested on the P4-PEG-OVA sensor surface to determine the level of non specific binding caused by the CBG in the serum. The serum samples were diluted with dilution factor of 1:25, 1:50, 1:100 and 1:200, and then injected over the P4-PEG-OVA sensor surface. With the 1:25 dilution of serum, the surface generated 142.1, 80.2 and 85.5 RU for each sample. As the dilution factor increased the surface response decreased and with the1:200 dilution the surface responses were 34.1, 23.2 and 21.8 RU (Figure 2.27). Therefore, the non specific binding from the serum sample to the P4-PEG-OVA is relatively high, hence sample pre-treatment is required for SPR analysis.

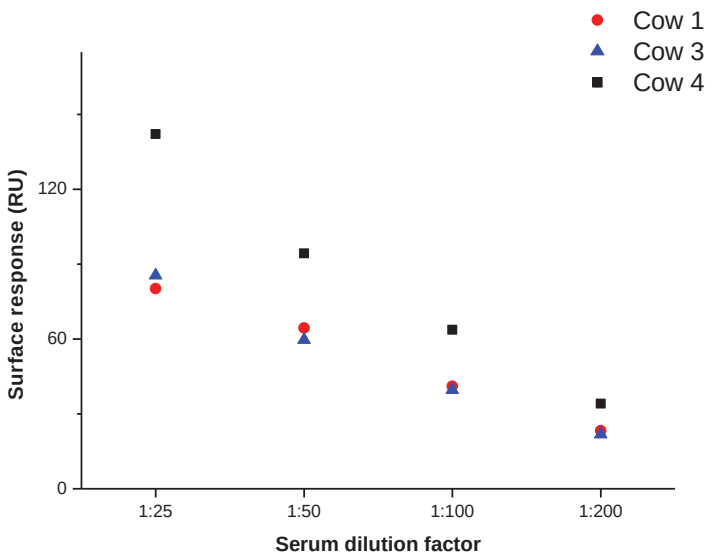

Figure 2.27 Bovine serum binding curve on a P4-PEG-OVA sensor surface.

2.4.2 Free P4 analysis

Approximately 2 to 10% of the total P4 in serum is unbound or free, which is in equilibrium with progesterone bound to the CBG.[36-39] A centrifugal filter with 3K molecular weight cut off, allowed the separation of free P4 from protein bound P4 into two fractions.

The filtered samples were mixed with mouse Anti-P4 (1.2 µg/mL) and then injected over the P4-PEG-OVA surface.

The results showed that (Figure 2.28) the filtering process reduced the non specific binding of CBG, but the concentrations of the free P4 in serum samples are fairly low and are at the limit of the detection range. Hence, the sample will require alternative treatment to remove CBG to avoid non specific binding of the sensor surface.

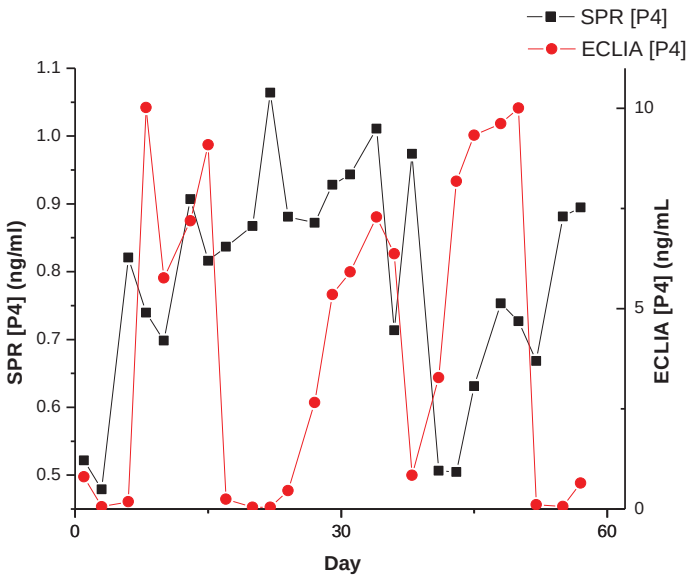

Figure 2.28 The SPR analysed P4 concentration in serum (free P4) and the ECLIA analysed P4 concentrations in serum samples were overlapped to monitor the P4 concentrations over 2 cycles.

-

2.4.3 Preparation of serum sample: solvent extraction

The P4 was extracted from the serum samples by performing simple solvent extraction steps. The carbonate-bicarbonate buffer with pH 10.4 was added to the serum samples to release bound progesterone.[40] After the addition of carbonate-bicarbonate buffer, the samples were shaken at room temperature for 18 hr at 200 rpm. Different organic solvents (15 mL each) were used to test the level of P4 extraction including, hexane, ethyl acetate and tetrahydrofuran (THF). Ethyl acetate has been commonly used for steroid extraction from biological material, while hexane has also been used for the progesterone extraction process.[40,41] For comparison purposes the heterocyclic THF was also used and a blank sample was prepared using the carbonate-bicarbonate buffer.

The mixtures were shaken at 300 rpm for 1 hour at room temperature, and then the samples were mixed with mouse Anti-P4 (1.2 µg/mL) and injected over a P4-PEG-OVA sensor surface. The resulting surface responses were compared to determine which solvent had the highest level of progesterone extraction.

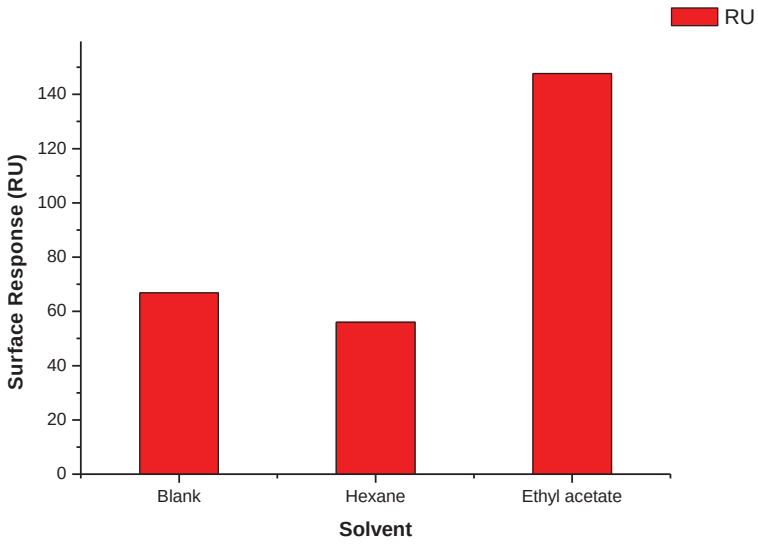

Figure 2.29 The surface responses of blank extraction, hexane extraction and ethyl acetate extraction of serum samples. The surface response is inverse proportional to the concentration of P4 in the sample. Hence, the ethyl acetate extracted sample presented the highest response compared with the blank (buffer) and hexane extracted samples.

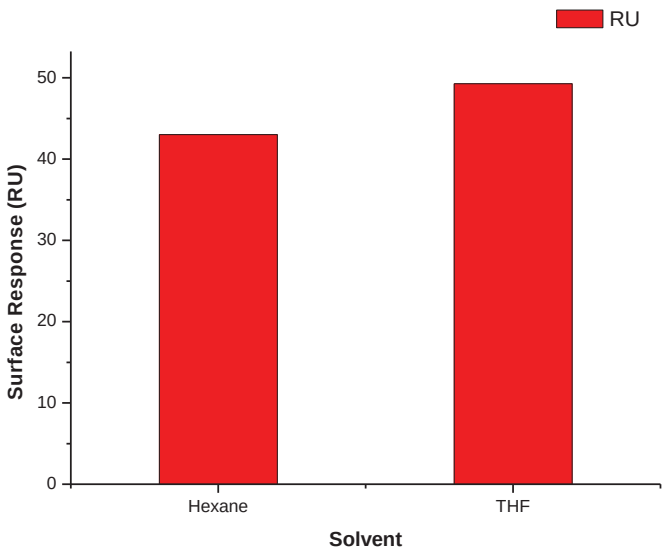

Figure 2.30 Surface response for a hexane extracted serum sample and a THF extracted serum sample.

The release of bound P4 is the crucial step in the extraction and it is understood that this is influenced by the carbonate-bicarbonate buffer and the extended mixing time. The blank sample generated a surface response of 66.8 RU, which was slightly higher than the hexane extracted sample (56.0 RU, Figure 2.29) followed by ethyl acetate (147.7 RU) which had the lowest extraction level (Figure 2.29). The THF extracted sample presented a slightly higher surface response (49.3 RU, Figure 2.30) than the hexane extracted sample (43.0 RU, Figure 2.30). Hence, it is clear that hexane had the highest extraction level for extracting progesterone from the serum samples. Therefore all samples were treated with carbonate-bicarbonate buffer to release the bound progesterone followed by hexane extraction.

2.4.4 Determination of P4 in bovine serum samples

The extracted serum samples were filtered through Amicon Ultra centrifugal filter (3K, Millipore) at 13.4 K rpm for 30 min. Both top and bottom fractions (the centrifugal filter separated the extracted sample into two fractions, the bottom fraction passed through the filter and the top fraction remained above the filter) were tested using mouse Anti-P4. Extracted serum samples were mixed with mouse Anti-P4 (1.2 µg/mL) and injected over the P4-PEG-OVA sensor surface. The P4 standard curve was used to extrapolate the P4 concentration in each sample and the concentration was plotted versus sampling day (Figure 2.31).

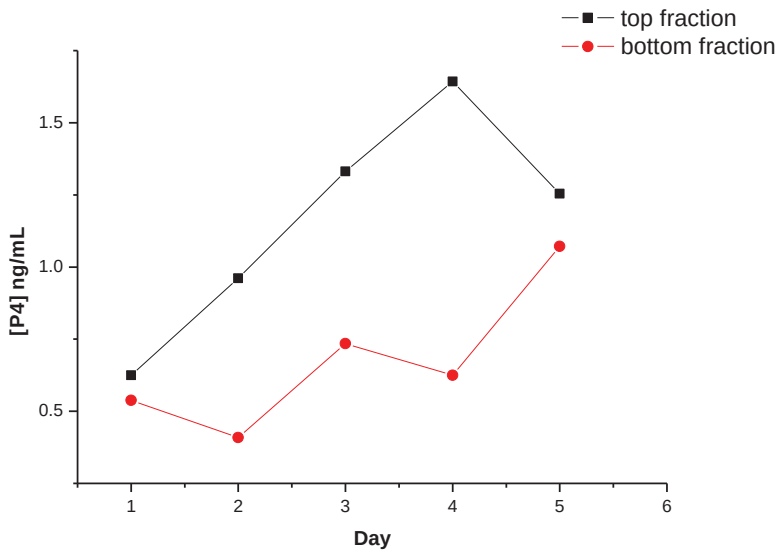

Figure 2.31 The P4 concentration of top (black) and bottom (red) fraction of the extracted and filtered serum samples.

The P4 concentrations from the extracted serum were approximately 1/3 of the actual P4 concentration (ECLIA analysis). It is suggested that there is a loss of P4 during the solvent extraction process as well as an incomplete extraction of P4 from the serum samples. The P4 should theoretically be completely extracted from the serum sample including the steroid protein bound P4. However, it is possible that 18 hrs of shaking the samples with carbonate-bicarbonate buffer was not sufficient to completely release the bound P4. After the addition of solvent, the sample was only shaken for 1 hr and this could also contribute to incomplete extraction. However, the level of extraction was consistent for all samples (approximately 1/3 of the P4 in serum samples was extracted and detected).

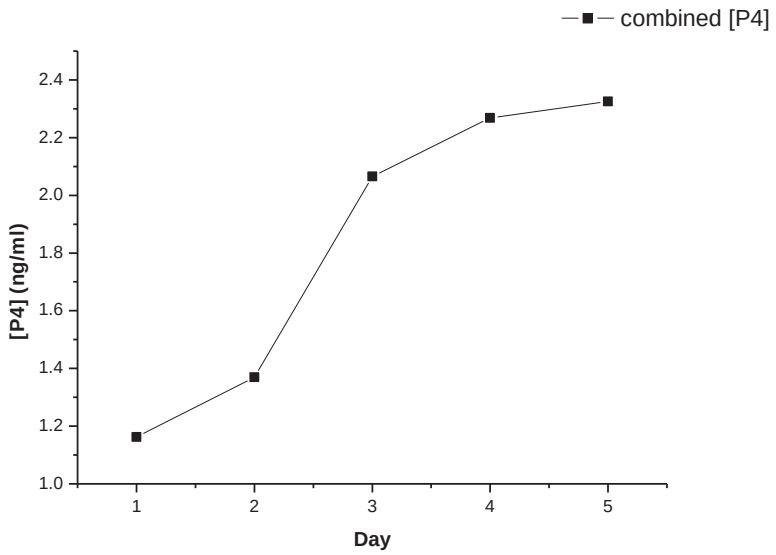

Figure 2.32 The combined P4 concentration from extracted serum samples.

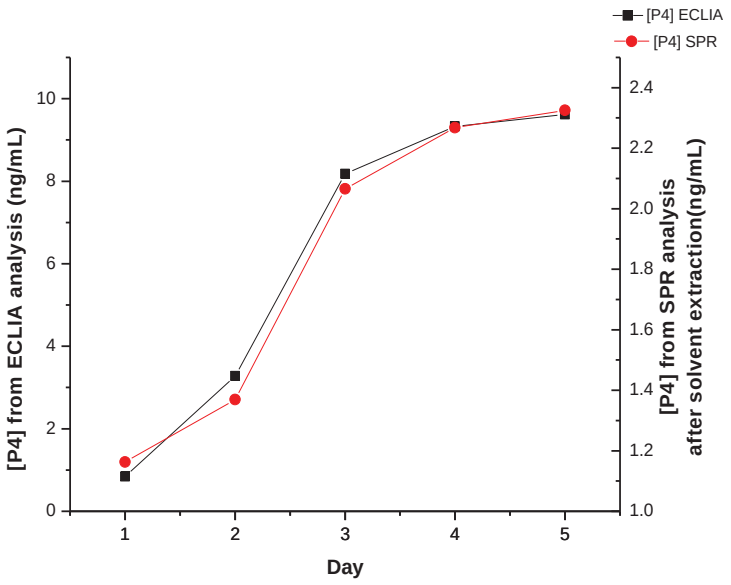

Figure 2.33 The independent analysis results overlapped with the SPR analysis results. The plot indicated that the SPR P4 level and the independent analysed P4 level have the same trend.

Nevertheless, the extrapolated P4 concentrations were still low compared with the independent P4 analysed results (ECLIA). It is clear that the trend of the P4 concentration levels (both fractions combined, Figure 2.32) for the solvent extracted samples matched the trend of the independent P4 analysed results (Figure 2.33).

The P4 inhibition assay was used to determine the level of P4 present in the serum sample. Hence the stability of a standard curve from the inhibition assay is very important. The slight variation of the standard curve affects the extrapolated P4 concentration significantly when the working range is narrow.

2.5 Determination of P4 in bovine milk samples

P4 is a hydrophobic and very fat soluble steroid, hence it is important to take consideration of the fat present in milk while analysing samples.

A simple protein precipitation step was carried out after homogenisation of the milk samples by sonication.[42] The milk samples were treated with acetonitrile to precipitate the protein in the milk sample followed by sonication and centrifugation of the mixture and removal of the precipitate. The samples were then freeze dried and reconstituted in SPR buffer. The concentration of P4 for each sample was extrapolated from the P4 standard curve and multiplied by the dilution factor (2). The extrapolated concentrations were plotted against the sample collection date then compared with the independent analysed result (ELISA analysis). For the accuracy of the assay development, three sets of milk samples from cow 1, 2, and 3 (see Appendix A.2.1,) were analysed and compared with ELISA analysed data.

2.5.1 Bovine milk 1

The extrapolated P4 concentration for bovine milk 1 was plotted versus the sample collection date. The plot clearly showed the gradual increase in P4 concentration, then the peak of the P4 cycle followed by the drop of P4 concentration (Figure 2.34). The assay clearly distinguished the peak of the P4 cycle with [P4] at 57.6 ng/mL and 0.60 ng/mL for the lowest [P4] of the cycle.

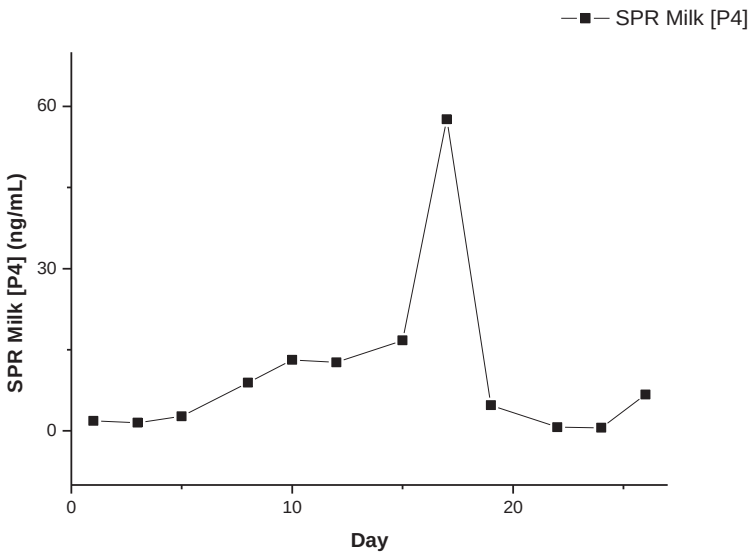

Figure 2.34 [P4] in bovine milk 1 analysed by SPR.

The SPR data were overlapped with ELISA analysed data (Figure 2.35), and it is clear that SPR assay could distinguish the peak of the cycle and the low [P4] in the cycle relatively well.

The [P4] data for the SPR analyses are approximately 4 times higher than from the ELISA assay, and the trend showed the consistency of P4 extraction from the raw samples.

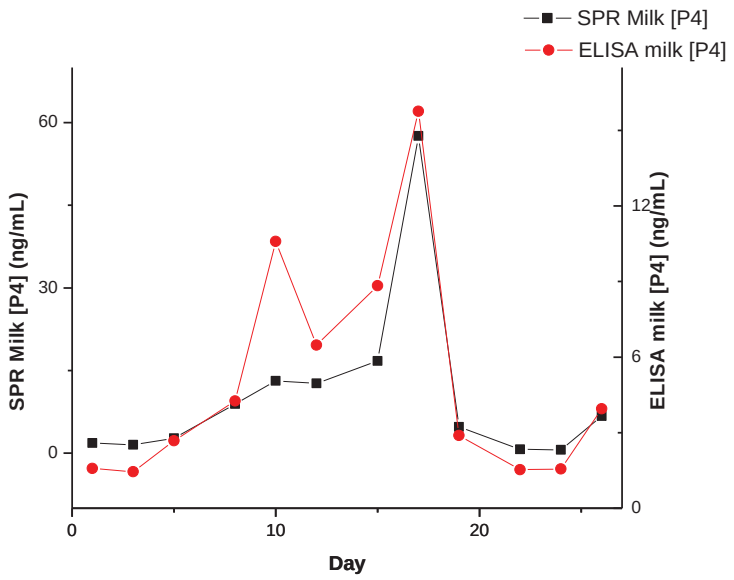

Figure 2.35 Overlapped spectra of SPR analysed milk 1 [P4] and ELISA analysed milk 1 [P4].

2.5.2 Bovine milk 2

The same assay and extrapolated method used before in 2.5.1 was repeated for milk sample 2. The two missing data points were due to the low surface response (Figure 2.36). The overlapped spectrum (Figure 2.37) showed that the general trend of the P4 cycle from SPR analysis fits the trend of the ELISA analysed [P4]. The assay was able to differentiate the peak and the low point of the P4 cycle.

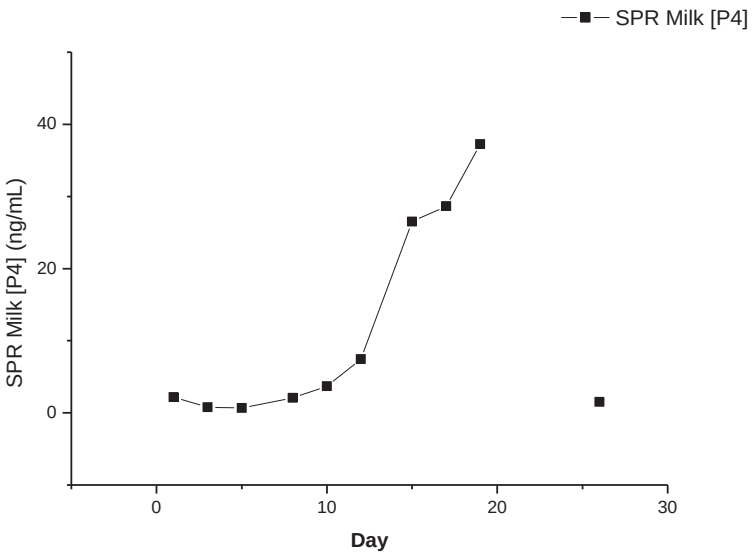

Figure 2.36 [P4] in bovine milk 2 analysed by SPR.

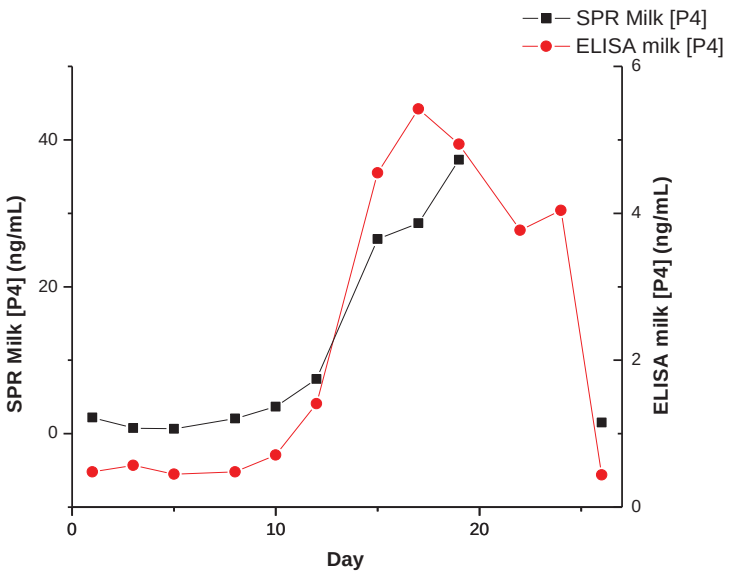

Figure 2.37 Spectra of SPR analysed milk 2 [P4] and ELISA analysed milk 2 [P4].

2.5.3 Bovine milk 3

Bovine milk 3 was also used for testing the SPR assay. The [P4] of each milk sample was extrapolated from the P4 standard curve and the extrapolated [P4] was plotted versus its sample collection data. One of the data points was out of the standard curve detection range (the slope of the standard curve), hence the missing data point (Figure 2.38). The [P4] at the peak of the P4 cycle was 112.5 ng/mL and 2.9 ng/mL at the lowest.

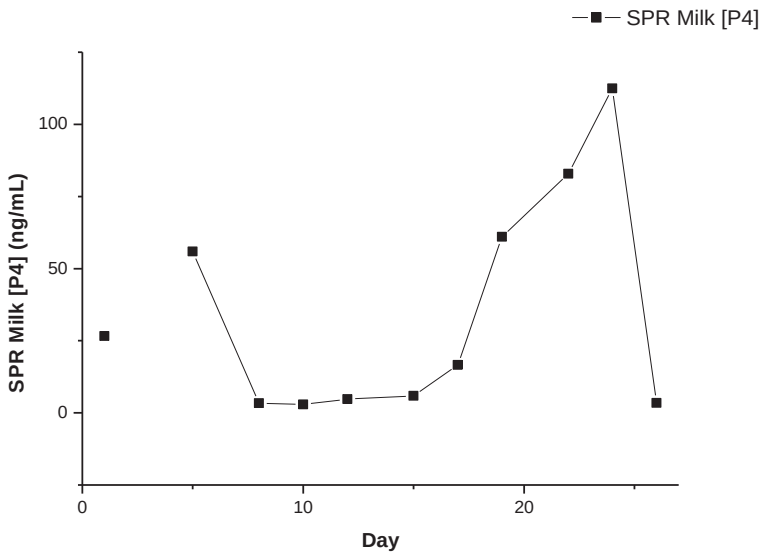

Figure 2.38 [P4] in bovine milk 3 analysed by SPR.

The overlapped spectra of SPR analysed data and the ELISA analysed data showed very similar trends of the P4 cycle (Figure 2.39). The [P4] from SPR data was approximately 16 times higher than the ELISA analysed data, but the trend of the cycle followed closely. It indicated that the extraction level and the analysed method were both consistent.

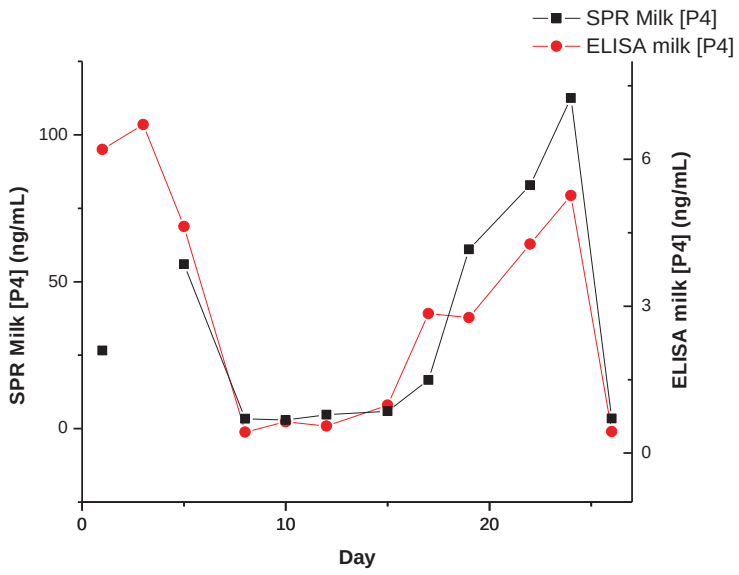

Figure 2.39 Spectra of SPR analysed milk 3 [P4] and ELISA analysed milk 3 [P4].

2.6 Conclusions

The studies showed that the linker length between the P4 molecule and OVA is an important feature for a SPR based sensor. As the linker size increased, the surface response increased. Different antibodies also affect the performance of the surface responses. Hence, it is essential to optimise the antibody binding condition. The linker with the highest surface response, P4-PEG-OVA was chosen to perform serum and milk sample analysis.

A P4-PEG-OVA sensor surface with mouse Anti-P4 antibodies improved the sensitivity of serum and milk sample analysis. The SPR analysed data was compatible with the ECLIA and ELISA independent analysis and the P4 cycle of each of the three bovine milk samples showed a very similar trend and the extraction level was also consistent.

It is clear that the P4-PEG-OVA sensor surface enables a rapid, simple and reliable P4 analysis for both bovine serum and milk sample and increasing the length of the conjugate linker has proven to be a potentially useful strategy for future advancement in this field.

The SPR data were consistently higher than the ECLIA data and this was most likely due to non-specific binding from the samples.

References

(1) Liedberg, B.; Nylander, C.; Lunstrom, I. *Sensors and Actuators* **1983**, *4*, 299-304.

(2) Pockrand, I.; Swalen, J. D.; Gordon, J. G. I.; Philpott, M. R. *Surface Science* **1978**, *74*, 237-244.

(3) Swalen, J. D.; Gordon, J. G. I.; Philpott, M. R.; Brillante, A.; Pockrand, I.; Santo, R. *American Journal of Physics* **1980**, *48*, 669-672.

(4) Ahmad, A.; Ramakrishnan, A.; McLean, M. A.; Breau, A. P. *Biosensors & bioelectronics* **2003**, *18*, 399-404.

(5) Komolov, K. E.; Senin, I. I.; Philippov, P. P.; Koch, K. *Analytical Chemistry* **2006**, *78*, 1228-1234.

(6) Nordin, H.; Jungnelius, M.; Karlsson, R.; Karlsson, O. P. *Analytical Biochemistry* **2005**, *340*, 359-368.

(7) Wegner, G. J.; Wark, A. W.; Lee, H. J.; Codner, E.; Saeki, T.; Fang, S.; Corn, R. M. *Analytical Chemistry* **2004**, *76*, 5677-5684.

(8) Nygren-Babol, L.; Sternesjoe, A.; Jaegerstad, M.; Bjoerck, L. *Journal of Agricultural and Food Chemistry* **2005**, *53*, 5473-5478.

(9) Huber, W.; Perspicace, S.; Kohler, J.; Muller, F.; Schlatter, D. *Analytical biochemistry* **2004**, *333*, 280-288.

(10) Miura, N.; Ogata, K.; Sakai, G.; Uda, T.; Yamazoe, N. *Chemistry Letters* **1997**, 713-714.

(11) Yu, Q.; Chen, S.; Taylor, A.; Homola, J.; Hock, B.; Jiang, S. *Sensors and Actuators, B: Chemical* **2005**, *B107*.

(12) Kausaite-Minkstimiene, A.; Ramanaviciene, A.; Ramanavicius, A. *Analyst* **2009**, *134*, 2054-2057.

(13) Indyk, H. E.; Filonzi, E. L. *Journal of AOAC International* **2003**, *86*, 386-393.

(14) Vaisocherova, H.; Mrkvova, K.; Piliarik, M.; Jinoch, P.; Steinbachova, M.; Homola, J. *Biosensors & bioelectronics* **2007**, *22*, 1020-1026.

(15) Hsieh, H. V.; Pfeiffer, Z., A. ; Amiss, T. J.; Sherman, D. B.; Pitner, J. B. *Biosensors & bioelectronics* **2004**, *19*, 653-660.

(16) Mariotti, E.; Minunni, M.; Mascini, M. *Analytica Chimica Acta* **2002**, *453*, 165-172.

(17) Tobiska, P.; Homola, J. *Sensors and Actuators, B: Chemical* **2005**, *B107*, 162-169.

(18) Kretschmann, E.; Raether, H. *Zeitschrift fuer Naturforschung, Teil A: Astrophysik, Physik und Physikalische Chemie* **1968**, *23*, 2135-2136.

(19) *Handbook of Surface Plasmon Resonance*; 1 ed.; Schasfoort, R. B. M.; Tudos, A. J., Eds.; Royal Society of Chemistry: Cambridge, **2008**.

(20) Daghestani, H. N.; Day, B. W. *Sensors* **2010**, *10*, 9630-9646.

(21) *Real-time analysis of biomolecular interactions : applications of BIACORE* Nagata, K.; Handa, H., Eds.; Springer: Tokyo, **2000**.

(22) BIACORE *BIACORE Technology Handbook*; AB ed.; BIACORE, **1998**.

(23) BIACORE; AB ed.; General Electric Healthcare: 2008.

(24) Liu, M.; Ning, B.; Qu, L.; Peng, Y.; Dong, J.; Gao, N.; Liu, L.; Gao, Z. *Sensors and Actuators, B: Chemical* **2012**, *161*, 124-130.

(25) Stevens, R. C.; Soelberg, S. D.; Near, S.; Furlong, C. E. *Analytical Chemistry* **2008**, *80*, 6747-6751.

(26) Medina, M. B. *Journal of Rapid Methods and Automation in Microbiology* **2005**, *13*, 37-55.

(27) Chung, K.; Hwang, H.; Lee, K. *Journal of Industrial and Engineering Chemistry* **2010**, *16*.

(28) Achilleos, C.; Tailhardat, M.; Courtellemont, P.; Le Varlet, B.; Dupont, D. *Toxicology in Vitro* **2009**, *23*, 308-318.

(29) Haughey, S. A.; Campbell, K.; Yakes, B. J.; Prezioso, S. M.; DeGrasse, S. L.; Kawatsu, K.; Elliott, C. T. *Talanta* **2011**, *85*, 519-526.

(30) Fonfria, E. S.; Vilarino, N.; Campbell, K.; Elliott, C.; Haughey, S. A.; Ben-Gigirey, B.; Vieites, J. M.; Kawatsu, K.; Botana, L. M. *Analytical Chemistry* **2007**, *79*, 6303-6311.

(31) Wu, Y. Q.; Mitchell, J.; Cook, C.; Main, L. *Steroids* **2002**, *67*, 565-572.

(32) Hosoda, H.; Miyairi, S.; Nambara, T. *Chemical & Pharmaceutical Bulletin* **1980**, *28*, 1294.

(33) Yoshida, H.; Nakai, S.; Nimbari, F.; Yoshimoto, K.; Nishimura, T. *Steroids* **1989**, *53*, 727-738.

(34) Hosoda, H.; Ushioda, K.; Shioya, H.; Nambara, T. *Chemical & Pharmaceutical Bulletin* **1982**, *30*, 202-205.

(35) Bieniarz, C.; Husain, M.; Barnes, G.; King, C. A.; Welch, C. J. *Bioconjugate Chemistry* **1996**, *7*, 88-95.

(36) *Steroid Analysis*; 2 ed.; Makin, H. L. J.; Gower, D. B., Eds.; Springer Netherlands: London, **2010**.

(37) van Wyk, V.; van Aarde, R. J.; Louw, A. I. *Comparative Biochemistry and Physiology, Part A: Molecular & Integrative Physiology* **1994**, *108A*, 265-271.

(38) Hammond, G. L.; Nisker, J. A.; Jones, L. A.; Siiteri, P. K. *Journal of Biological Chemistry* **1980**, *255*, 5023-5026.

(39) Shintani, K.; Yoshida, N.; Sekiba, K. *Endocrinologia Japonica* **1987**, *34*, 221-230.

(40) Lee, H.; Chang, J.; Lee, G. *Analytical and Bioanalytical Chemistry* **2010**, *396*, 1713-1719.

(41) Supko, J. G.; Phillips, L. R. *Journal of Chromatography, B: Biomedical Applications* **1995**, *666*, 157-167.

(42) Beckonert, O.; Keun, H. C.; Ebbels, T. M. D.; Bundy, J.; Holmes, E.; Lindon, J. C.; Nicholson, J. K. *Nature Protocols* **2007**, *2*, 2692-2703.

Chapter 3

Lateral flow immunoassay for progesterone sensing

3.1 Introduction

A rapid membrane-based assay which comprises an analyte and antibody conjugate being chromatographed on a porous membrane can be referred to as a lateral flow device (LFD). The LFDs can be used as a qualitative or semi-quantitative detection system for many analytes. The basic concept of LFDs was introduced in the 1960s, and the first lateral flow immunoassay (LFIA) was developed based from a latex agglutination assay in 1956.[1] LFIA is an immunoassay adapted to operate along a single axis test strip format. The principle of LFIA is the same as ELISA where the antibody detects the analyte, after labelling to generate a visible signal.

The LFIA technology has been refined and established in the early 1980s and the development of a solid phase rapid test was driven by the need for a human pregnancy test. In 1988, the first commercial application of LFIA was Unipath's Clearview pregnancy test.[2]

The first application of a LFIA system used colloidal gold particles and this was in 1980,[3] since such gold nanoparticles are useful for conjugation to antibodies.[4,5] Gold nanoparticles (AuNPs) are readily available, highly visible, and conjugate to most immunoglobulins easily.[6-9] The sizes of AuNP commonly used for LFIA are from 20 to 40 nm. The AuNP conjugates produce stable labels for LFIAs, and they have become one of the commonly used signal generators (labels).[10-12]

There are many advantages of LFIAs including the portability, stability, speed, flexibility, and ease of use. The major advantages are that the technique could be performed with minimum training, and no expensive apparatus was required. The prepared strips can be stored for a long period of time without refrigeration, and this enabled off-laboratory a-point-of-care analysis.

LFIAs are rapid and cost-effective compared with other commercially available immunoassays and they can also be brought to the market relatively quickly with lower costs. In recent years, LFIA has become a popular technique as a diagnostic method. They are commonly used for detecting hormones,[3,13] viruses,[14,15] toxic compounds and metabolic

disorders.[11,16,17] Despite the potential for wide applications, LFIAs for progesterone determination in bovine milk have not been commercialised.[18]

There are still limitations of LFIAs, one being that they have not been useful for quantitative tests. Our study focused on the application of LFIA, in combination with gold nanoparticles, to validate the developed immunoassay for progesterone sensing. The goal of the study was to develop a non-laboratory rapid hormone assay for onsite progesterone analysis. The bovine serum and milk samples were collected from cows that were used in a trial to validate the use of LFIA. All blood and milk samples (from cow 1, 2, 3 and 4 see Appendix A.2.1) were collected every 2 days for a period of 8 weeks and all samples were analysed using electrochemiluminescence immunoassay (ECLIA) and enzyme-linked immunosorbent assay (ELISA) by NZVP independently to validate the new LFIA assay (the P4 concentrations from each assay were plotted versus the sample collection day/date). The details for sample collection are described in Appendix A.2.1.1 and A.2.1.2.

3.2 LFIA system

The LFIA system is based on the movement of liquid by capillary attraction through the detection region where the analyte interacts with the attached partner molecule for specific interactions.

The LFIA strip sensor was developed using anti progesterone-gold (Anti-P4-Au) conjugates. The details for the preparation of the half strips are described in the Appendix (A.3.4). The samples and the conjugates were introduced by immersing the LFIA strip in the solution well of a microtiter plate containing the sample.

The two main assay types described briefly in Chapter 1 (section 1.2) are (i) sandwich format and (ii) the competitive format. In a sandwich format, the sample migrates from the sample pad through the conjugate pad to bind with the analyte specific antibody then migrates through the membrane till it reaches the detection region. A sandwich format is suitable for larger analytes which have multi epitopes such as protein.

The competitive assay is primarily used for detecting small molecules and antigenic molecules which have only one epitope because of their small size. There are two possible configurations for a competitive assay; in one configuration (configuration A), the conjugate pad comprises the labelled antigen with an antigen-specific antibody immobilised onto a matrix such as nitrocellulose as the test line. The labelled antigen competes with the antigen in the sample to bind to the test line. The second configuration (configuration B) consists of a labelled antibody and a protein conjugated antigen immobilised as a test line. The antigen in the sample binds to the labelled antibody and migrates through the detection region. And for configuration B, the concentration of the analyte is inversely proportional to the signal generated on the test line.

The choice of membrane material and labelling particle are crucial for a LFIA system. The membrane must bind the test and control line materials irreversibly by either electrostatic or hydrophobic interactions.[22] Nitrocellulose is the most commonly used membrane for LFIA[23-25]. The protein of the immobilised ligand binds to the nitrocellulose membrane via electrostatic interaction between the strong dipole-dipole interaction of the nitrate ester and the protein peptide bonds. There is a range of nitrocellulose membranes with different pore sizes ranging from 0.005 to 12 μm. The porosity of the membrane is determined by the volume of air in a three-dimensional membrane structure, and it is one of the important factors of a LFIA system since it directly affects the flow rate of the system.

The membrane used in LFIA studies was Hi Flow Plus 75 from Millipore which has a capillary flow time of 75 ± 19 sec/4 cm.

The labelling material is the other important parameter of the LFIA system. The labelling materials including gold nanoparticles (AuNPs), coloured polystyrene (latex beads), fluorescent nanoparticles and magnetic particles have been studied and used for development of LFDs. AuNPs has been used extensively in LFIA systems since they can be easily conjugated to protein via tryptophan, lysine, and cysteine residues, and are relatively cheap.

A competitive assay (configuration B) is suitable for a small molecule such as progesterone (P4), where the analyte (P4) is conjugated with ovalbumin (OVA) to form the capture molecule for the test line. The P4 is conjugated with OVA because the molecular weight of P4 is relatively low. The analyte-protein conjugate P4-PEG-OVA was sprayed onto commercially available nitrocellulose cards as the test line and a rat anti IgG was sprayed as the control line. The test and control lines were then developed into two signal generators. Therefore, the format for the one assay used for the P4 studies was a half strip which comprised a nitrocellulose membrane, and an absorbing pad (Figure 3.1).

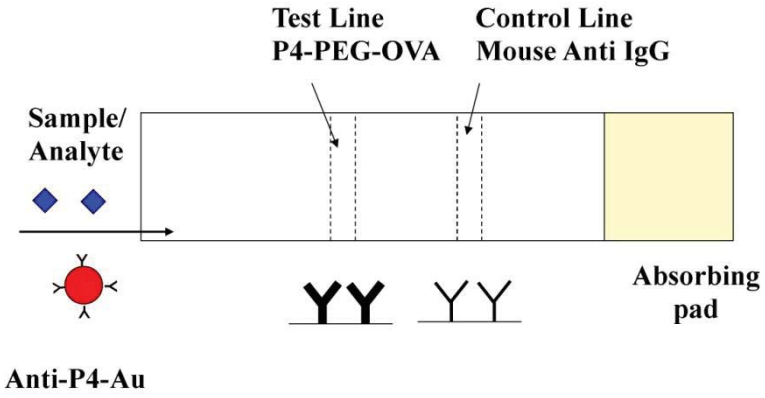

Figure 3.1 Development of a one step assay with Anti-P4-Au conjugates. P4-PEG-OVA and rat anti IgG served as test and control lines.

The assay used an Anti-P4-Au conjugate as the signal generator (label), the P4-PEG-OVA conjugate as the test line and the mouse anti IgG as the control line. The mixture of Anti-P4-Au and a range of free P4 standards were used to develop the standard curve for sample analysis. The free P4 standard in the mixture was competing for the binding to the Anti-P4-

Au with the sprayed P4-PEG-OVA test line. As the concentration of the free P4 standards increased, the signal generated by anti-P4-Au binding to P4-PEG-OVA line decreased as the antibody bound to the conjugate signal progressively neutralised. The concentration of the free P4 is inversely proportional to the signal generated by the Anti-P4-Au on the test line. The intensity of the test and control lines were quantified using an in-house system (Figure 3.2).

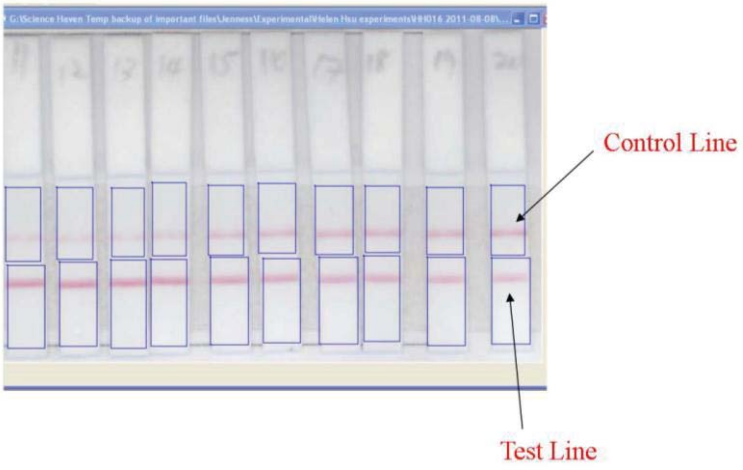

Figure 3.2 The image of the strips were obtained by using a photoscanner. The intensity of control and test lines on the test strips were read and quantified using the strip reader system.

3.2.1 Processing methodologies

The strip images are scanned using a photocopy scanner (HP), the intensities of the test and control lines on the strips being quantified using a proprietary strip reader (Version 2.00, Simon Brown, Launceston, Tasmania, Australia). The data obtained from the strip reader were then corrected by performing statistical analysis. The absolute intensity was calculated by dividing the intensity of the test line (T) by the sum of the test and control line intensities (T+C), and the result (T/(T+C), intensity) was plotted versus logistic concentration of the standard with OriginLab.

The plotted data was then used to fit a dose-response curve (Boltzmann Sigmoidal) with variable slope (OriginPro 7.0) to generate the standard curve. A dose-response curve is commonly used to plot the results of *in vitro* experiments where the known concentrations of drugs/hormone versus the response such as enzyme activity or secretion of a hormone. The X-axis plots the concentration of the analyte and the Y-axis plots the responses. The shape of

a dose-response curve is dependent on the system and the standard shape of a dose response curve is shown in Figure 3.3.

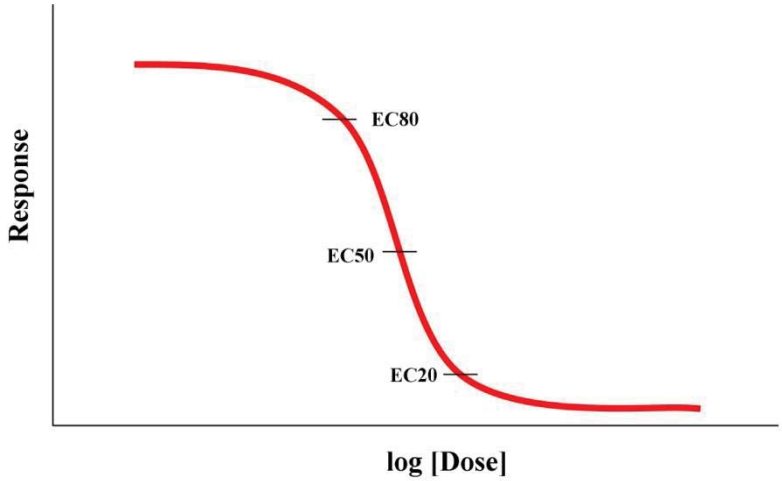

Figure 3.3 A typical shape of a dose-response curve where the response depends on the dose of the drug (drug concentration).

A standard dose-response curve is defined by four parameters: the baseline response, the maximum response, the slope of the curve, the drug concentration which provokes a response half way between the baseline and the maximum response. The slope of a dose-response curve is important for the concentration extrapolation process as a steeper curve will have a higher slope factor and a shallower curve has a lower slope factor; the calculated concentration can be affected greatly if the slope is steep.

3.3 Development of the P4-PEG-OVA sensor strip

3.3.1 Antibody titration

The antibody titration process is important for determining the appropriate pH/concentration of antibody which are required for stabilising the gold nanoparticles. The pH of the gold nanoparticles is generally determined by titration using K_2CO_3, and considering that the physiological pH of blood is 7.365 the chosen pH for gold nanoparticles was pH 7.4. The concentration of the Anti-P4 used for assays was determined by an antibody titration experiment. A 0.1 mg/mL solution of Anti-P4 stock solution was prepared and the matrix was set up in 1 mL cuvettes with different protein concentrations as shown in Table 3.1.

Table 3.1 Antibody titration concentrations

Stock [Anti-P4] (mg/mL)	Anti-P4 (µL)	Buffer (µL)	[Anti-P4] (µg/mL)
0	0	50	0
0.1	7	43	13
0.1	3	17	65
1	6.5	44	130
1	9.75	40	195
1	13	37	260
Stock [Anti-P4] (mg/mL)	Anti-P4 (µL)	Au, NaCl (µL)	Titration[Anti-P4] (µg/mL)
0	50	500, 100	0
13	50	500, 100	1
65	50	500, 100	5
130	50	500, 100	10
195	50	500, 100	15
260	50	500, 100	20

500 µL of colloidal gold (40 nM, pH 7.4) was added to each cuvette and mixed thoroughly and allowed to stand at room temperature for 2 minutes. 100 µL of NaCl (10% w/v) was added to each cuvette a minute apart. The solutions were left standing for 5 minutes and then

the UV/visible absorbance was determined by scanning from 300 to 800 nm. The UV/visible spectrum of a blank Au solution was also plotted followed by a determination of the maximum absorbance peak for each antibody concentration (Figure 3.4).

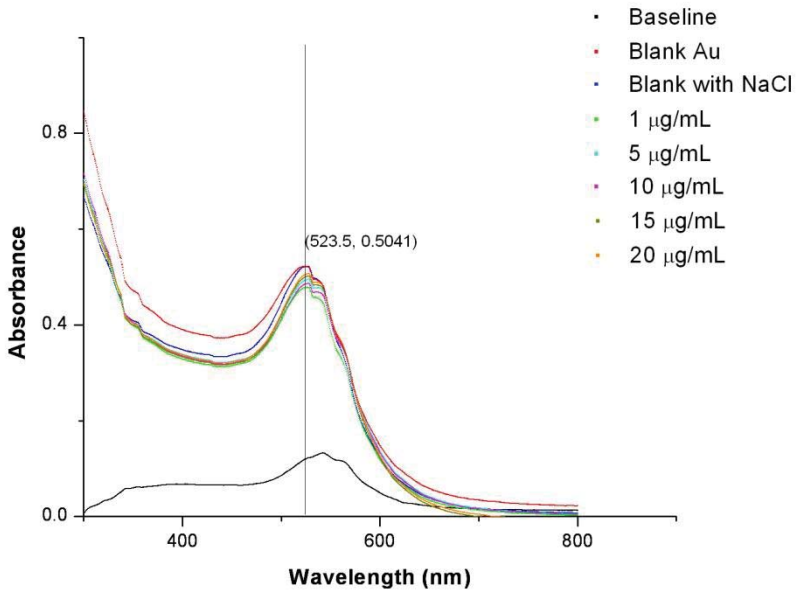

Figure 3.4 UV/visible spectra of an antibody titration, where the λ_{max} of the blank Au solution was at 523.5 nm.

Table 3.2 Absorbance and λ_{max} obtained from antibody titration

Antibody (μg/mL)	Absorbance at 523.5 nm	λ_{max} (nm)
0	0.5218	523.5
1	0.4774	526.0
5	0.4937	527.0
10	0.4840	528.0
15	0.4988	528.0
20	0.5041	528.0

Table 3.2 was constructed by determining the absorbance at 523.5 nm, the lambda(max) (λ_{max}) of blank Au solution. The antibody concentration selected was based on the minimum

amount of antibody required to stabilise the gold nanoparticles and the concentration gave the results that were closest to the blank solution.

The results indicated that at 20 μg/mL the Anti-P4 had an absorbance closest to the blank Au solution, but required a high concentration of Anti-P4. At 15 μg/mL the Au nanoparticles were stabilised by the antibody and generated a reasonably close absorbance spectrum compared to the blank Au solution. Hence the concentration of the Anti-P4 chosen for antibody-Au nanoparticles conjugation was 15 μg/mL.

3.3.2 Conjugation of Anti-P4 to gold nanoparticles

The use of gold colloidal particles as a versatile and efficient template for the immobilisation of biomolecules has been recognised since the 1980s,[27] and Au nanoparticles (AuNPs) have been commonly used as the labelling or enhancement particles in biosensing.[28-31] The concentration of Anti-P4 determined from the antibody titration (section 3.3.1) was used for the conjugation of Anti-P4 to AuNPs. 15 μg/mL of Anti-P4 (Serotech) was conjugated to 10 mL of AuNPs (40 nm, pH 7.4) and the details of the conjugation process are described in Appendix A.3.5.

3.3.3 Development of the P4-PEG-OVA strip

A commercially available nitrocellulose membrane (Millipore) was assembled using an absorbent pad (Millipore). The membrane consisted of a test line (P4-PEG-OVA) and a control line (rabbit anti-mouse IgG, Sigma M6024). The stock solution of P4-PEG-OVA (6.4 mg/mL) and IgG was diluted to 1 mg/mL using 10x PBS buffer (pH 7.4) and Milli-Q H_2O then sprayed onto the membrane. The sprayed membranes were dried at 40 ℃ for 1 hour and then cut into 5 mm width strips and sealed stored in a dry-box at room temperature.

3.3.4 The P4 binding curve

The concentration of the Anti-P4-Au used for the P4 assays was determined by developing the P4-PEG-OVA test strip binding curve. The strips were tested with a series of solutions with different Anti-P4-Au concentrations (0.1 µg/mL to 1.2 µg/mL, Figure 3.5) with three replicates. The results were plotted and the concentration of Anti-P4-Au which was sufficient to perform the assay was determined.

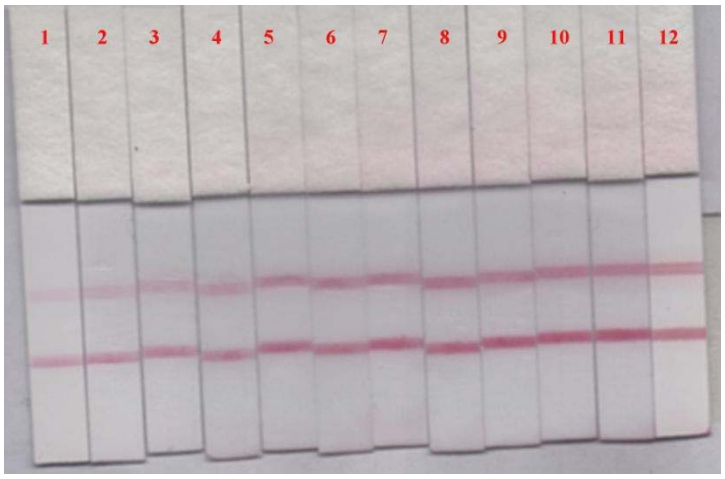

Figure 3.5 P4-PEG-OVA strips with varied Anti-P4-Au concentrations (strips 1 to 12, 0.1 µg/mL to 1.2 µg/mL). As the concentration of Anti-P4-Au increased from A1 to A12 the intensity of both test and control lines increased.

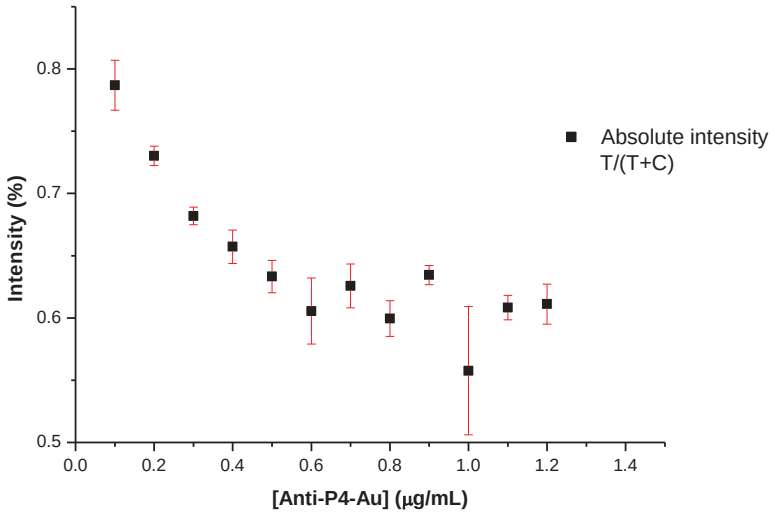

Figure 3.6 A P4-PEG-OVA binding curve indicated 0.1~0.3 µg/mL of Anti-P4-Au should be sufficient for assay development.

The statistical analysis method was applied to analyse the intensity of the test and control lines; where T/(T+C) represents the absolute intensity of the test line (the ratio of the intensity of the test line to the sum of the test and control line.

As the Anti-P4-Au concentration increased, the absolute intensity (T/(T+C)) decreased. As the concentration of Anti-P4-Au increased, the non-specific interaction between the Anti-P4-Au and the control line also increased. Hence it is important to select a suitable concentration to generate signals and also minimise the amount of Anti-P4-Au in each assay.

The strips from the binding curve (Figure 3.5, Figure 3.6) showed that a 0.5 μL (0.1 μg/mL) per solution well contained a sufficient amount of Anti-P4-Au to generate signals for both test and control line for analysis. 2.0 μL of the stock Anti-P4-Au (0.4 μg/mL) was the maximum amount of Anti-P4-Au required to generate signals. Hence, 0.5 μL of the stock Anti-P4-Au was selected as the antibody concentration for all LFIA analyses.

3.3.5 The P4 standard curves

3.3.5.1 Concentration scouting

The P4 concentration scouting for the standard curve was performed using P4-PEG-OVA sensor strips. The concentrations of the P4 standard solutions used in the initial standard curve scouting were the same as used in the SPR P4 concentration scouting (see section 2.3.4.3) and were from 0 to 10800 ng/mL (the concentration range 0 ng/mL to 1.08 ng/mL in ~0.1 ng/mL increments). Each solution well contained Anti-P4-Au, P4 standard solution and HBS-EP^{+} buffer.

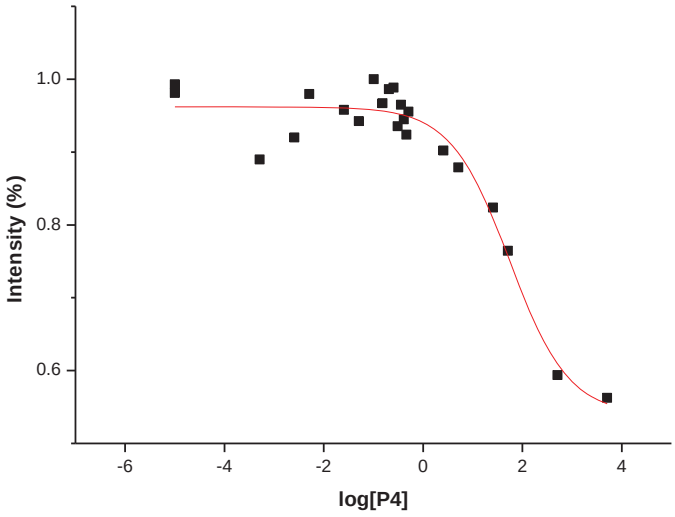

Figure 3.7 A P4 standard curve scouting to establish the concentrations for P4 standard solutions.

From the plotted and fitted standard curve, it was clear that with the LFIA system, the detection sensitivity was not as responsive as SPR sensing (Figure 3.7). The LFIA system was not able to clearly detect the low concentrations used in the SPR sensing system (0 to 1.08 ng/mL). Hence the concentrations selected for the LFIA standard curve were increased compared to the original SPR P4 standard curve concentrations.

3.3.5.2 The P4 standard curve established with the P4-PEG-OVA test strips

The assay was developed using the Anti-P4-Au conjugate and with P4-PEG-OVA capture line test strips. The concentrations of the P4 standard solutions were selected after concentration scouting and then used to determine the P4 standard curve. The assay consisted of Anti-P4-Au (0.5 µL), P4 standard solution (37 uL), and HBS-EP^{+} buffer (32 µL) as running buffer and each point ran in triplicate. The dose-response fit showed that the P4 standard curve of a P4-PEG-OVA strip has a working range of 0.2 ng/mL to 38 ng/mL (EC80 and EC20) with EC50 2.8 ng/mL (Figure 3.8).

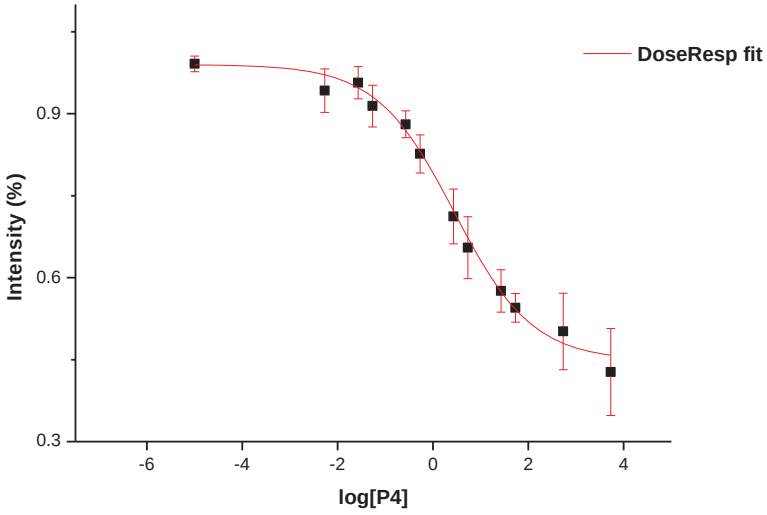

Figure 3.8 The P4 standard curve obtained from the P4-PEG-OVA test strips. The standard curve was calibrated with triplicate measurements. The error bars represented the standard deviation of the measurements.

3.4 Determination of P4 in bovine serum using LFIA

3.4.1 Preliminary free P4 analysis

It is known that only approximately 2% of the total P4 in serum is unbound, or free, and it is in equilibrium with the P4 bound to the corticosteroid binding globulin (CBG).[32-35] In order to separate the unbound/free P4 from the bulk of the serum, a separation process was carried out. The centrifugal filter allowed the separation of small molecules from higher molecular weight proteins. Theoretically, using a centrifugal filter, proteins larger than 3 kDa will be trapped on the upper layer of the centrifugal filter, and the bottom layer filtrate will contain molecules/proteins smaller than 3 kDa, which allowed the separation of the unbound P4 in the serum. Each bovine serum sample was spun down using a centrifugal filter (3K, Millipore) to remove the proteins present in the serum. The bottom fraction of the sample (20 μL) which contained lower molecular weight molecules was used for assay development. The P4 standard curve was used to calculate the free P4 concentration in the serum (Figure 3.8). It suggested the concentration of free P4 in the treated (spun down) serum sample was not within the detection range. The intensity of the strips was plotted versus the sample collection day/date (not the day of estrous cycle) from the animal (Figure 3.9) and this showed the variations between the triplicates. The free P4 analysis in a serum sample requires further investigation and an increase in the sample volume used in the assay may be needed.

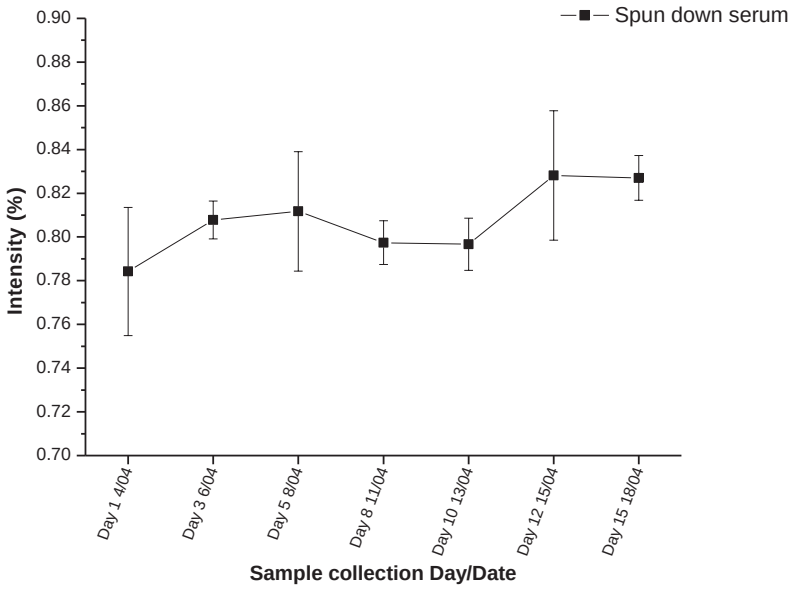

Figure 3.9 Intensity of control serum samples after protein separation using a centrifugal filter. The results indicated the concentrations of the free P4 present in serum samples may be too low for the sensing strip to detect.

Further investigations of free P4 analysis were carried out using serum samples collected from cow 3. The samples were also spun down using the centrifugal filters, and the volume of spun down serum used for assay development was increased to 37 µL. The P4 standard curve was used to calculate the free P4 concentration present in the serum sample. The extracted serum sample showed no clear indication of a P4 cycle (Figure 3.10). It is likely the concentration of free P4 in the serum sample was low and it was out of the detection range of the established standard curve.

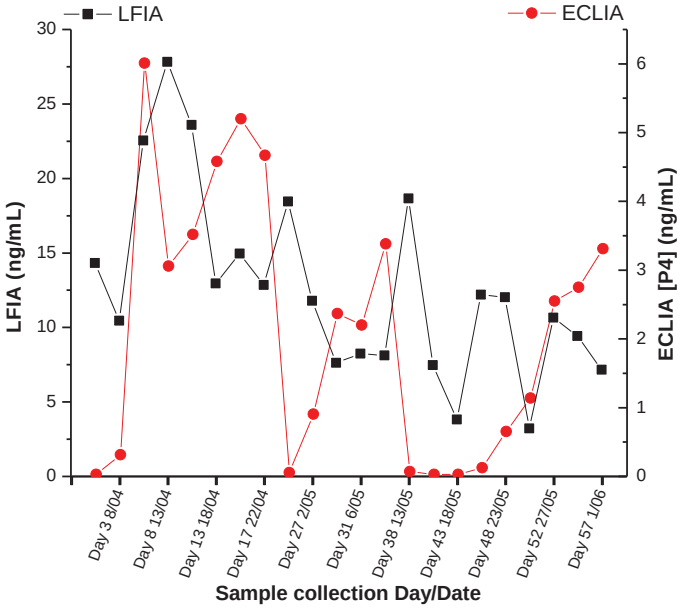

Figure 3.10 P4 concentrations of cow 3 in spun down serum samples.

It was clear that there are limitations for free P4 analysis using P4-PEG-OVA LFIA strips. Hence, serum 3 was used for testing an alternative sample preparation method.

The serum samples were diluted in PBS buffer (1:10 dilution) and LFIA analyses were carried out. The P4 concentrations were plotted versus the sample collection dates (Figure 3.11), then compared with ECLIA analysis data. The calculated concentrations from the serum samples were approximately 10% compared to the ECLIA analysed data, which was expected because of the sample dilution. The results of LFIA analysis using diluted serum samples showed the assay was able to indicate the peak of the P4 cycle and the general trend of the P4 cycle matched the ECLIA P4 cycle. Hence, the serum dilution preparation was preferred over the free P4 analysis.

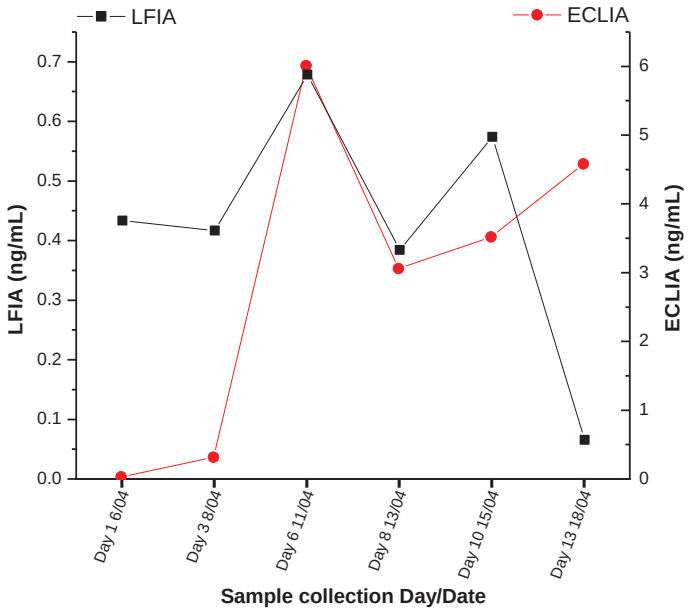

Figure 3.11 The serum samples from cow 3 were tested and the results compared with the ECLIA analysis.

3.4.2 Bovine serum samples analysis

The serum samples from cow 1 were used for P4 analysis. The P4 standard curve with established concentrations was used to calculate the P4 concentration in the serum samples.

3.4.2.1 P4 standard curves with low [P4] serum samples

The previously established P4 standard curve with selected concentrations was used to develop a standard curve with spiked serum (with known P4 concentration). From the strips used from serum dilution assay, it was clear that with the 1:10 serum dilution the strips still showed a noticeable background colour. Hence, before using the developed assay to measure the serum samples, the serum matrix effects in the format were assessed and corrected with a serum sample which contained the lowest P4 concentration (0.045 ng/mL from ECLIA analysis), which was used as a blank standard. The diluted serum samples (1:5 and 1:10 dilution) were used for the assay.

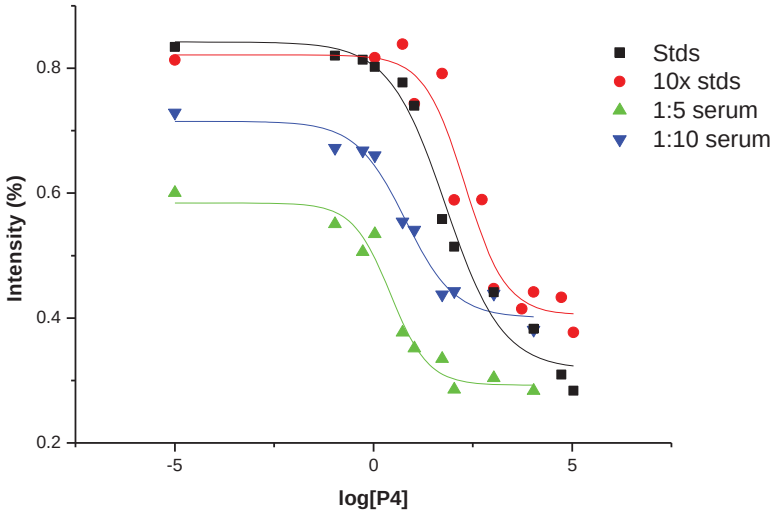

Figure 3.12 P4 standard curves to test the matrix effect from the serum sample as well as the sensitivity of the assay by using different sets of P4 standards.

The P4 standard curves containing the spiked serum were compared with the non-spiked P4 standard curves. The standard curve shifted slightly (decreased in intensity at the lower concentration end of the standard curve), but overall the intensity of the spiked serum strips have increased compared with the normal standard curve (Figure 3.12). The increase in

intensity was not expected because as the concentration of the standards increased, the intensity is expected to decrease. The spiked standard curve with the 1:10 dilution serum showed a noticeable decrease in intensity, and the effect was more significant in the standard curve spiked with 1:5 dilution serum. The intensity of the standard 0 ng/mL with spiked serum was plotted with the standard curve (Figure 3.13).

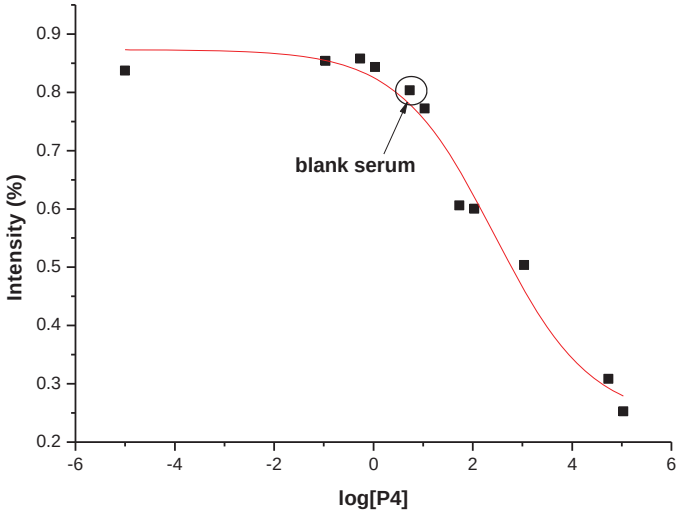

Figure 3.13 Serum with no standards fitted within the working range of the P4 standard curve.

The intensity of the serum sample which was used as the blank solution to spike the standard curve lay on the working range of the standard curve. This suggested that with a blank serum, there will still be background intensity, which is likely to be caused by the non-specific binding/matrix effect. In a biological system, matrix components present in biological samples can affect the response of the analyte which are termed generally as matrix effects.

3.4.2.2 Serum analysis for cow 1

The samples collected from cow 1 were tested with the P4-PEG-OVA sensor strips. The P4 standard curve and the P4 standard curve spiked with the 1:10 dilution serum gave a reasonable estimate of the background intensity generated by the blank serum sample (see section 3.4.2.1). The normalised spiked standard curve was compared with the non-spiked standard curve (Figure 3.14).

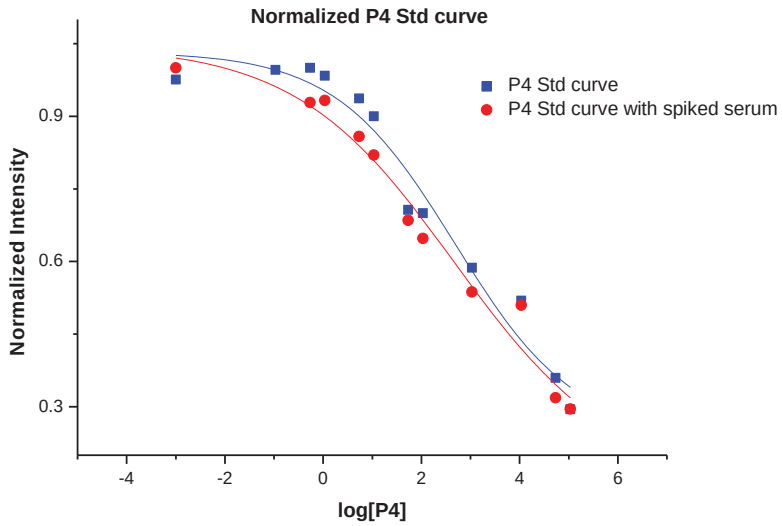

Figure 3.14 Comparison between a normalized P4 standard curve and a normalized P4 standard curve with spiked low [P4] serum sample.

The shifting of the standard curve downwards indicated that the sensitivity of the standard curve decreased as expected. The intensity deviated more at the top (lower P4 concentration end) than the bottom (higher concentration end) of the standard curve. It is possible there are some effects caused by the blank serum on the assay which only resulted in a slight shift of the standard curve, and it is likely due to the non-specific binding and matrix effects.

The serum samples were diluted (1:10) and analysed using the developed assay and the details are described in Appendix A3.8. The plotted standard curve (with spiked serum) was used to calculate the P4 concentration in the samples (Figure 3.15).

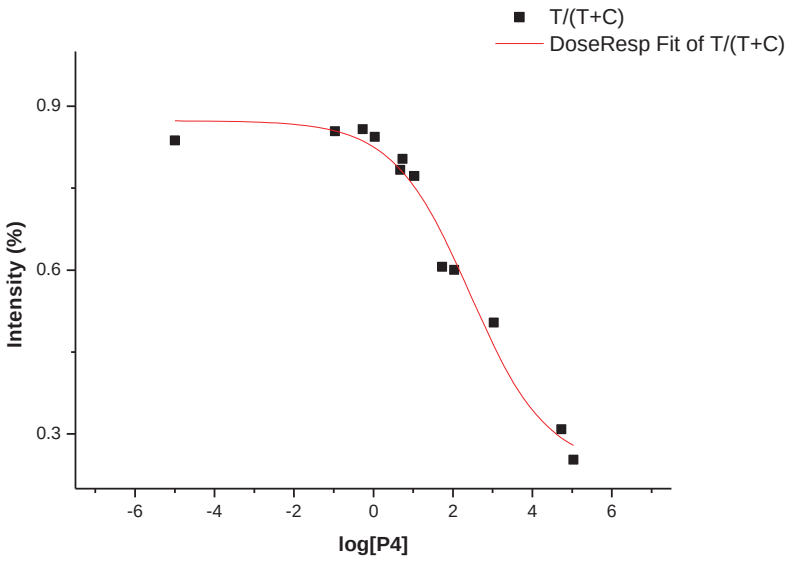

Figure 3.15 P4 standards were spiked with a serum sample which contained a low concentration of P4.

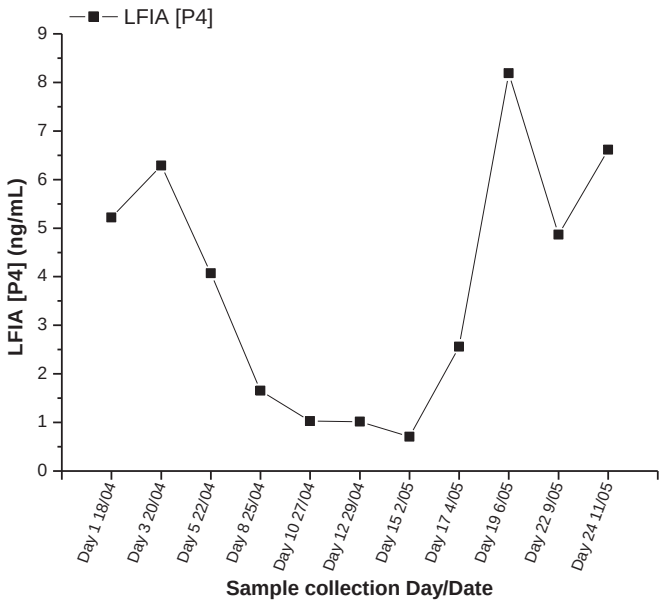

Figure 3.16 LFIA analysis of serum 1, which showed a distinct P4 cycle.

The P4 concentration calculated in the serum samples was plotted versus the sampling date (Figure 3.16). Unlike the assay for a filtered serum sample (section 3.4.1), the P4 concentration plot showed a clear P4 cycle.

The plotted P4 cycle of cow 1 was compared with the corresponding P4 concentrations from the ECLIA P4 analysis (Figure 3.17) for the serum samples.

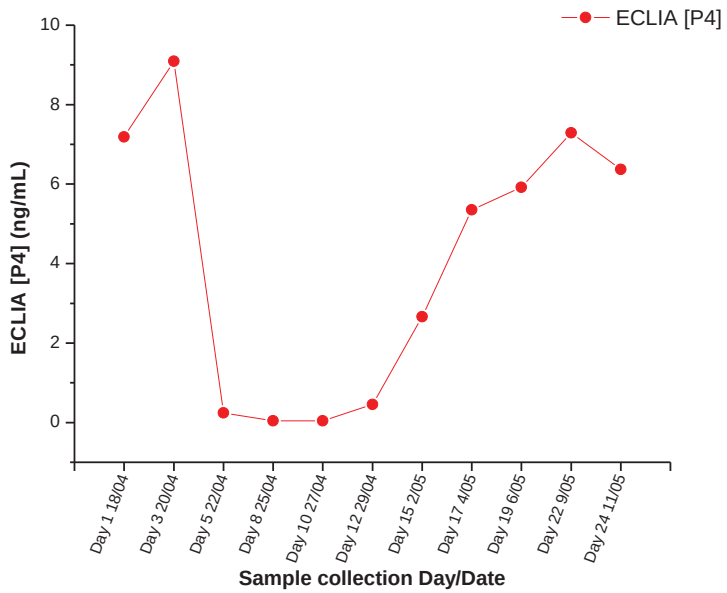

Figure 3.17 ECLIA analysis of serum from cow 1, which was used as a standard to validate the assays. The serum samples showed one complete P4 cycle with the two ends of the plot having high P4 concentration and low P4 concentrations in between, and this followed the normal trend for a bovine P4 cycle.

From the electrochemiluminescence immunoassay (ECLIA) analysis, the P4 concentration decreased significantly on Day 5 and the concentration then stayed low for approximately 1 week and the P4 concentration increased steadily for the next 9 days. This is presumably as a restart of ovulation and corpus luteum formation. It would be expected that had samples been collected from 3 and 4 days the P4 concentration would decrease to the baseline again. The P4 concentrations from serum 1 showed a typical P4 cycle in bovine serum.

The P4 concentrations obtained using the two different analytical techniques were overlapped and the general trend of the cycles compared (Figure 3.18). The LFIA method was able to differentiate the increase in concentration from the first day to the third day. The significant decrease in concentration was detected by the ECLIA on the fourth day (third data point on the plot), and the LFIA also detected the reduction in P4 concentration but reduced more slowly. For both assays, the concentration of P4 remained low for approximately a week and then the P4 concentration increased again, as another corpus luteum was established which linked to the next P4 cycle.

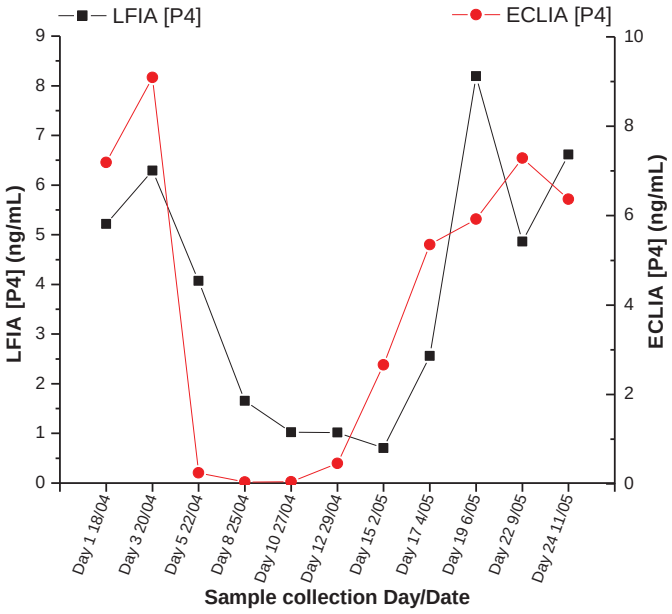

Figure 3.18 Overlapped plots of ECLIA analysis and LFIA analysis of serum 1.

The P4-PEG-OVA sensor strip appeared to overestimate the sample concentration at lower P4 concentrations (between the two peaks). The standard curve was corrected by spiking blank serum to the P4 standard solutions. However, the overestimation of the concentration still appeared in the lower P4 concentrated samples. The overestimation of P4 concentration was possibly due to the non-specific binding of the CBG. The effect in higher P4 concentrated serum samples was not as significant. However, the general trend of the LFIA P4 cycle followed the ECLIA P4 cycle, and the LFIA analysis method was able to distinguish between the high and low concentration points of the cycle.

The samples from cow 1 were repeated using LFIA six months later and the concentrations were plotted versus the ECLIA results.

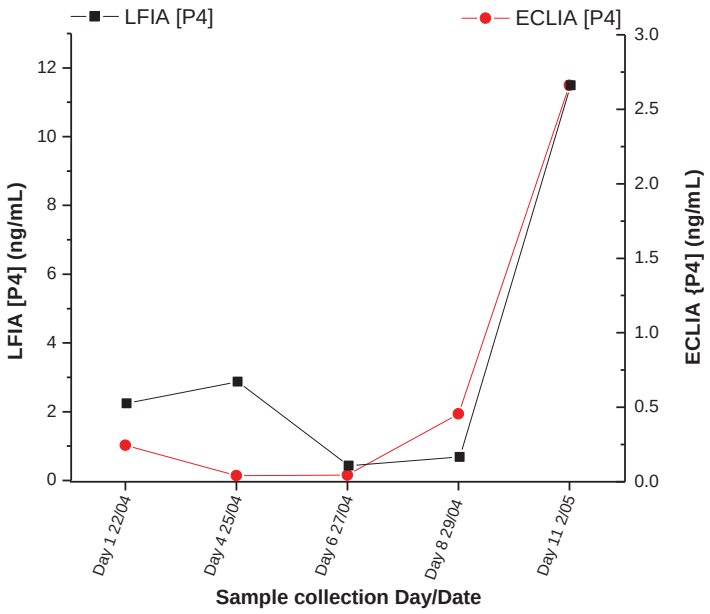

Figure 3.19 Serum samples from cow 1 repeated for P4 concentration 6 months later. The pro-estrus and metestrus profile from LFIA analysis matched the profile from ECLIA analysis.

The serum samples were retested using the same assay with the same batch of strips (prepared/sprayed on the same date). The same batch of Anti-P4-Au was initially used to analyse the serum samples, but as the intensity generated by them had reduced from what they were previously, a new batch of Anti-P4-Au was conjugated and used for the assay.

The LFIA still overestimated the P4 concentration in lower concentrated serum samples (Figure 3.19), but allowed the detection and distinguishing of the high and low P4 concentrations in a P4 cycle.

The assay was performed with the same protocols as before but with serum samples from cow 2. The overall trend of the P4 cycle still matched the ECLIA P4 cycle adequately (Figure 3.20).

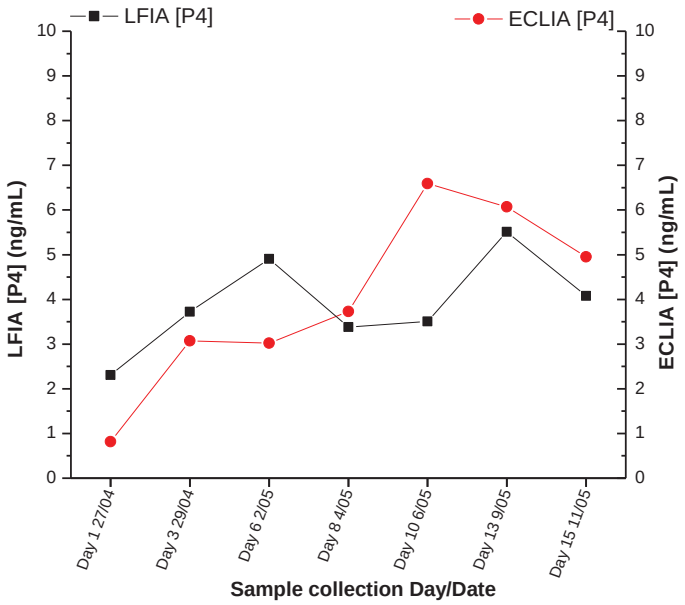

Figure 3.20 Overlapped LFIA P4 cycle and ECLIA P4 cycle for Serum 2.

It is clear that without sample pre-treatment, the non-specific binding/matrix effect can be reduced by diluting the serum samples. The LFIA analysis can be carried out by simple serum dilution using PBS buffer and could potentially be used for an easy and quick semi-quantitative P4 cycle analysis. It could distinguish between oestrus and the luteal phase which can have commercial implications with further refinement.

3.5 Bovine milk progesterone

An ELISA-based kit for an on-farm determination of progesterone in milk has been developed.[36] The method works well but the cost may be prohibitive.

For LFIA analysis, there are issues for small molecule analysis in milk where fat and protein molecules are present. A trial assay was carried out by using 5 μL of raw milk with an antibody conjugate (Anti-P4-Au). Only in a few samples did the Anti-P4-Au elute successfully from the solution well and bind to both test and control lines. A few strips also had binding at both the test and control lines but with a thin layer of fat/protein aggregated at the bottom of the strips. However, in the majority of the samples the fat present in the milk samples inhibited the flow of the fluid in the assay and coagulated with Anti-P4-Au at the bottom of the strips (see strips 6-11 Figure 3.21). Therefore the milk samples required prior treatment/preparation before the assays could be performed.

Figure 3.21 The assay using milk samples (the strips were numbered from 1 to 12 according to their sample collection date) without treatment/preparation resulted in coagulation of the milk fat/protein with the Anti-P4-Au at the bottom of the strip. The bottom of samples 6 to 11 showed the fat and protein deposits.

To prevent coagulation the initial sample preparation included using simple dilutions with PBS buffer (10 mM) and the aggregation level of Anti-P4-Au was reduced significantly. The samples were analysed in duplicates so that the accuracy and the reproducibility of the assay could be compared.

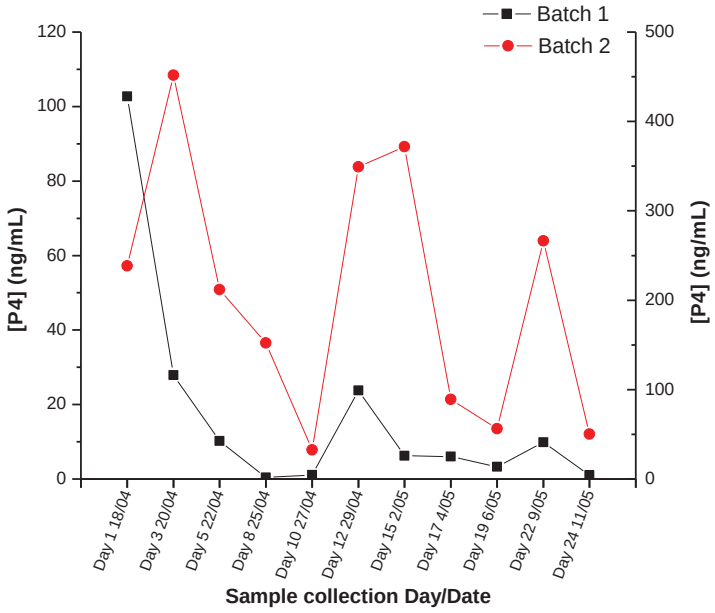

Figure 3.22 Comparison of [P4] from two batches of LFIA analysis using diluted milk samples from cow 1. The two batches analysed from the same assay were not consistent. Therefore the milk samples required further treatment.

The results indicated that upon dilution of the milk samples, the assay was eluted successfully, but the P4 concentration analysed from batch to batch varied significantly and it was out of the acceptable error range (Figure 3.22). This is most likely due to the milk samples not being homogeneous despite the sonication process.

Therefore, the method was not satisfactory for the assay development and required further modification.

3.5.1 Independent analysis

The profile of the P4 cycle in bovine serum should be similar to the profile of the P4 cycle in bovine milk. The P4 concentration in bovine milk should be higher than in serum because P4 has a high affinity for fat. Hence the LFIA analysed P4 concentrations in milk samples were initially compared with the ECLIA serum P4 concentrations and a similar P4 cycle profile was expected.

The independent ELISA analysis for milk samples showed a basal level of P4 concentration from Day 1 to Day 3. The P4 concentration started to increase from Day 5 to Day 10 and decreased to 6.48 ng/mL on Day 12 (Figure 3.23). The P4 concentration continued to increase to the maximum on Day 17 and then started to decrease back to its basal concentration. The duration of the P4 cycle was approximately 21 days.

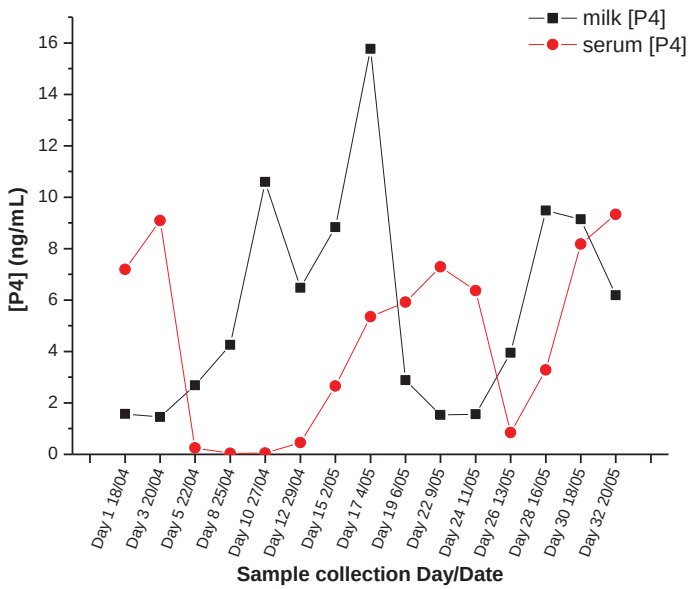

Figure 3.23 NZVP milk and serum samples of cow 1 did not have the same P4 cycle profile.

The ECLIA analysis for the serum samples showed a different trend of the P4 cycle. The P4 concentration increased from 7.19 ng/mL on Day 1 to 9.09 ng/mL on Day 3 and dropped back to the basal concentration (from 0.041 to 0.46 ng/mL) until Day 12. The P4 concentration then increased from Day 15 to Day 22 (2.66 ng/mL to 7.29 ng/mL) and dropped to 0.84 ng/mL on Day 26. The P4 concentration did not stay at a basal level but increased to 3.28 ng/mL on Day 28 followed by 8.18 ng/mL on Day 30 and 9.33 ng/mL on

Day 32. From the graph (Figure 3.23), it suggested that Day 10 was the beginning of the new P4 cycle, and from Day 17 to Day 24 the P4 remained high and Day 26 was the end of the estrous cycle, which lasted 16 days and was shorter than a typical P4 cycle (21 days).

The bovine estrous cycle is known to recur on average every 21 days, so the shortened P4 cycle for cow 1 was unusual. The P4 cycle profile of the serum samples was expected to be similar to the milk P4 cycle profile,[37,38] but the independent ECLIA and ELISA analysis suggested otherwise.

In this study, the serum and milk P4 concentrations obtained from independent analysis were used as a standard for LFIA development in serum and milk P4 analysis. The P4 cycle profile was used to compare/determine the accuracy of the LFIA technique.

3.5.2 P4 standard curves for milk analysis

The standard curve was tested for the milk sample by comparing the normal standard curve to the standard curve with increased P4 concentration and the standard curve spiked with a milk sample. The standard curve was spiked with 5 µL of fat-removed, diluted milk (with a P4 concentration of 0.041 ng/mL). The intensity decreased as expected as a function of increasing concentration in the spiked standard curve and it indicated that the milk samples would also reduce the sensitivity of the assay slightly with just using 1:10 dilution (Figure 3.24). In the assay which contained twice as much of the P4 standard solution (10 µL was used instead of 5 µL in standard assay), the intensity increased slightly and the dose response curve fitted reasonably well. However, the slope became steeper compared with the normal standard curve (Figure 3.24).

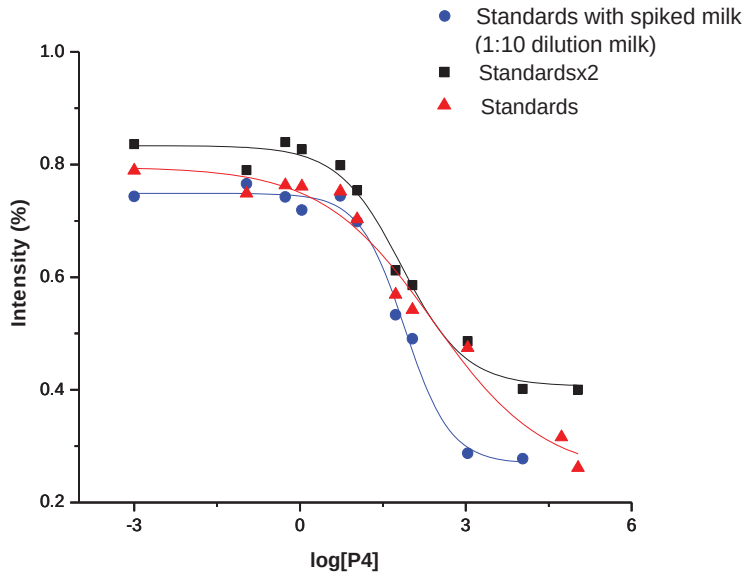

Figure 3.24 Standard curve spiked with a milk sample.

The standard curve spiked with a milk sample (Figure 3.24) indicated that the background signal/matrix effect from the milk sample was apparent even with fat removal and sample dilution steps. It is important to develop an assay, which enables the estimation of the matrix effect separate from the milk samples. Alternatively, the sample treatment/preparation method can be improved and modified to eliminate the non-specific binding and matrix effect.

3.5.3 Milk sample preparation

The preparation method was modified by removal of the fat contained in the milk sample by centrifuging the samples at 13400 rpm for 10 min. The assays were performed using 5 µL of a fat-removed milk sample with a 1:10 dilution with PBS buffer (10 mM). The strips clearly indicated that the issues of coagulation of the milk sample and aggregation of the Anti-P4-Au were both resolved by this method (Figure 3.25).

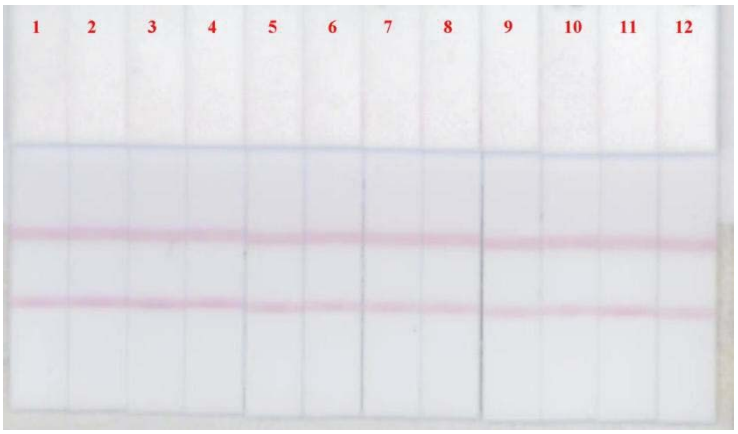

Figure 3.25 The sensor strips (the strips were numbered from 1 to 12 according to their sample collection date) from fat-removed, diluted milk samples.

The calculated P4 cycle was overlapped with the P4 cycle obtained from the ELISA analysis, and the result indicated that the matrix effect from the milk sample resulted in an overestimation in the P4 concentration (Figure 3.26). However, the general trend of the P4 cycle resembles the ELISA P4 cycle. Hence by carrying out the assay after the removal of fat would allow qualitative P4 sensing using P4-PEG-OVA strip sensors.

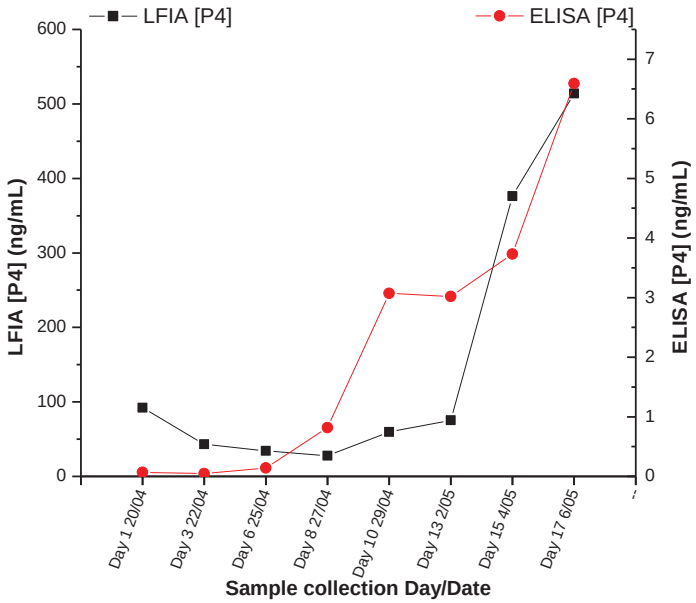

Figure 3.26 The P4 standard curve was used to calculate the P4 in milk samples from cow 1.

To facilitate development towards a quantitative P4 sensor strip, a trial of milk protein and fat precipitation was carried out for the sample preparation. The precipitated samples were used to perform the P4 assay (Figure 3.27), although the solvent selected for protein precipitation affected the nitrocellulose membrane. Therefore the sample preparation method was altered for the LFIA setup.

The established standard curve used for serum analysis was also used for milk analysis. Pre-treatment of the milk samples to remove the fat and protein was carried out for all samples by precipitation using acetonitrile (see Appendix A.3.9 for details).

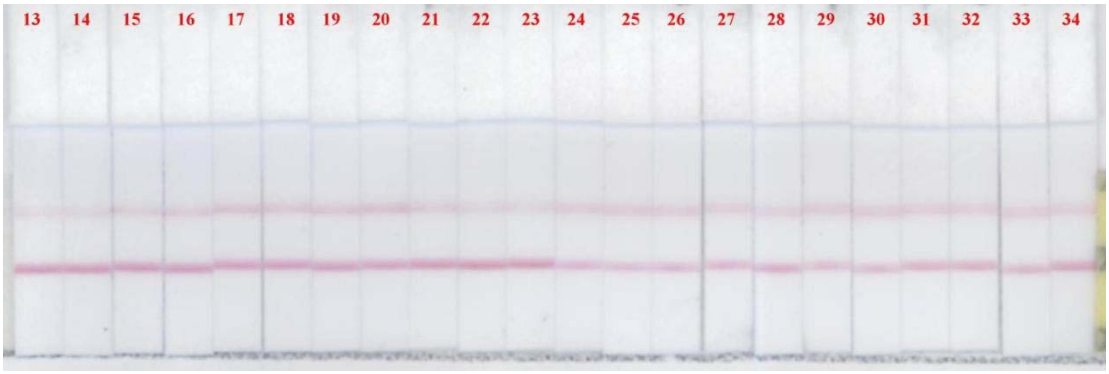

Figure 3.27 The sensor strips (the strips were numbered from 13 to 34 according to their sample collection date) were allowed to develop in the solution well which contained the analysed solution for 20 min. The strips were scanned and analysed using the strip reader. The variation in colour intensity of the sample strips suggested a difference in [P4] in the milk samples from cow 1.

3.5.4 Comparison of the P4 LFIA analysis to the independent ELISA analysis of milk samples after protein and fat removal

The milk samples from cow 1 and 2 were used for LFIA analysis. The samples prepared followed the protein and fat precipitation protocol,[39] and the excess solvent (acetonitrile) was removed by freeze drying overnight (see Appendix A.3.9).

The freeze dried milk samples were used for the assay development with the established P4 standard curve. 5 µL of freeze dried milk were used for the assay which contained 32 µL of PBS (10 mM), 38 µL of Anti-P4-Au and the assay was allowed to develop for 20 min before the quantitative analysis.

The calculated P4 concentration of cow 1 was plotted versus the sampling date. The P4 concentration increased from Day 1 to Day 8 (from 0.85 ng/mL to 5.86 ng/mL) and decreased to 0.12 ng/mL on Day 10 which indicated the tested samples covered part of an estrous cycle. The absence of a basal P4 concentration suggested the pro-estrus and diestrus stages were not included in the test samples (Figure 3.28).

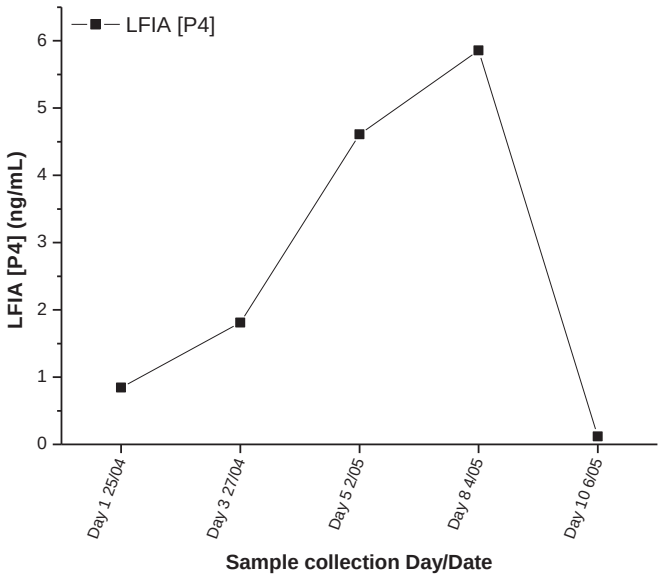

Figure 3.28 The P4 cycle from cow 1 analysed from LIFA, the samples showed only a partial estrous cycle which resembled a typical bovine estrous cycle.

The P4 cycle determined from LFIA was overlapped with the ELISA analysed P4 cycle (Figure 3.29).

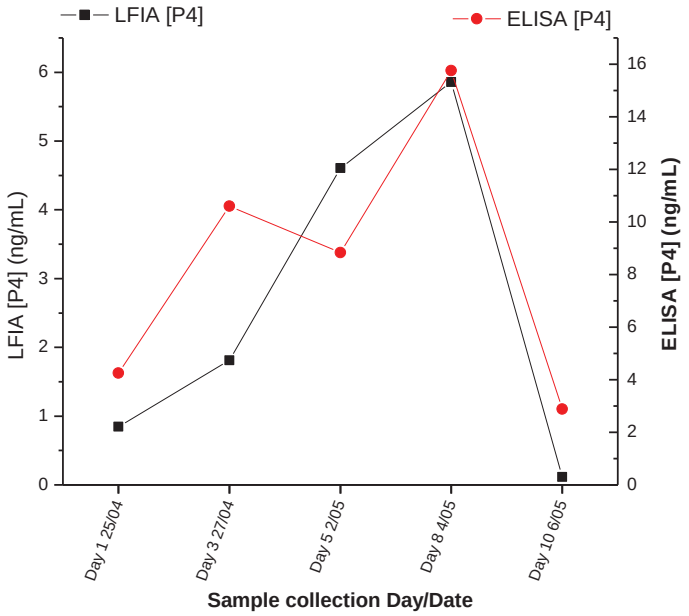

Figure 3.29 The LFIA analysed P4 cycle was overlapped with the ELISA analysed P4 cycle of cow 1.

The ELISA analysed P4 cycle showed an increase of P4 concentration from 4.26 ng/mL to 10.6 ng/mL from Day 1 to Day 3, and a decrease to 9.86 ng/mL on Day 5. The concentration then increased to the peak of the P4 cycle (15.8 ng/mL) followed by a drop to 2.89 ng/mL on Day 10. The ELISA analysed P4 cycle also suggested the test samples validated the P4 cycle profile analysed from LFIA since the trend of metestrus and diestrus resembled a typical estrous cycle. The concentrations calculated from LFIA analysis were consistently lower than the ELISA analysed concentrations (~1/3 to 1/5 of the ELISA analysed concentrations). The loss of P4 in the milk samples was likely to be caused by the sample preparation step. Each milk sample was prepared after the samples had been thawed over ice. The milk samples were mixed by vortex and then the protein precipitation step was carried out. The solvent added to the samples allowed the protein and fat to be removed from them. P4 is known to have high affinity for fat. Hence it is possible the precipitation process still allowed some P4 residues to remain in the precipitated fat layer.

To improve the efficiency of P4 extraction, the sample preparation protocol was modified by increasing the mixing time prior to the precipitation process. The precipitated milk samples were sonicated for 10 minutes, and this was followed by freeze drying of the extracted milk samples. The assay was performed after carrying out the modified protein precipitation protocol. It was allowed to develop for 20 minutes and this was followed by a quantitative analysis using the strip reader. The established P4 standard curve was used to calculate the P4 concentration in the treated milk samples.

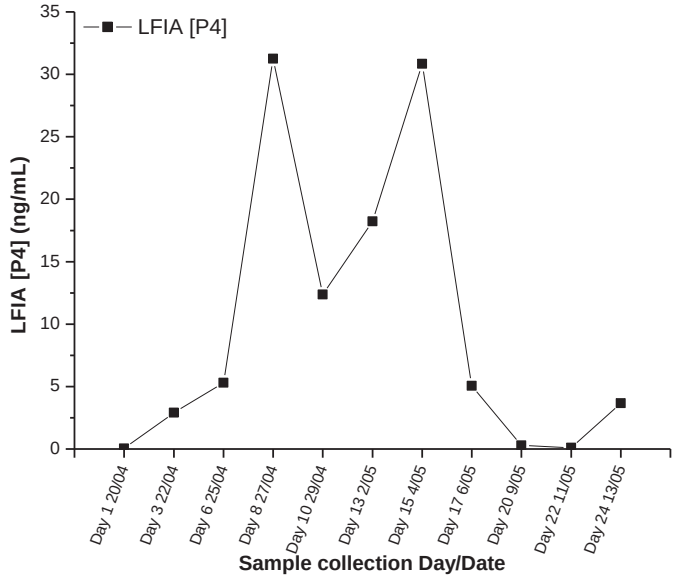

Figure 3.30 LFIA analysed milk sample (after removal of fat and protein) showed a full P4 cycle of cow 1.

The P4 concentrations in the milk samples were calculated using the LFIA P4 standard curve and also plotted versus the sample collection date. The P4 concentration increased from the basal concentration on Day 1 to Day 8 followed by a sudden decrease in concentration on Day 10. The concentration then increased and reached the peak of the P4 cycle on Day 15, and on Day 19 it decreased and then back to the basal concentration on Day 20-22 (Figure 3.30). The LFIA P4 cycle was overlapped with the ELISA P4 cycle so the results could be compared with the two methods (Figure 3.31).

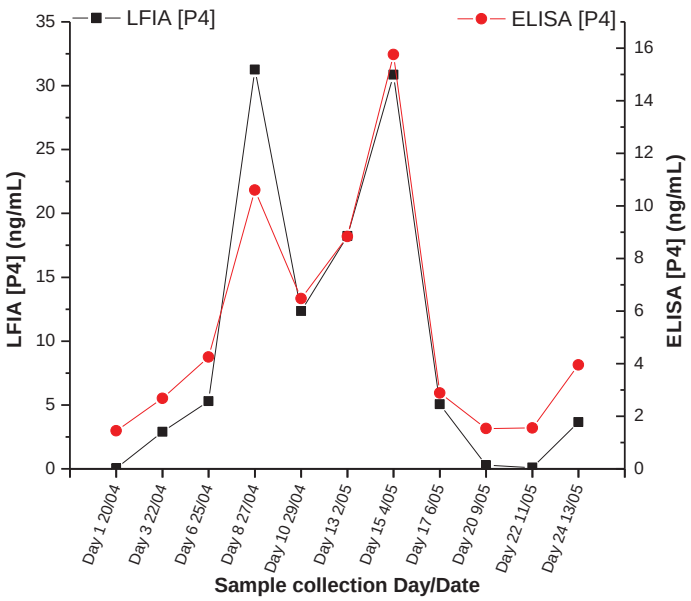

Figure 3.31 Overlapped ELISA and LFIA P4 cycles of cow 1. The profiles of the P4 cycles matched but with an overestimation of the P4 concentration from LFIA.

The ELISA results showed a gradual increase in P4 concentration from Day 1 to Day 8, followed by a sudden decrease in P4 concentration on Day 10 to 6 ng/mL which increased again from Day 13 to Day 15. The concentration of P4 decreased significantly on Day 17 and remained low till Day 22. The ELISA result indicated the milk samples collected had a full estrous cycle which typically averages 21 days (Figure 3.31). The LFIA method clearly overestimates the concentrations by approximately 3 times. On Day 8, the P4 concentration was expected to be lower than the P4 concentration on Day 15, but it appeared to be an overestimation with this particular sample. The rest of the test samples followed the trend of the P4 cycle profile for both LFIA and ELISA.

The P4 analysis method developed for cow 1 was performed on the milk samples from cow 2 and compared with the ELISA P4 cycle. The plot showed a P4 cycle without the basal P4 concentration in pro-estrus stage. The P4 concentration increased from Day 1 and decreased slightly from Day 3. The P4 concentration then suddenly increased on Day 8 and remained high till Day 17, which indicated a clear P4 cycle (Figure 3.32).

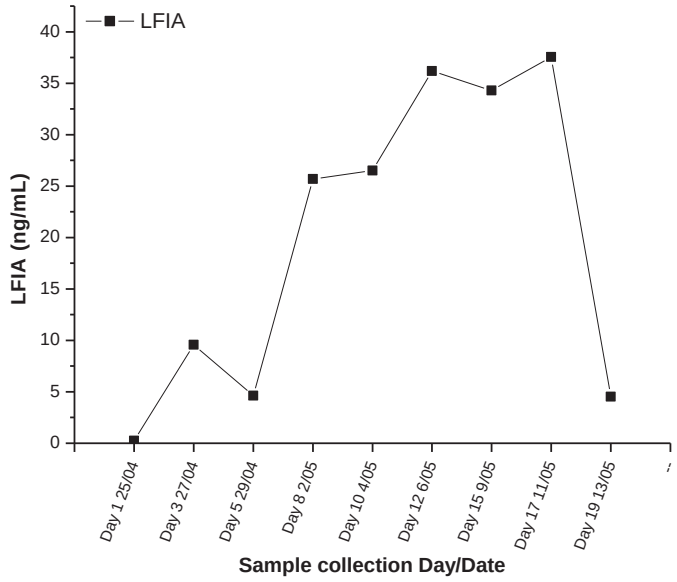

Figure 3.32 LFIA analysis of milk samples from cow 2 after protein and fat removal.

The ELISA P4 cycle showed a similar gradual increase in P4 concentration from Day 1 to Day 5, which indicated the LFIA method was possibly overestimating the concentration on Day 3 or underestimated the concentration on Day 5. The LFIA method was not able to distinguish the peak of the cycle on Day 10, but was able to indicate the end of the P4 cycle, which is important for estrus detection (Figure 3.33).

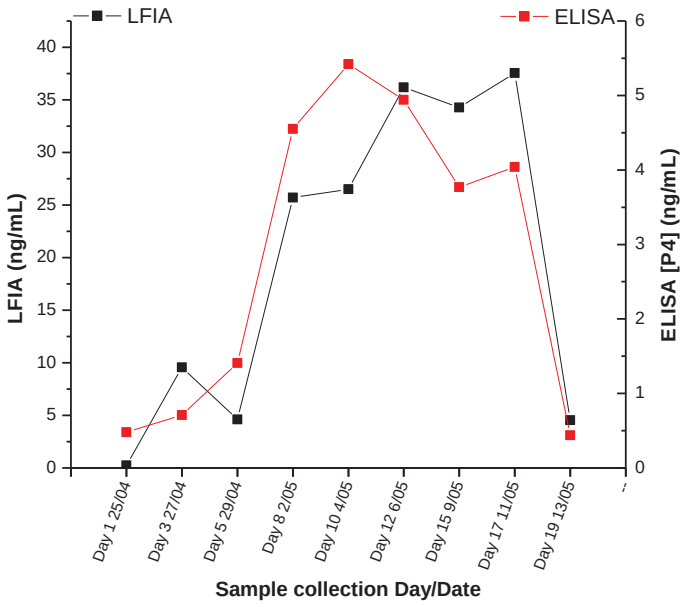

Figure 3.33 Overlap of the LFIA P4 cycle and the ELISA P4 cycle. The general trend of the P4 cycle was demonstrated by using the LFIA method for milk sample analysis on cow 2.

The concentrations obtained from LFIA analysis were still consistently higher than the concentrations from ELISA analysis. However, the general profile of the P4 cycle from LFIA did not match as closely as the previous analysis using milk samples from cow 1. It is possible the assay was less sensitive due to the antibody dissociation from the AuNPs' surface and this process usually results in the precipitation of AuNPs (the antibody-AuNP conjugates are generally stable for approximately 6 months).

The analysis was repeated using milk samples from cow 2 with newly conjugated Anti-P4-Au. The assays were carried out using the same conditions and method. The calculated P4 concentrations showed a long period of basal concentration. The P4 concentration spiked on Day 15 and peaked on Day 17, followed by slight decrease on Day 19 and continued till Day 22 (Figure 3.34).

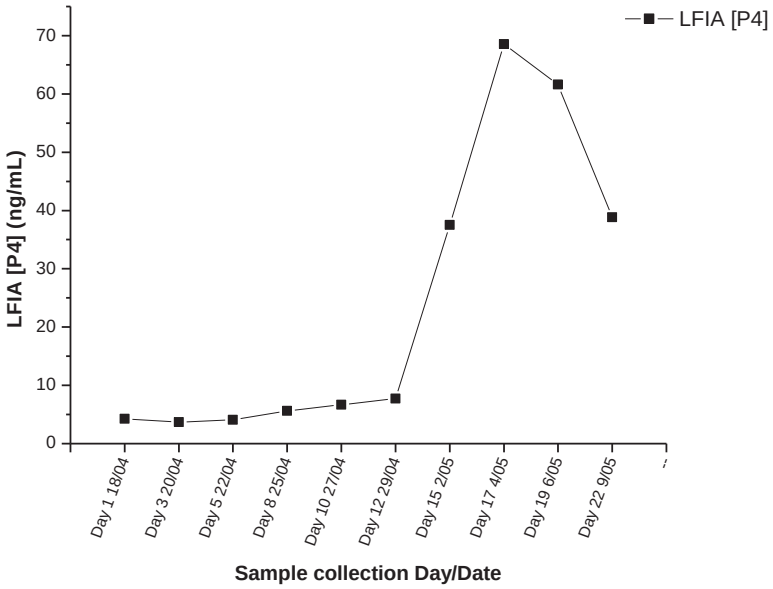

Figure 3.34 A repeat of the P4 cycle of cow 2 analysed by LFIA with newly conjugated Anti-P4-Au.

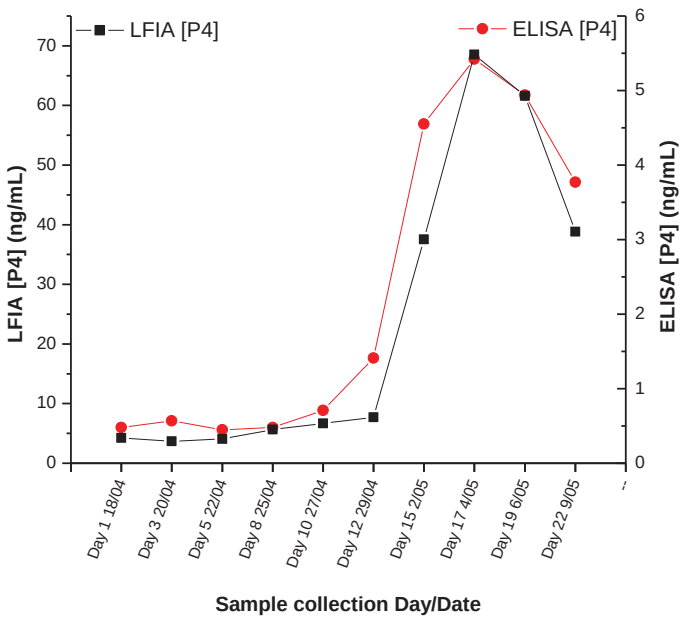

Figure 3.35 Overlap of the repeat LFIA analysed P4 cycle and ELISA analysed P4 cycle for cow 2.

The overlapped cycle showed the P4 cycle analysed from ELISA had the same long period of basal concentration as from LFIA. The P4 profile obtained from LFIA resembled that of the ELISA analysed P4 cycle. The LFIA assay was able to distinguish the basal concentration in pro-estrus stage, and the increase in P4 concentration in the metestrus stage and diestrus stage where the P4 concentration decreased (Figure 3.35). The assay still overestimates the

concentration (approximately 10 times higher), but it is most likely due to the matrix effect from the milk sample regardless of the protein precipitation and extraction process. However, after completion of the analysis of a full set of milk samples, the results indicated that the sample preparation method and the LFIA assay allowed the profile of the estrous cycle to be established.

3.6 Conclusions

The new P4 linker P4-PEG-OVA discussed in chapter 2 as a base sensor for SPR studies was incorporated into LFIA studies as well. The P4-PEG-OVA linker was used as the test line on a test strip with IgG as control line. The P4 standard curve was established and used for both serum and milk analysis.

The P4 analysis for a diluted serum sample was carried out using LFIA and compared with independent ECLIA analysed P4 concentrations. The LFIA methods showed a good P4 fitting profile but with an overestimate of P4 concentration.

The major issues for milk analysis using LFIA are the fat and protein present in the sample. The milk sample required pre-treatment to remove them in order to be able to perform the assay.

The matrix effects from both serum and milk samples were not completely removed after the sample pre-treatment, but reduced significantly. For a ligand-binding type of assay such as LFIA, non-specific interactions between the biological components with the assay components and the surface are the major cause of matrix effects. The matrix effects were likely caused by the matrix component (in the sample) bound to the antibody (assay component) non-specifically in the LFIA which led to inaccurate quantitation for the assay.

The reagent (Anti-P4-Au) used for the assay has a shelf life of approximately 6 months and requires refrigeration at 4 ℃. The sensor strips also have a long shelf life of over 8 months and with no special storage requirements.

With appropriate sample pretreatment the milk P4 cycle obtained from LFIA analysis resembled the independent ELISA analysed P4 cycle. In conclusion, the results indicated that the LFIA method can be a potentially quick, easy and cost effective semi-quantitative P4 analysis for serum and milk samples.

References

(1) Plotz, C. M.; Singer, J. M. *The American Journal of Medicine* **1956**, *21*, 888.

(2) *Immunoassays in Agricultural Biotechnology*; Shan, G., Ed.; John Wiley & Sons, Inc.: New Jersey, **2011**.

(3) Leuvering, J. H. W.; Thal, P. J. H. M.; Van der Waart, M.; Schuurs, A. H. W. M. *Fresenius' Zeitschrift fuer Analytische Chemie* **1980**, *301*, 132.

(4) Karra, S. R.; Schibli, R.; Gali, H.; Katti, K. V.; Hoffman, T. J.; Higginbotham, C.; Sieckman, G. L.; Volkert, W. A. *Bioconjugate Chemistry* **1999**, *10*, 254.

(5) Hu, F.; Cutler, C. S.; Hoffman, T.; Sieckman, G.; Volkert, W. A.; Jurisson, S. S. *Nuclear Medicine and Biology* **2002**, *29*, 423.

(6) Nie, S.; Emory, S. R. *Science* **1997**, *275*, 1102.

(7) Rosi, N. L.; Giljohann, D. A.; Thaxton, C. S.; Lytton-Jean, A. K. R.; Han, M. S.; Mirkin, C. A. *Science* **2006**, *312*, 1027.

(8) Sperling, R. A.; Rivera Gil, P.; Zhang, F.; Zanella, M.; Parak, W. J. *Chemical Society Reviews* **2008**, *37*, 1896.

(9) Grzelczak, M.; Perez-Juste, J.; Mulvaney, P.; Liz-Marzan, L. M. *Chemical Society Reviews* **2008**, *37*, 1783.

(10) Ayong, L. S.; Tume, C. B.; Wembe, F. E.; Simo, G.; Asonganyi, T.; Lando, G.; Ngu, J. L. *Tropical medicine & international health : TM & IH* **2005**, *10*, 228.

(11) Delmulle, B.; De Saeger, S. M. D. G.; Sibanda, L.; Barna-Vetro, I.; Van Peteghem, C. H. *Journal of Agricultural and Food Chemistry* **2005**, *53*, 3364.

(12) Mettler, M.; Grimm, F.; Capelli, G.; Camp, H.; Deplazes, P. *Journal of Clinical Microbiology* **2005**, *43*, 5515.

(13) van Amerongen, A.; Wichers, J. H.; Berendsen, L. B. J. M.; Timmermans, A. J. M.; Keizer, G. D.; van Doorn, A. W. J.; Bantjes, A.; van Gelder, W. M. J. *Journal of Biotechnology* **1993**, *30*, 185.

(14) Oku, Y.; Kamiya, K.; Kamiya, H.; Shibahara, Y.; Ii, T.; Uesaka, Y. *Journal of Immunological Methods* **2001**, *258*, 73.

(15) Salomone, A.; Mongelli, M.; Roggero, P.; Boscia, D. *Journal of Plant Pathology* **2004**, *86*, 43.

(16) Klewitz, T.; Gessler, F.; Beer, H.; Pflanz, K.; Scheper, T. *Sensors and Actuators, B: Chemical* **2006**, *B113*, 582.

(17) Fernandez-Sanchez, C.; McNeil, C. J.; Rawson, K.; Nilsson, O.; Leung, H. Y.; Gnanapragasam, V. *Journal of Immunological Methods* **2005**, *307*, 1.

(18) Posthuma-Trumpie, G. A.; Korf, J.; van Amerongen, A. *Analytical and Bioanalytical Chemistry* **2009**, *393*, 569.

(19) Noakes, D. E. *Fertility and obstetrics in cattle*; 2 ed.; Blackwell Science: Oxford, **1997**.

(20) *Factors affecting Calf Crop: Biotechnology of Reproduction*; 1 ed.; Fields, M. J.; Sand, R. S.; Yelich, J. Y., Eds.; CRC Press: New York, **2002**.

(21) Lehrer, A. R.; Lewis, G. S.; Aizinbud, E. *Animal Reproduction Science* **1992**, *28*, 355.

(22) Millipore Corporation. *Rapid Lateral Flow Test Strips: Considerations for production development*, **2008**, http://www.millipore.com/techpublications/tech1/tb500en00.

(23) Leung, W.; Chan, P.; Bosgoed, F.; Lehmann, K.; Renneberg, I.; Lehmann, M.; Renneberg, R. *Journal of Immunological Methods* **2003**, *281*, 109.

(24) van Dam, G. J.; Wichers, J. H.; Ferreira, T. M. F.; Ghati, D.; van Amerongen, A.; Deelder, A. M. *Journal of Clinical Microbiology* **2004**, *42*, 5458.

(25) Jin, S.; Chang, Z. Y.; Xu, M.; Min, C. L.; Wei, H.; Sheng, L. Y.; Hong, G. X. *Clinical and Diagnostic Laboratory Immunology* **2005**, *12*, 198.

(26) Reis, M. F.; Aniceto, P.; Aguiar, P.; Simao, F.; Segurado, S. *International Journal of Hygiene and Environmental Health* **2007**, *210*, 419.

(27) Rembaum, A.; Dreyer, W. J. *Science* **1980**, *208*, 364.

(28) Jiang, X. Q.; Waterland, M.; Blackwell, L.; Wu, Y. Q.; Jayasundera, K. P.; Partridge, A. *Steroids* **2009**, *74*, 819.

(29) Souza, G. R.; Christianson, D. R.; Staquicini, F. I.; Ozawa, M. G.; Snyder, E. Y.; Sidman, R. L.; Miller, J. H.; Arap, W.; Pasqualini, R. *Proceedings of the National Academy of Sciences of the United States of America* **2006**, *103*, 1215.

(30) Huang, Y.; Chiang, C.-Y.; Lee, S. K.; Gao, Y.; Hu, E. L.; De Yoreo, J.; Belcher, A. M. *Nano Letters* **2005**, *5*, 1429.

(31) Dragnea, B.; Chen, C.; Kwak, E.; Stein, B.; Kao, C. C. *Journal of the American Chemical Society* **2003**, *125*, 6374.

(32) *Steroid Analysis*; 2 ed.; Makin, H. L. J.; Gower, D. B., Eds.; Springer Netherlands: London, **2010**.

(33) van Wyk, V.; van Aarde, R. J.; Louw, A. I. *Comparative Biochemistry and Physiology, Part A: Molecular & Integrative Physiology* **1994**, *108A*, 265.

(34) Hammond, G. L.; Nisker, J. A.; Jones, L. A.; Siiteri, P. K. *Journal of Biological Chemistry* **1980**, *255*, 5023.

(35) Shintani, K.; Yoshida, N.; Sekiba, K. *Endocrinologia Japonica* **1987**, *34*, 221.

(36) Simersky, R.; Swaczynova, J.; Morris, D. A.; Franek, M.; Strnad, M. *Veterinarni Medicina* **2007**, *52*, 19.

(37) Gowan, E. W.; Etches, R. J. *Theriogenology* **1979**, *12*, 327.

(38) Laing, J. A.; Heap, R. B. *British Veterinary Journal* **1971**, *127*, XIX.

(39) Beckonert, O.; Keun, H. C.; Ebbels, T. M. D.; Bundy, J.; Holmes, E.; Lindon, J. C.; Nicholson, J. K. *Nature Protocols* **2007**, *2*, 2692.

Chapter 4

Toward an alternative sensing material for SPR sensing: Polyhydroxyalkanoate granules

4.1 Introduction to polyhydroxyalkanoates

Polyhydroxyalkanoate (PHA) granules are spherical inclusions produced by bacterial fermentation, and are formed by biopolymerization occurring within bacterial cells. The PHA granules are synthesized by most bacteria when nutrients are limited, the bacteria converts the excess carbon intracellularlly into insoluble spherical inclusions. PHAs have many interesting properties such as biocompatibility, biodegradability, and they are a renewable resource.

PHAs have been applied to the medical field to develop implants such as heart valves, stents and bone scaffolding.[1,2] It has also been suggested that PHA polyesters can be a new substitution for polyolefin containers, plastic films and bags. Although there are considerable industrial interests in PHAs, the main problem in the manufacture and commercialization of PHA polyesters as a new source of biodegradable plastics is the significant cost of the substrate used for the growth of the microorganisms. Researchers have been seeking alternative inexpensive carbon sources such as plant oils,[3,4] molasses,[5,6] starch,[7,8] whey[9] and industrial wastes[10,11]. Polyhydroxybutyrate (PHB) and poly(3-hydroxybutyrate-co-3-hydroxyvalerate) (PHBA, a PHA copolymer) are still the main members of PHAs which are mass produced commercially, and it is recognised that PHA production capacity will increase due to the high demand.

The size and the functionality of PHAs also provide applications to drug delivery, diagnostics, bioseparation and protein immobilisation. The nano/micro size of this biological material gives it great potential for drug delivery, imaging/biomarker (with fluorescence property) and biosensors.

4.2 Polyhydroxyalkanoate granules

Microorganisms are known to form spherical inclusions intracellularly, and the inclusions can be divided into two main categories, the inorganic and organic inclusions. Examples of inorganic inclusions are magnetosomes and biopolymers are examples of organic inclusions.

Polyhydroxyalkanoates (PHAs) are the organic water insoluble organic polyesters composed of (R)-3-hydroxy fatty acids which are synthesised by a wide range of prokaryotic microorganisms. The key enzyme of the PHAs biosynthesis is PHA synthase which is responsible for the polymerisation of the (R)-3-hydroxyacyl-CoA thioester monomer to the respective polyester.

PHA appear within the cell as intracellar granules, with molecular weights of up to 2 x 10^6 kDa and dimensions typically around 0.2 to 0.5 μm.[12] PHAs are made by the cell when one of the nutrients such as nitrogen, phosphate or iron is limited, so the excess carbon source is stored as polyester granules. The organism can store up to 80% of its body weight in the form of PHAs. Poly-(R)-(3-hydroxybutyrate), P2HB in *Bacillus megaerium* is the first PHA to have been reported in the literature by M. Lemoigne in 1926.[13]

Polyester synthases are the key enzymes used in the formation of polyesters. There are four major classes of polyester synthases: Class I, II, III, and IV. Class I and II comprise enzymes consisting of only one type of subunit (PhaC) with molecular weight ranges from 61 to 73 kDa.[14] Both Class I and Class II polyester synthases preferentially utilized CoA thioesters of various (R)-3-hydroxy fatty acids, where Class I had a preference for (R)-3-hydroxy acids comprising 3-5 carbon atoms but Class II had a preference for similar acids containing 6-14 carbon atoms.[15,16]

Class III polyester synthases consist of two different subunits PhaC and PhaE where the molecular weight of both subunits is around 40 kDa. It prefers CoA thioesters of an (R)-3-hydroxy fatty acid comprising 3-5 carbon atoms.[17,18] Class IV polyester synthases (*Bacillus megaterium*) are similar to Class III, and consists of two subunits, PhaC (~40 kDa) and PhaR (~22 kDa).[19,20] This classification of synthases does not allow polyester inclusion of the synthases from *Thiocapsa pfennigii*, *Aeromona punctata*, and *pseudomonas* sp.61-3 due to substrate specificity.[21]

The exact structure of PHA granules has not been fully determined. However, the results from small-angle neutron scattering are consistent with the phospholipid monolayer model which is shown in Figure 4.1.[22,23]

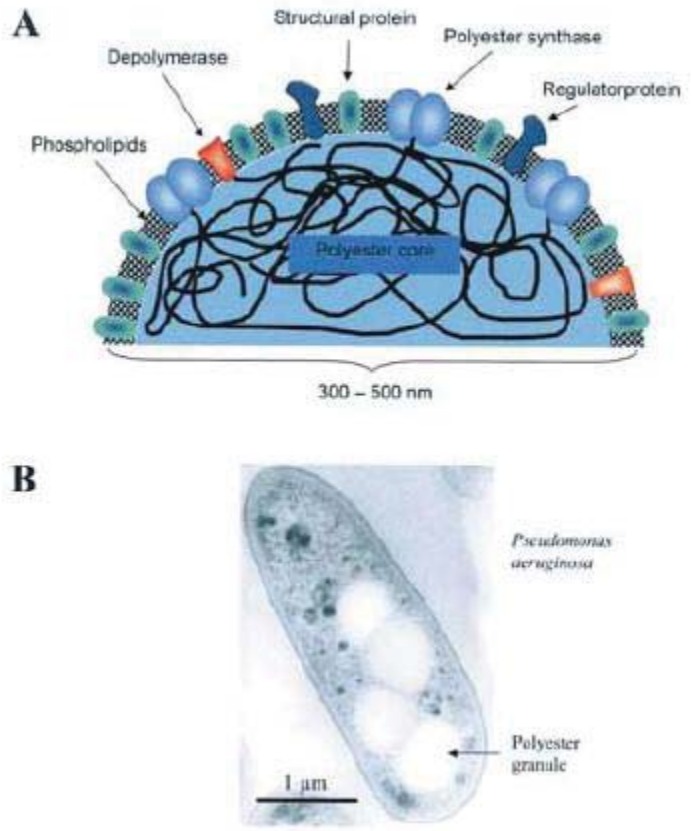

Figure 4.1 A) Proposed structure of a polyester granule. The small water insoluble inclusions are formed with a amorphous polyester core with polyester synthase covalently attached to the surface.[15] B) Electron microscopy image of *Pseudomonas aeruginosa* accumulating polyester granules.[15]

4.2.1 Formation of polyester granules

The small water-insoluble polyester granules are formed with an amorphous polyester core with polyester synthase covalently attached to the surface. There are two proposed models for polyester granule formation as depicted in Figure 4.2. The micelle model (Figure 4.2A) outlines the *in vitro* formation in the absence of phospholipids, and the Budding model (Figure 4.2B) predicts that the granules are formed at the cytoplasmic membrane. In the latter the water soluble polyester synthase is converted into amphipathic molecules which then undergo self-assembly in the membrane or cytosol.

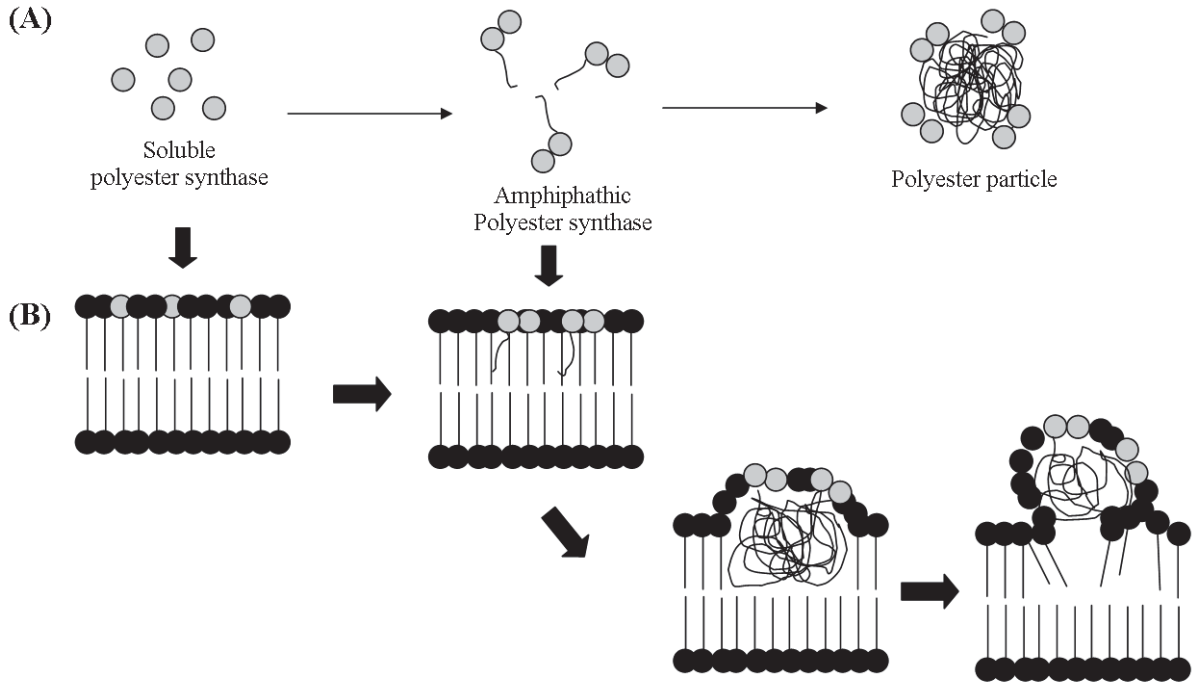

Figure 4.2 Model of polyester granule formation. A) Micelle model, and B) Budding model.[24]

4.2.2 Multifunctional inorganic binding beads

The genetically engineered polypeptides for inorganics (GEPIs) represent another class of sensing materials and could be utilised and developed into many applications in different areas including engineered probes for targets recognition, multi-drug delivery, heterofunctional nanoassemblers, biocompatible surface for therapeutics, biomineralisation, morphogenesis, and tissue engineering.

One type of the GEPIs selected (by phage display or cell surface display) were the gold binding proteins that were isolated as extracellular loops of maltoporin which subsequently fused to the amino terminus of the alkaline phosphatase with retention of gold binding activity. The 14 amino acids motif, MHGKTQATSGTIQS, GBP-1 does not contain cysteine which is known to bind to gold via the thiol linkage.[24]

A study of GBP-1 has been done using surface plasmon resonance spectroscopy on a metallic gold surface and the result showed that in order to increase the binding activity, the amino acid sequence needed to be repeated at least 3 times to give 3R-GBP-1.[25]

Genetic fusion of GEPIs to polyester synthase (PhaC) or already engineered PhaC enables the production of polyester granules which have the properties of binding to a specific inorganic metal and biological molecules (Figure 4.3).[24]

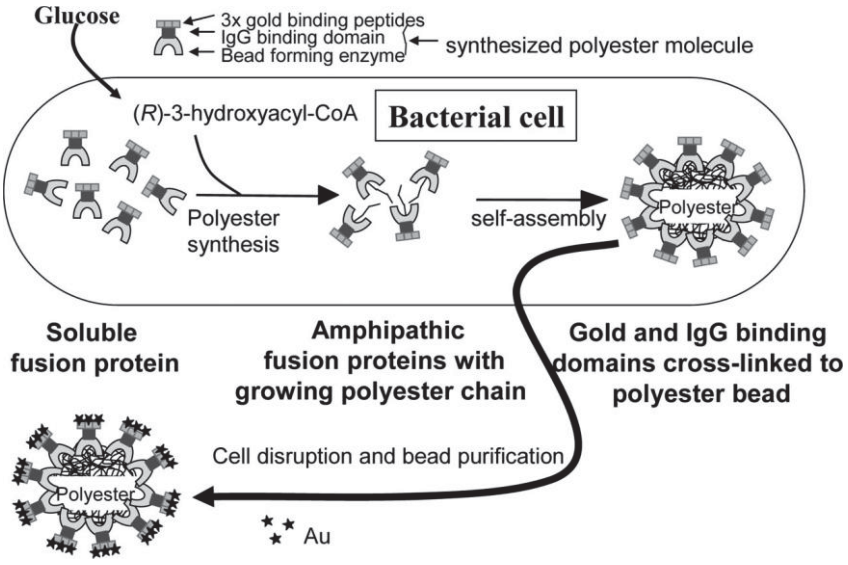

Figure 4.3 Genetically fused 3R-GBP-1, bead formation enzyme (polyester synthases) and extra binding domain protein (IgG) enable the formation of polyester inclusion within the bacterial cell.[24]

The antibody binding domain of protein A (ZZ domain) from *Staphylociccus aureus* was used for additional binding functionality which enables the formation of the spherical polyester inclusion to bind any specific antibody as well as inorganic metals.

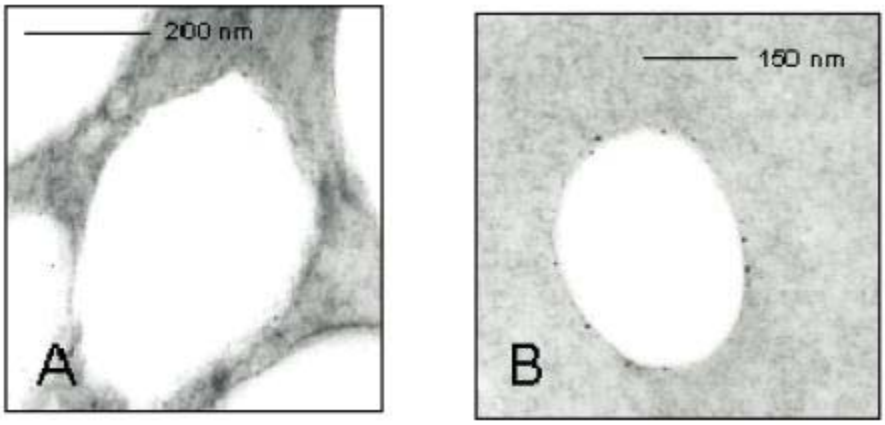

Figure 4.4 TEM images of PHA beads after incubation with colloidal gold, with PHA beads A displaying the ZZ(-)PhaC protein at the surface and PHA beads B containing the engineered protein 3xGN-G_5-ZZ(-)PhaC on the surface with gold nanoparticles. Figure A shows no gold attached but Figure B does.[24]

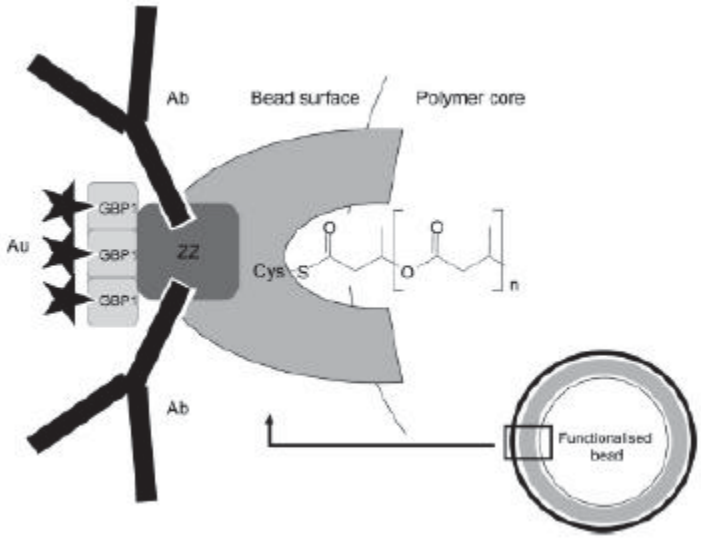

Figure 4.5 Scheme of the surface of a bifunctional gold/antibody binding PHA bead.[24]

The addition of (R)-3-hydroxyacyl-CoA promotes the polyester synthesis. The water soluble fused protein was then fused with the growing polyester chain to initiate the self-assembly process resulting in the gold and IgG binding domains cross-linked to the polyester bead. The

polyester beads are isolated by disruption of the bacterial cell followed by purification and the desired metal (Au in this case) can then be incubated onto the beads (Figure 4.4) (see Appendix A.4.1).

It is possible to synthesise the polyester beads with gold and silica as well as antibody binding capability as multifunctional beads.

The formation of the bifunctional gold/antibody binding beads requires that 3GBP-1 is fused with the PhaC protein, then the beads are formed and coated with the protein within the bacterial cells. The soluble PhaC protein is then covalently linked with the core of the polyesters (Figure 4.5).[26,27] The polyester can be stained with dye in order to closely monitor the beads' formation using a fluorescence microscope.

There are a few potential applications for GEPIs (Figure 4.6), however, their multi-binding function may allow SPR and LFIA based sensor development.

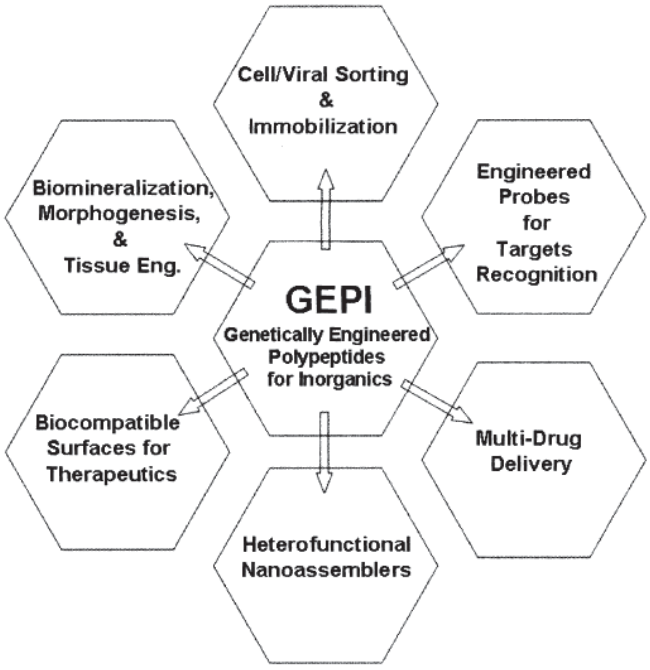

Figure 4.6 There are many possible applications for GEPI, including biosensing studies.[21]

4.3 Applications of PHA granules

There are many potential applications for PHAs within the medical and pharmaceutical industries because it is both biocompatible and biodegradable. The PHA copolymer, poly(3-hydroxybutyrate-co-3-hydroxyvalerate)(3HBV) is less stiff but a tougher polyester than PHA, which may be used as packaging material. The biodegradable polymers such as P(3HBV) are frequently used in tissue engineering, and are often used in bone plates, osteosynthetic material and surgical sutures. It is also used as slow release agents for drugs and hormones deliveries.[28] However, the rate of biodegradation is too slow in the human body; hence there are restricted uses of the material.

PHAs also bind to many antibodies (both monoclonal and polyclonal, Figure 4.7) with somewhat high binding affinity, hence it has been used as a purification tool for IgG.[29]

MONOCLONAL			POLYCLONAL	
Human	IgG_1	++++	Rabbit	++++
	IgG_2	++++	Cow	++
	IgG_3	---	Horse	++
	IgG_4	++++	Goat	-
Mouse			Guinea pig	++++
	IgG_1	+	Sheep	+/-
	IgG_{2a}	++++	Pig	+++
	IgG_{2b}	+++	Rat	+/-
	IgG_3	++	Mouse	++
Rat			Chicken	---
	IgG_1	---	Human IgG	++++
	IgG_{2a}	---	Human IgM	---
	IgG_{2b}	---	Human IgD	---
	IgG_{2c}	+	Human IgA	---

Figure 4.7 Binding affinity of a ZZPhaC polyesters for various antibodies, where (----) represents weak binding affinity, and (++++) represents strong binding affinity.

4.4 Surface applications

It is known that 3GNZZPhaC beads bind to gold nanoparticles (AuNPs) due to the infusion of GBP, hence the beads were immobilised to a Au coated surface to observe the binding property. Methods needed to immobilise the beads included dip coating, spin coating, microplotting, and simple immobilisation. The ability of 3GNZZPhaC to bind to the Au surface is important as this will determine whether the 3GNZZPhaC beads may be a useful material for surface sensing. In the present study the first two methods were trialled and will now be discussed.

4.4.1 Dip coating

Dip coating is a common method to fabricate a thin film on a desired substrate surface. The substrate is immersed in the coating material at constant speed. The repeat steps of immersing the substrate into the coating material, pulling out the substrate from the solution and allowing the coating material to deposit on the substrate (with drainage of the excess liquid as well as evaporation of the solvent from the liquid), enables a thin film to be deposited onto the substrate surface.

The sample solution of 3GNZZPhaC was prepared in HBS-EP^+ buffer (10 mM, pH 7.4, the SPR buffer), and the gold coated mylar chip was cleaned with ethanol, air dried and then attached to the dip coating setup (Figure 4.8). The gold coated mylar chip was dip coated for 1 hour followed by washing with Milli-Q H_2O and then subjected to fluorescence and SEM microscopic studies.

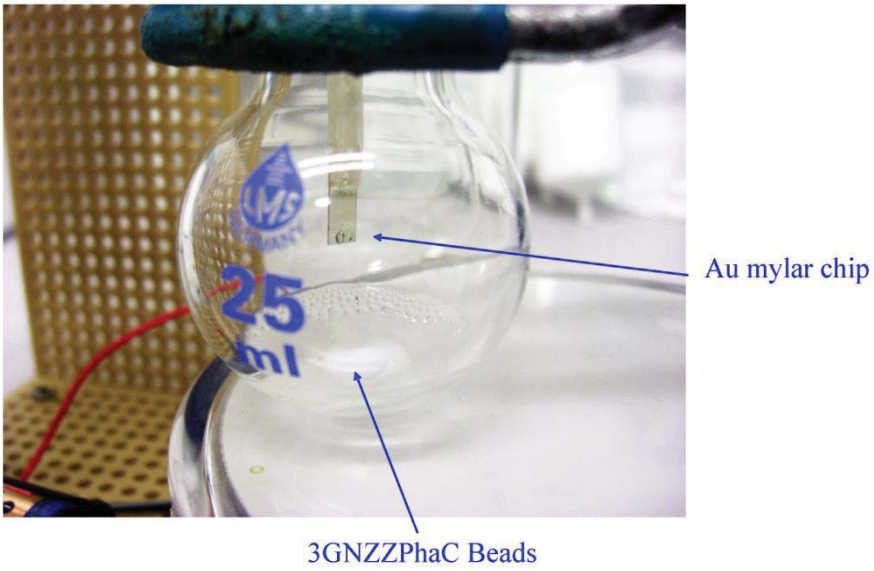

Figure 4.8 The dip coating set up for 3GNZZPhAC beads. The Au coated mylar chip was dip coated with 3GNZZPhaC beads followed by washing of the surface with Milli-Q H_2O. To reduce aggregation of the 3GNZZPhaC beads, the bead solution was under continuous stirring while the Au chip underwent the dip coating process.

4.4.2 Spin coating

Spin coating is also a common procedure to produce a uniform thin film. An excess amount of coating solution is placed on the substrate, then rotated at constant speed to evenly distribute the solution by centrifugal force using a spin coater.

0.5 μL of the 3GNZZPhaC bead solution (10 ng/mL) was deposited onto the surface of a gold coated microscope slide (1 cm x 1 cm). The sample was coated at 1000 rpm for 2 minutes 20 seconds in HBS-EP^+ buffer (10 mM, pH 7.4) and the slide was subjected to SEM analysis.

4.5 Flow cell system

The interaction between the analyte and the sensor chip occurs in the micro fluidic system. Hence the micro fluidic system is the most crucial component of the SPR system. The flow cells are formed by pressing the sensor chip against the set of open channels on the surface of the integrated micro fluidic cartridge (IFC). The IFC consists of a series of micro channels and membrane valves encased in a plastic housing which controls the liquid flow to the sensor surface.

A model flow cell system was constructed for the purpose of determining the binding interaction between PHA beads and the Au surface. It was constructed using a polycarbonate slice to imitate the SPR X100 micro fluid channels which consisted of an inlet, and an outlet and a single channel (Figure 4.9). The 1 mm channel was carved into the polycarbonate slice with two holes drilled downwards to connect with the inlet and outlet paths.

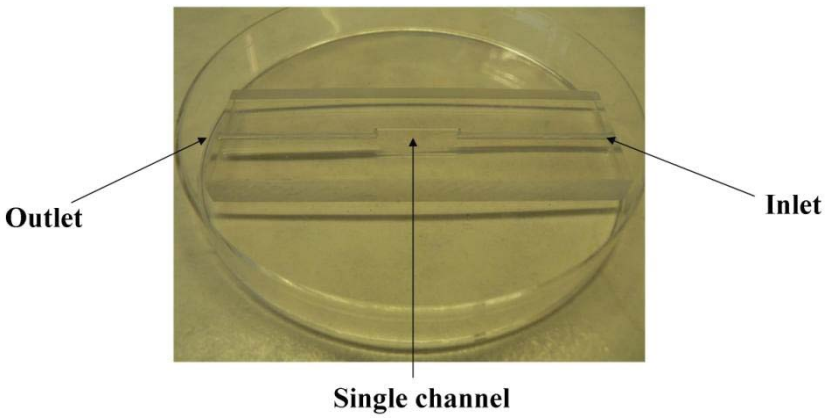

Figure 4.9 Flow cell with an inlet and an outlet and a single channel.

As a gold sensor surface is required for a SPR sensing system, a Au coated sensor chip was also designed and fabricated for the flow cell. Microscope slides were cut and cleaned with methanol and then sonicated for 15 minutes and dried. The glass slices were then gold sputtered coated at 18~20 mA for 6 minutes (Figure 4.10). Double sided tape was cut into shape (cutting out where the channel goes through) and used to seal the flow cell.

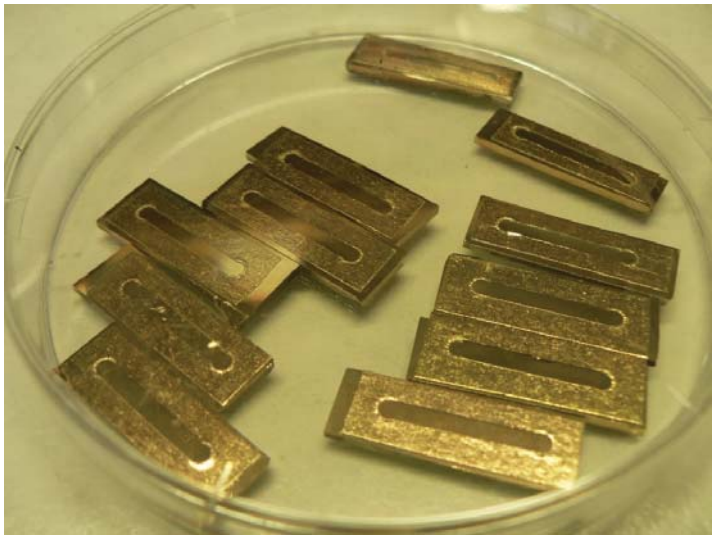

Figure 4.10 Glass surfaces coated with gold acting as a sensor chip for the SPR sensing system.

Non-gold-sputtered coated slides (Figure 4.11) were also cut and fabricated following the same method as before to use as a reference to monitor the non-specific binding.

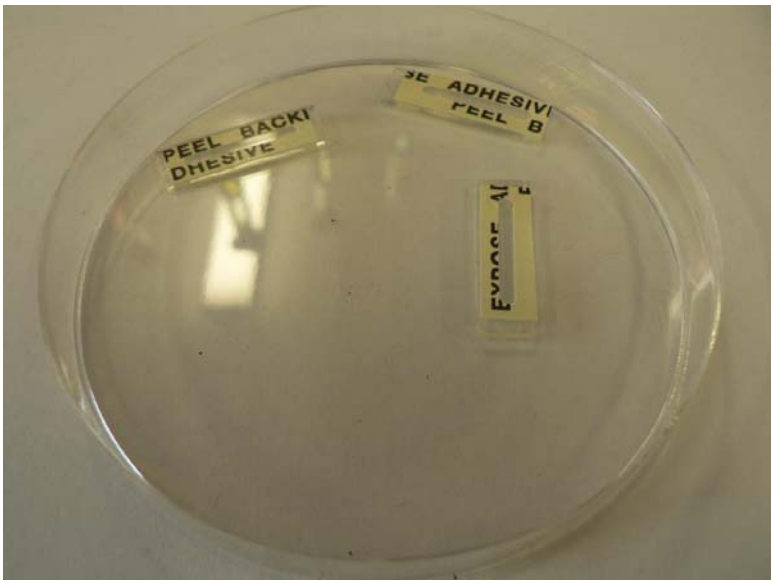

Figure 4.11 Reference glass slide with double-sided tape.

The upper layer of double-sided tape was removed and the glass slide was sealed onto the flow cell (Figure 4.12, Figure 4.13). The top face of the flow system is where the binding should occur similar to the SPR system. The inlet and outlet tubes were attached to the flow cell unit and attached to a 1 mL syringe.

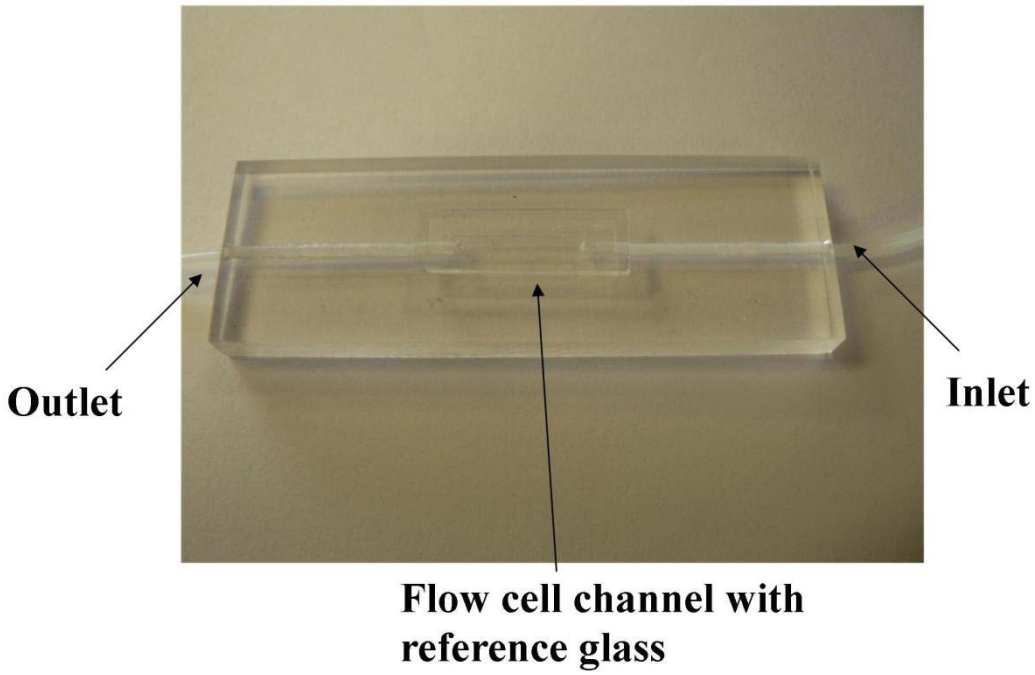

Figure 4.12 The flow cell channel was sealed with the reference glass slide and with inlet and outlet tubes attached to the flow cell system.

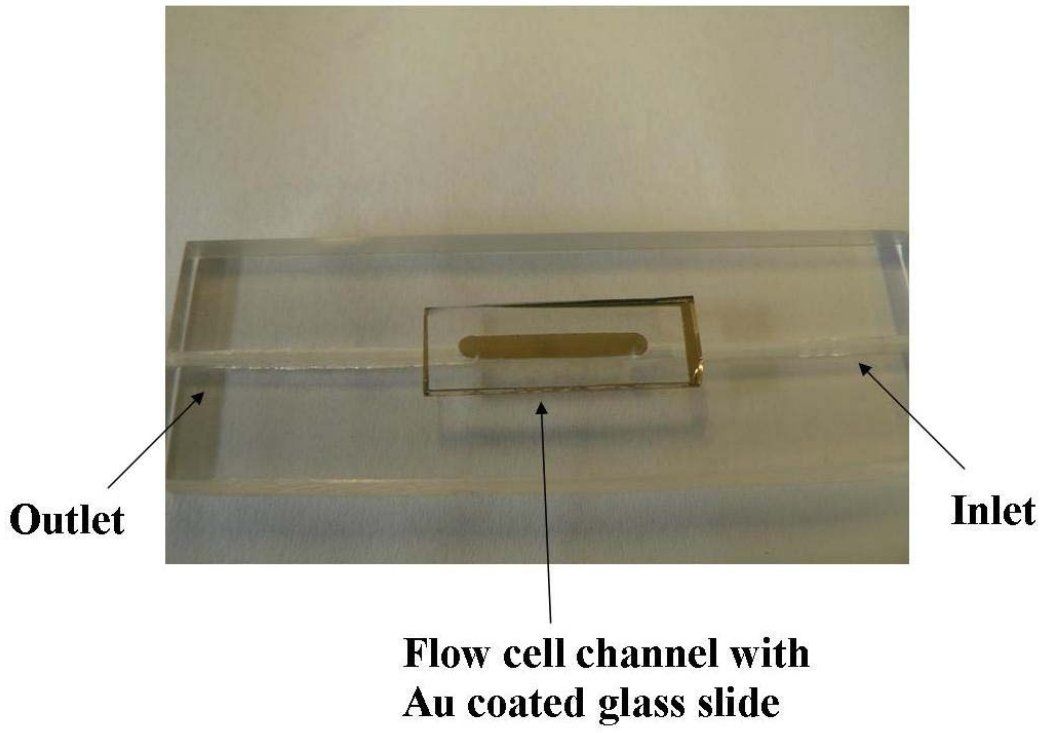

Figure 4.13 The flow cell channel was sealed with the Au coated glass slide and with inlet and outlet tubes attached to the flow cell system.

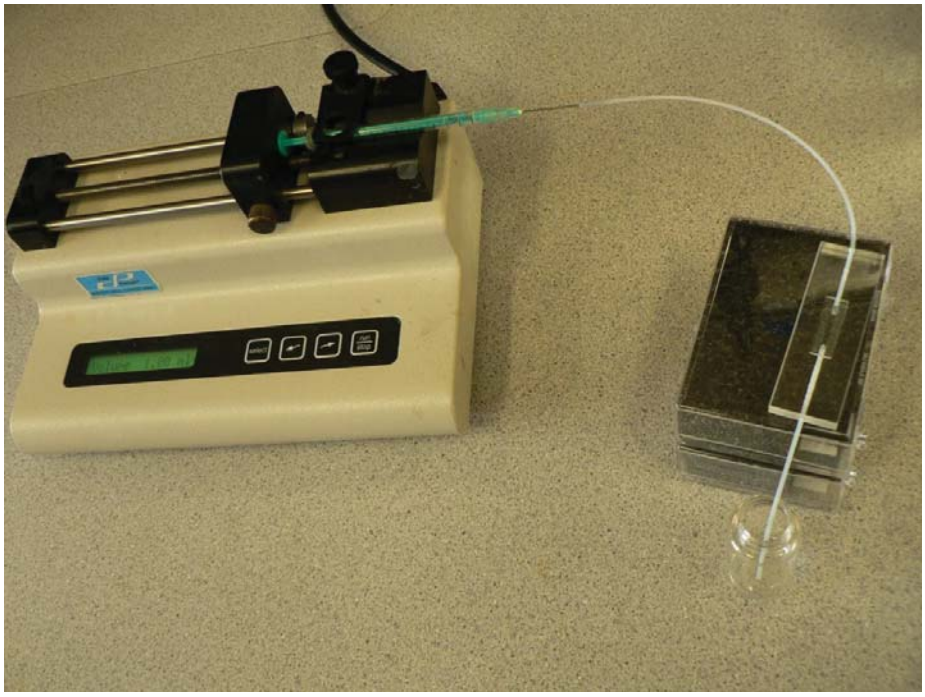

Figure 4.14 F**low cell system setup. The single flow cell system with reference glass slide was attached to syringe pump from the inlet tube and injected with a 3GNZZPhaC bead solution at 2 mL/hr. The residue solution flowed through the flow cell channel and exited from the outlet tube.**

The flow cell was sealed with a reference glass slide then attached to a syringe pump (Figure 4.14). The 3GNZZPhaC bead solution (1 mL, 1 ng/mL, wet weight) was injected at 2 mL/hr followed by injection of 100 μL of Milli-Q H_2O to remove salt residues in the tubing and on the sensor surface. The glass slide was then taken off carefully for further SEM analysis. The flow cell was cleaned with methanol and air dried.

The procedure was repeated with Au coated slides with in injection volumes of 1 mL, 2 mL and 3 mL respectively. The Au coated slides were subjected to SEM analysis, and the SEM images showed that the 3GNZZPhaC beads bound to the surface under a continuous flow system and the number bound increased as the injection volume increased.

4.6 Microscopy studies

4.6.1 Scanning electron microscopy studies

The scanning electron microscopy technique enables the study of sample surfaces with high resolution and allows confirmation of the surface immobilisation.

Sample slides were taped to an aluminium stub using double sided tape, the sample slide and the stub was then connected using a drop of silver paint (at the edge of the slide and the stub). The sample was then Au sputtered coated for 200 s using a BAL-TEC SCD 050 sputter coater.

4.6.1.1 3GNZZPhaC immobilisation on the Au surface

The samples obtained from simple surface immobilisation studies showed impurity residues even after washing with buffer and Milli-Q H_2O. The sample was subjected to fluorescence microscopy imaging to confirm the immobilisation level. The image was recorded and the 3GNZZPhaC beads (with Nile red dye) were attached to the Au surface (Figure 4.15).

A SEM image (Figure 4.16, Figure 4.17, and Figure 4.18) of the 3GNZZPhaC beads showed the impurity was mostly aggregated and embedded in the solvent (HBS-EP^+ buffer) residues. It is most likely that the washing method did not clean up the solvent residues thoroughly and the drying process (under air vacuum) also may have contaminated the surface. The nature of the 3GNZZPhaC beads could also be the reason why they aggregated rather than being spread on the Au surface evenly.

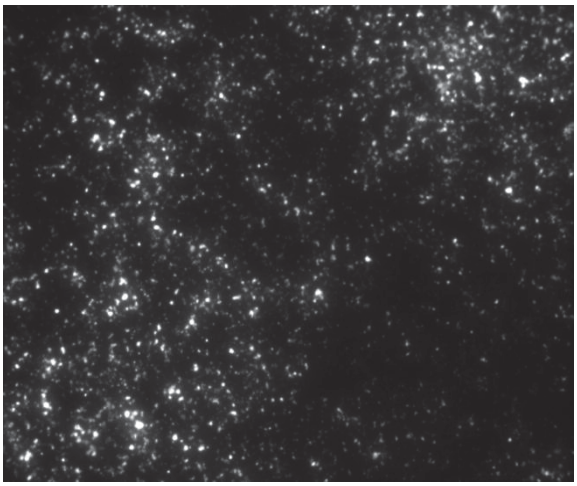

Figure 4.15 The cores of 3GNZZPhaC beads were stained with Nile red dye then immobilised onto the gold surface. The fluorescence image (40x magnification) of 3GNZZPhaC beads at after immobilisation showed they were still present after the washing process.

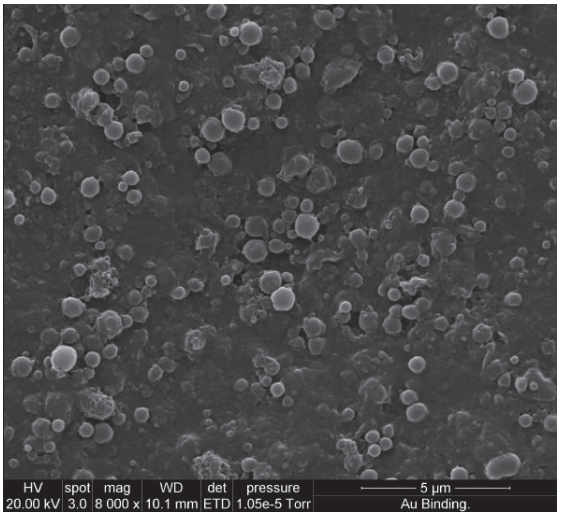

Figure 4.16 A SEM image (8,000x magnification) of 3GNZZPhaC beads after surface immobilisation. The larger 3GNZZPhaC beads were embedded within the solvent residues/contaminants.

However, there were a few beads scattered on the surface without any aggregation, but still with residues surrounding it (Figure 4.17). The 3GNZZPhaC beads appeared to be "sticky", the beads were embedded within the solvent residues or contaminants (Figure 4.16). The interaction between the Au surface and 3GNZZPhaC was expected since 3GNZZPhaC beads bind to AuNPs.[24]

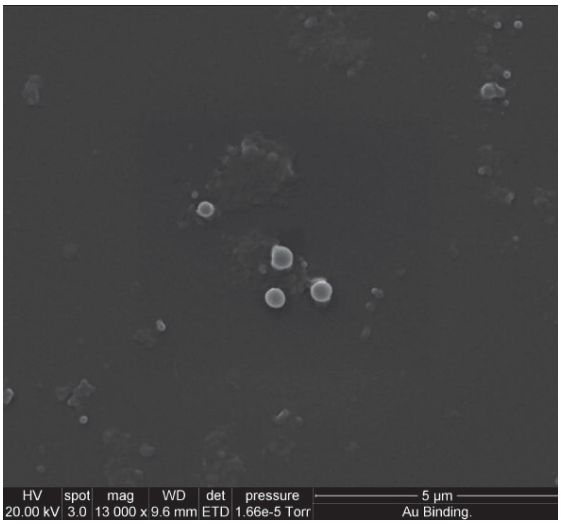

Figure 4.17 Aerial view of an SEM image (13,000x magnification) of 3GNZZPhaC beads after surface immobilisation. There were single layer beads scattered on the surface after cleaning. However, there were residues/ contaminants that still remained.

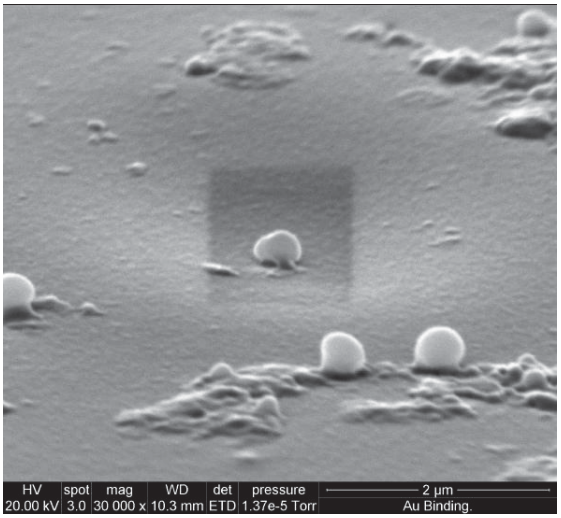

Figure 4.18 Close up (tilted 90°) of an SEM image (30,000x magnification) of 3GNZZPhaC beads after surface immobilisation. It is quite clear that the beads are attached to the surface with the residues/ contaminants "sticking" to it.

4.6.1.2 SEM of ZZPhaC immobilisation on the Au surface

After the ZZPhaC solution (which has the same functionality of 3GNZZPhaC except that the gold binding 3GN component was absent) was immobilised onto the Au surface, the sample was washed with Milli-Q water repeatedly to remove solvent residues and unbound polyesters. SEM images (Figure 4.19, Figure 4.20, Figure 4.21), clearly showed that the ZZPhaC beads were still attached/bound to the gold surface.

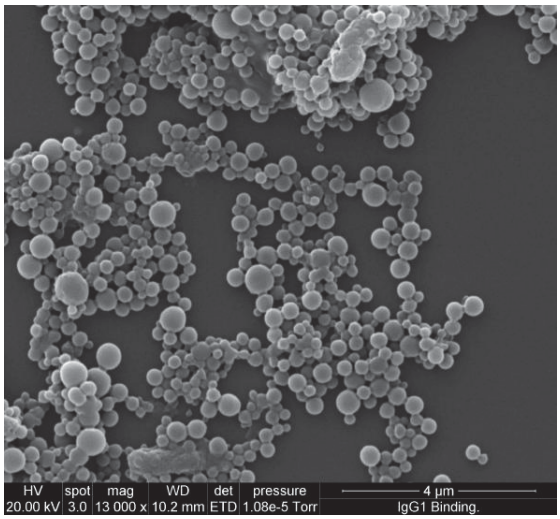

Figure 4.19 Aerial view of an SEM image (13,000x magnification) of ZZPhaC beads after surface immobilisation. The ZZPhaC beads are coagulated on the Au surface.

However, the nature of the interactions between the beads and the gold will require e.g. Raman spectroscopic study and X-ray crystallographic study (see Appendix A.4.6 and A.4.7).

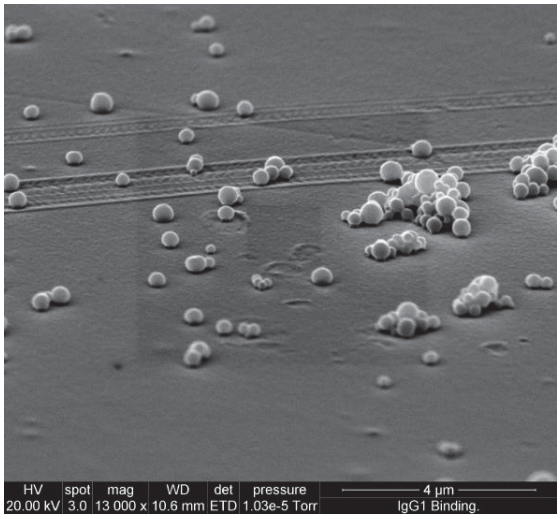

Figure 4.20 SEM image (13,000x magnification) of ZZPhaC beads after surface immobilisation. Some of the beads scattered on the surface with no aggregation.

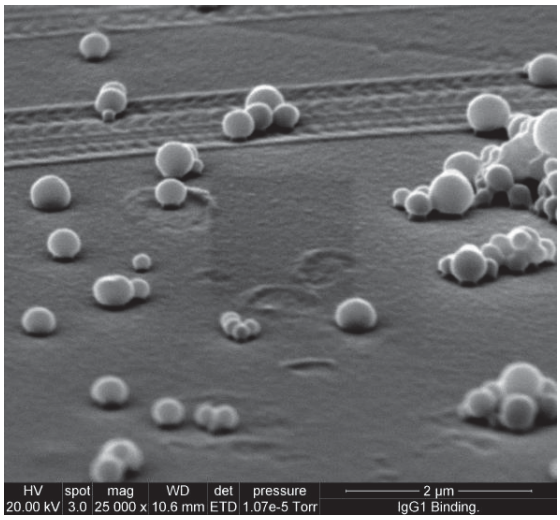

Figure 4.21 Close up (tilted 90°) of an SEM image (25,000x magnification) of ZZPhaC beads after surface immobilisation. The scattered single beads were attached to the Au surface with no solvent residues after cleaning the surface (residues showed in a 3GNZZPhaC sample).

The SEM images indicated that the immobilisation method is more suitable for ZZPhaC beads. The method gives no obvious surface contamination (solvent residues or other

unknown substances) and the scattered single beads were still attached to the surface after cleaning the surface several times.

The results from SEM suggested that the ZZPhaC beads even without the 3GN component, still bound to the Au surface like the 3GNZZPhaC beads. Both 3GNZZPhaC and ZZPhaC beads could potentially be used as SPR capture ligands if coagulation issues can be removed and it becomes possible to replace the dextran matrix in a CM5 chip for the Biacore instrument.

4.6.2 Preliminary atomic force microscopy (AFM) studies

The atomic force microscope is a powerful tool for imaging and surface characterisation. It allows high resolution imaging studies, measuring and manipulating matter at the nanoscale. The AFM comprises a cantilever with a probe to scan the specimen surface. The operation mode for AFM studies involved a tapping mode with a golden silicon cantilever (Ultrasharp, Noncontact NSG II). The Asylum Research MF-3D instrument was used for the surface profiling (Figure 4.22).

Figure 4.22 The Asylum Research MFP-3D model was used for surface profiling.[30]

A 3GNZZPhaC solution (0.1 µg/mL) was deposited on to a Au coated glass by spin coating at 6000 rpm for 2 min. The golden silicon cantilever was used to scan over the surface with tapping mode. The beads were distributed and bound throughout the Au surface (Figure 4.23).

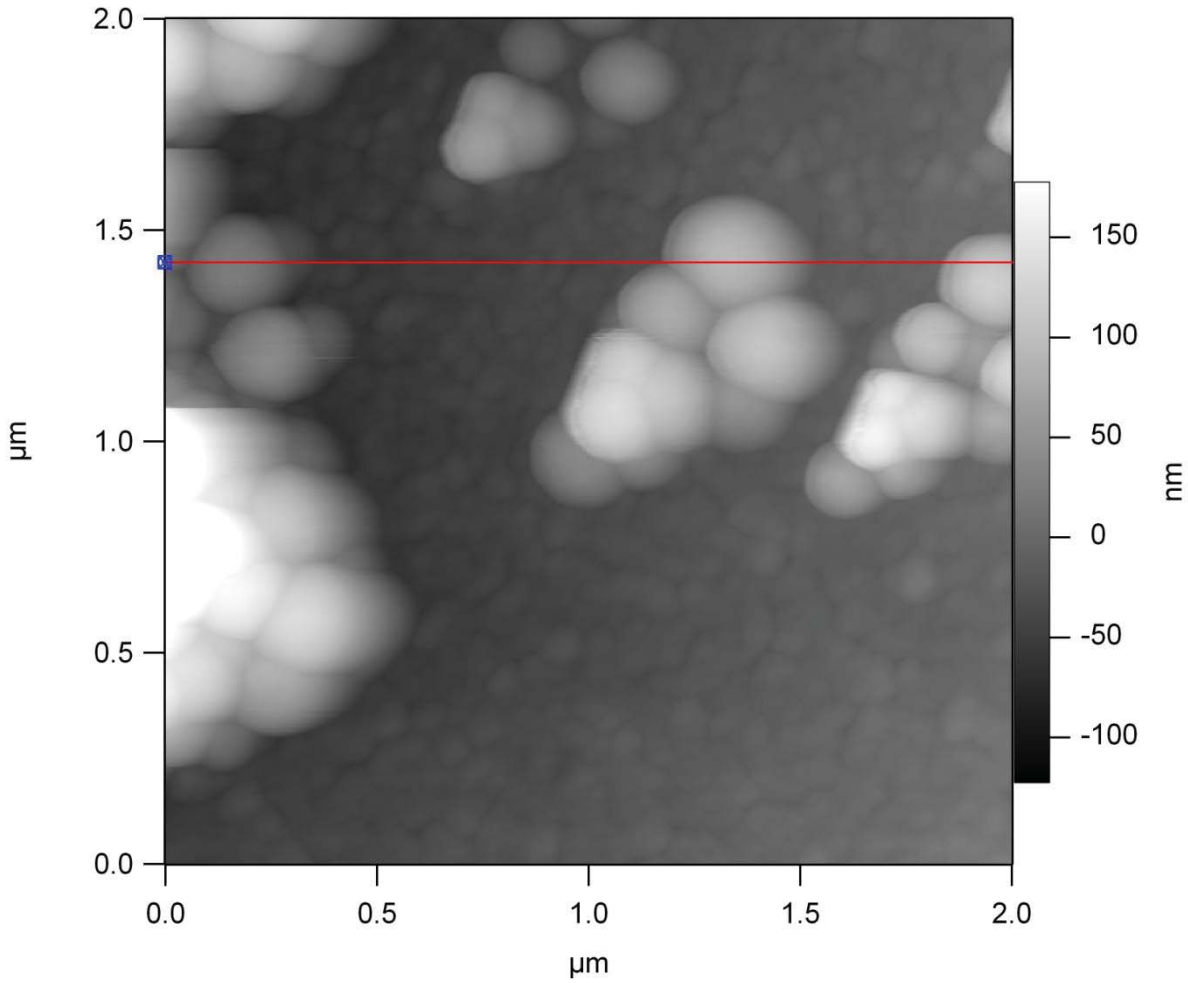

Figure 4.23 Surface profiling of the 3GNZZPhaC beads.

The surface profiling showed that the beads were approximately 100 nm in width and 150 nm at their highest point (Figure 4.24), these dimensions being significantly smaller than expected.

This suggested that the 3GZZNPhaC beads are a potential material for surface immobilisation, but only if coagulation issues could be resolved.

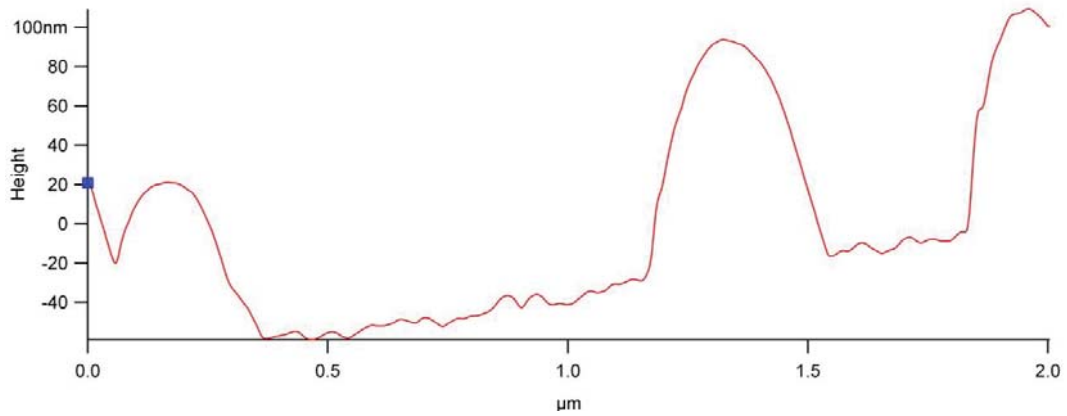

Figure 4.24 Surface profiling of 3GNZZPhaC beads on a Au coated surface.

In principle, it is possible to measure the interaction between the 3GNZZPhaC beads and the Au surface, which indicates the binding strength and the suggested methods include mounting the 3GNZZPhaC beads onto the cantilever and measure the force constant between the beads attached and the Au surface. The alternative possible method would be to use a Au coated cantilever and measure the interaction between the cantilever and the beads on the surface (in solution). Unfortunately, as these studies were going to take months to complete, it was not possible to embark on this line of investigation using the AFM technique.

4.7 The selection of ZZPhaC beads as an alternative SPR sensing material

The SPR phenomenon can only be detected within approximately 300 nm above the gold surface. A commercially available sensor chip such as CM5 consists of a carboxymethylated dextran layer (approximately 100 nm) which occupies 1/3 of the available space above the gold surface. In order to increase the sensitivity of the SPR signal, it is preferable to develop a new sensor chip which eliminates the dextran matrix.

An important aim left in this study was to test ZZPhaC beads as a possible alternative material to develop a new matrix free SPR sensor chip (Figure 4.25).

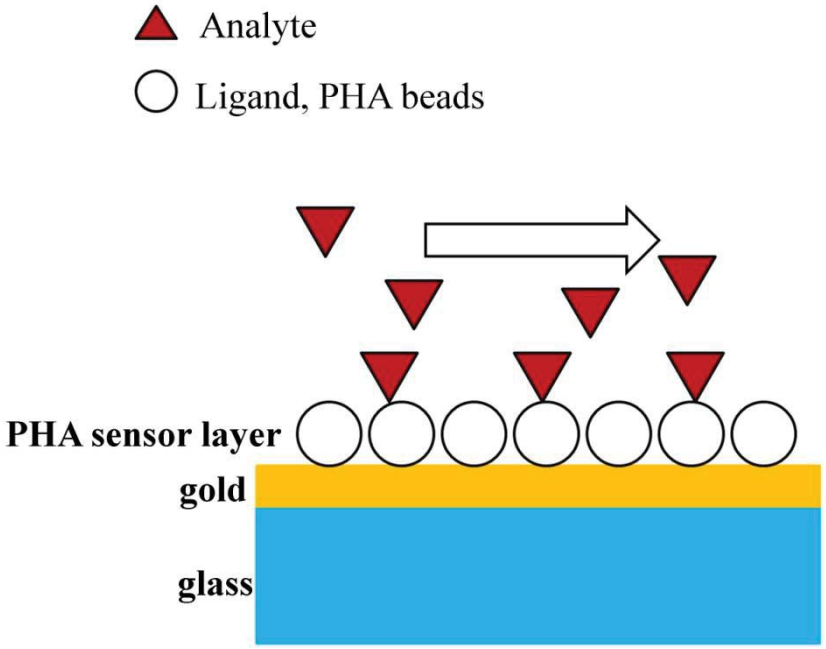

Figure 4.25 Schematic diagram of a SPR sensor with immobilised PHA beads. The multifunctional PHA beads are able to bind to the gold surface as well as the analyte.

From the surface studies including the methods of immobilising both 3GNZZPhaC and ZZPhaC beads onto Au coated surface, it is clear that both beads interact with the Au surface. The surface interaction between the beads and the surface was relatively stable. From SEM and AFM microscopy studies, both beads were bound to the Au surface after the rinsing and cleaning process to remove excess material. From the flow cell studies, the results suggested that it is possible to slowly immobilise the beads onto the Au surface.

Since ZZPhaC beads presented similar binding stability from the studies and due to the size of 3GNZZPhaC (approximately 100~500 nm), ZZPhaC beads (approximately 50~100 nm) were tested as an alternative SPR sensing material.

4.7.1 Preliminary binding test

4.7.1.1 Outside immobilisation of ZZPhaC beads

The Au sensor chip is commonly used for self-assembled monolayers and other modifications to study the interaction between surface materials and biomolecules.[31-37] Hence the commercially available SIA Kit Au was ideal for ZZPhaC bead studies. The unmounted gold surface was used as a binding surface for the ZZPhaC beads.

The outside immobilisation method is often used for immobilising a small molecule which requires organic solvents to maintain solubility. Many organic solvents are not compatible with the IFC and flow system in a Biacore instrument; hence the immobilisation step must be performed outside the instrument. The outside immobilisation can be achieved by pipetting the solution directly onto the sensor chip, and the success or failure of the procedure can only be determined by performing a binding test with an analyte. The coagulation issue of the beads (both 3GNZZPhaC and ZZPhaC beads) observed from surface studies (see section 4.6) suggested they may aggregate during the immobilisation process and may cause issues in the IFC and flow system. Hence the outside immobilisation technique was chosen for preparing the Au-ZZPhaC sensor surface.

Outside immobilisation was initially performed to assess the surface response of ZZPhaC surface with rat anti-progesterone (IgG concentration 0.1 mg/mL).

ZZPhaC (1 ng/mL, wet weight) was immobilised onto a Au sensor chip (Biacore) by depositing the ZZPhaC bead solution onto the surface and allowing binding to occur for 10 minutes. The Au surface was rinsed with Milli-Q H_2O to remove excess bead solution, potential unbound beads and salt from the buffer solution. The Au sensor chip was dried using oil free compressed air and assembled with the sensor chip cassette holder.

4.7.1.2 Binding tests using rat Anti-P4 on a ZZPhaC surface

The ZZPhaC immobilised Au chip (Au-ZZPhaC chip) was cleaned and dried using Milli-Q H_2O and then docked onto the X100 SPR instrument. The rat Anti-P4 solution was used to test the binding performance of the ZZPhaC surface in order to compare with the binding performance of the three P4 linker surfaces. Each of the rat Anti-P4 solutions (2.5, 5 and 10 µg/mL) was injected over the Au-ZZPhaC surface at 5 µL/min for 120 s. The surface was regenerated by 3 injections of NaOH (30 s, 50 mM).

After the baseline of each cycle of injection was established, the binding for FC1 and FC2 occurred. The stability of the flow cells was calculated by subtracting the FC2 response from FC1, which resulted in a relative response from the antibody and surface interaction (RU). The sensorgram and the surface responses of both flow cell 1 (FC1) and flow cell 2 (FC2) indicated the binding had occurred for each rat Anti-P4 concentration (Figure 4.26, Figure 4.27). As the rat Anti-P4 solution was injected over the Au-ZZPhaC surface, the baselines (absolute responses) of both flow cells were monitored to ensure the Au-ZZPhaC surface was stable, and the ZZPhaC beads were not removed from the Au surface under a closed flow cell system.

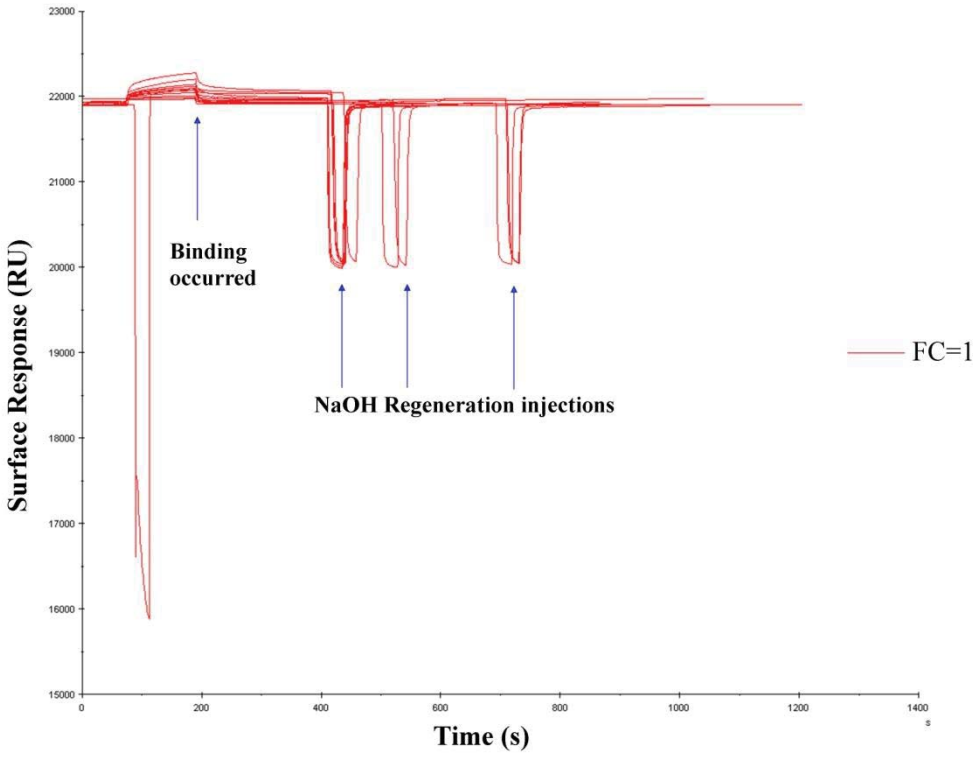

Figure 4.26 Sensorgram of rat Anti-P4 binding to the Au-ZZPhaC surface in FC1.

The baseline indicated that the ZZPhaC beads were reasonably stable and three injections of NaOH (50 mM) were sufficient to regenerate the ZZPhaC bead surface. The sensorgrams for FC1 and FC2 were similar because both flow cells consisted of the same binding material due to outside immobilisation.

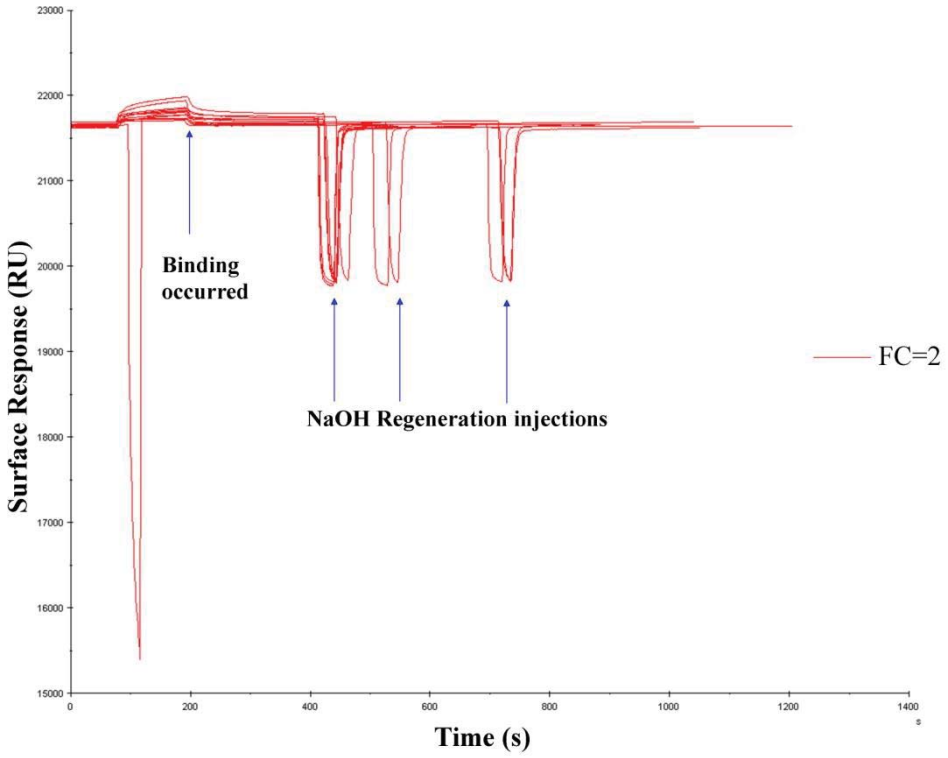

Figure 4.27 Sensorgram of rat Anti-P4 binding to the Au-ZZPhaC surface in FC2.

Rat Anti-P4 solution was injected over the sensor surface to observe the binding activity of the ZZPhaC beads (Figure 4.30). The surface responses of FC1 and FC2 to the rat Anti-P4 were similar at 5 µL/min injection rate (Table 4.1). The Au sensor surface was immobilised by depositing the bead solution outside of the SPR instrument, hence the surface response for both FC should be similar (Figure 4.28).

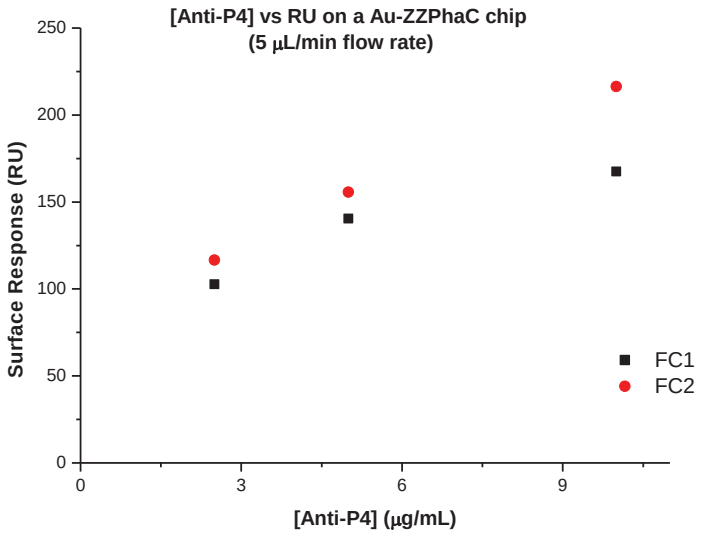

Figure 4.28 The rat Anti-P4 was tested on a ZZPhaC surface with a flow rate of 5 µL/min.

A 2.5 µg/mL solution of rat Anti-P4 was injected over the ZZPhaC surface for 120 s at 5 µL/min, FC1 had a surface response of 102.7 RU and FC2 was 116.6 RU. The RU from FC2 was 13.5% higher than FC1. As the concentration of rat Anti-P4 increased to 5 µg/mL the surface response of FC1 was 140.5 RU and FC2 was 155.6 RU (10.7% higher than FC1). The final injection of 10 µg/mL of rat Anti-P4 gave 167.5 RU for FC1 and 216.3 RU for FC2, showing that FC2 generates a 29% higher surface response than FC1. It is possible the FC2 consisted of a higher bead distribution when the beads were immobilised onto the Au surface. Hence the surface responses of FC2 were all higher than FC1.

Table 4.1

[Rat Anti-P4] (µg/mL)	FC1 (RU)	FC2 (RU)	Variation between FC1 & FC2 (%)
2.5	102.7	116.6	13.5
5.0	140.5	155.6	10.7
10.0	167.5	216.3	29.1

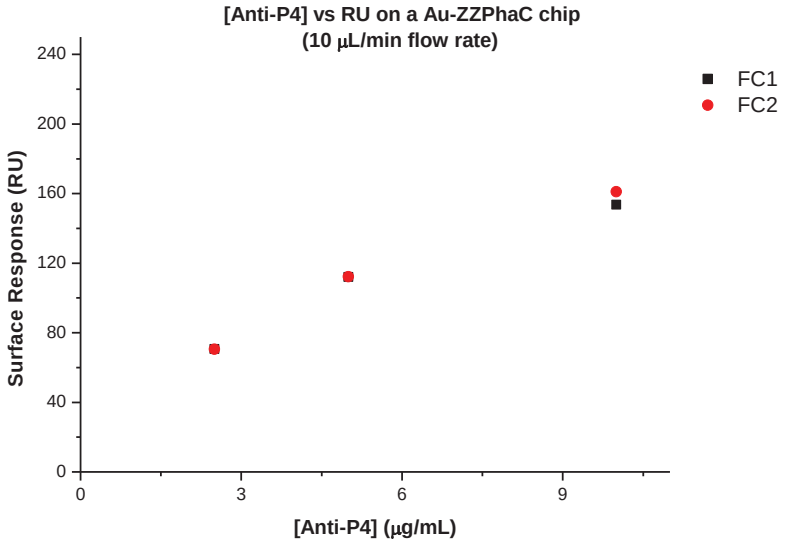

Figure 4.29 The rat Anti-P4 was tested on a ZZPhaC surface with a flow rate of 10 µL/min.

Table 4.2

[Rat Anti-P4] (µg/mL)	FC1 (RU)	FC2 (RU)	Variation between FC1 & FC2 (%)
2.5	70.7	70.5	0.28
5.0	112.0	112.2	0.17
10	153.6	161.1	4.88

The ZZPhaC bead surface binding performance was also tested with rat Anti-P4 at an injection rate of 10 µL/min. The surface responses of FC1 and FC2 were consistently close and the surface responses showed that at 10 µL/min injection rate (Table 4.2), the surface response variation between the two flow cells was reduced (Figure 4.29). It is likely that rat Anti-P4 requires an extended association time (to bind to the ZZPhaC beads). Hence using a higher flow rate (10 µL/min) resulted in lower responses for both FC1 and FC2.

The binding curve was repeated with a flow rate of 5 µL/min and the variation in surface response between FC1 and FC2 increased. It is possible that the beads on the surface of FC1 degenerated which led to a reduction in binding response. It could also be caused by more FC1 binding sites becoming available as the excess beads were removed under the continuous flow system (Figure 4.30).

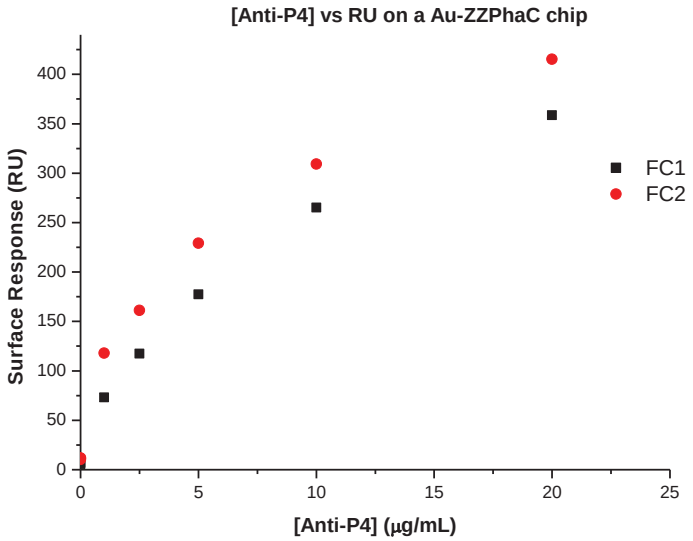

Figure 4.30 Binding performance of rat Anti-P4 on a ZZPhaC sensor surface with a flow rate of 5 µL/min. The sensor surface was immobilised outside of the SPR instrument, hence the FC1 and FC2 surface response units should be relatively similar.

The sensor chip was subjected to SEM analysis after the cursory binding curves testing (Figure 4.31, Figure 4.32, and Figure 4.33). The SEM image (Figure 4.31) showed impurities on the sensor surface; the impurities were most likely introduced in the process of outside immobilisation (outside of the SPR instrument).

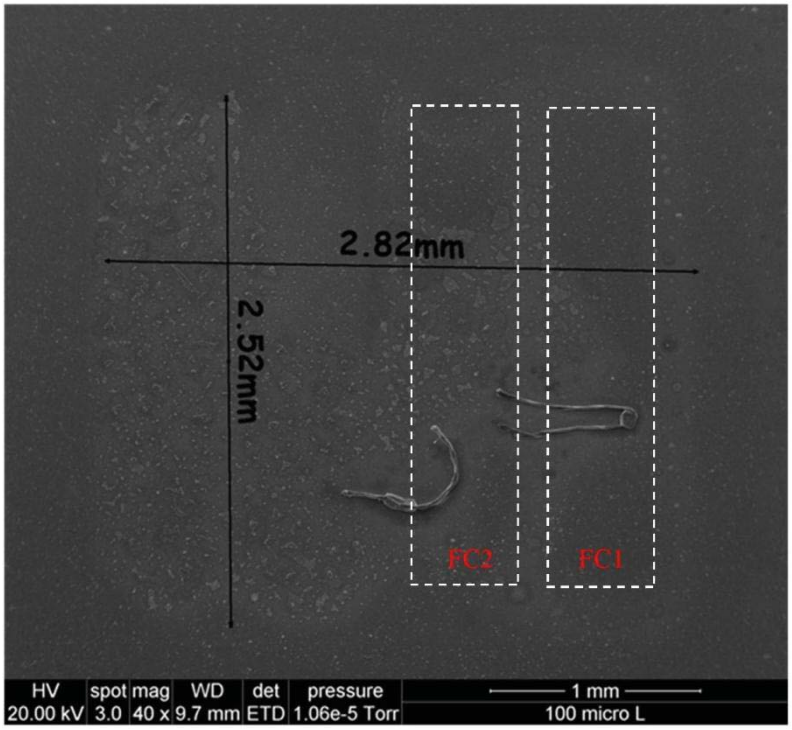

Figure 4.31 The ZZPhaC beads immobilised on the commercially available Au sensor surface. The surface appeared to have a large amount of salt present which was from the buffer residues (40x magnification). FC1 and FC2 are visibly coated with salt residues and ZZPhaC beads.

It was also clear that the sensor surface was not completely occupied with the ZZPhaC beads (Figure 4.32). Hence the immobilisation concentration can be increased for future reference. The SEM image also showed that the aggregation level of the ZZPhaC beads was high (Figure 4.33), and this probably resulted in a decrease in binding sensitivity of the Au-ZZPhaC surface. To achieve a monolayer sensor surface, the concentration of ZZPhaC beads should not be lower than 1 ng/mL and the immobilisation process of the ZZPhaC beads should be gradual.

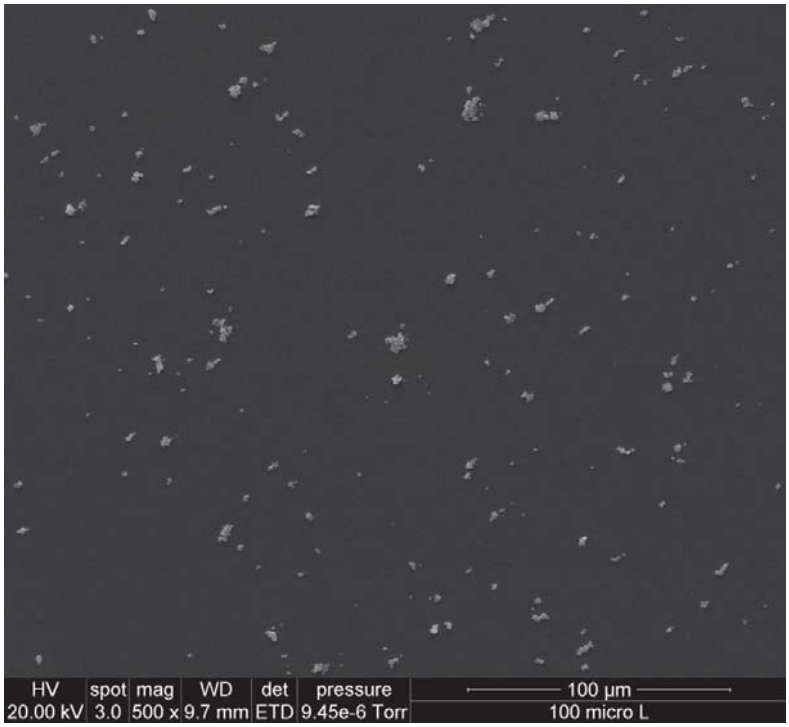

Figure 4.32 The sensor surface with ZZPhaC beads immobilised outside of the SPR instrument. The beads were scattered along the gold surface with aggregation (500x magnification).

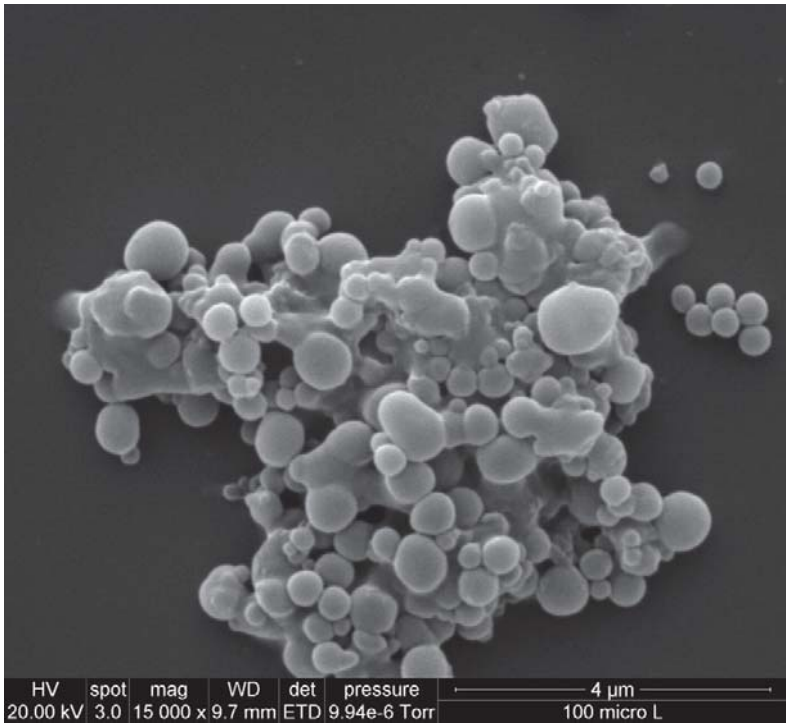

Figure 4.33 Outside surface immobilisation of ZZPhaC beads. A significant amount of aggregation occurred (15,000x magnification) and this would hinder the binding response of the Anti-P4.

4.7.1.3 ZZPhaC immobilisation (in Biacore X100)

A standard surface immobilisation process includes: activation of the surface, immobilisation of the material, and deactivation of the surface. However, for a Au surface without any binding material on the surface, the activation step by injection of EDC and NHS was skipped since the reagents are used to activate the carboxylic group on the sensor surface (see Chapter 2 section 2.2).

To immobilise the ZZPhaC beads on the Au surface an initial concentration of 1 ng/mL was used, which was the same as that used for outside SPR immobilisation discussed in section 4.7.1. The first injection of ZZPhaC beads indicated that no binding had occurred on the Au surface (Figure 4.34). Several short injections (24 s) of the ZZPhaC bead solution at a rate of 5 µL/min showed that there was very low binding on the Au surface (Figure 4.35). The low surface response (immobilisation level) was likely due to the low immobilisation concentration of the ZZPhaC beads. The normal deactivation step of injecting ethanolamine was also not performed in this procedure, since there are no unreacted carboxylic groups on the surface and injecting ethanolamine would potentially block the binding site on the ZZPhaC beads.

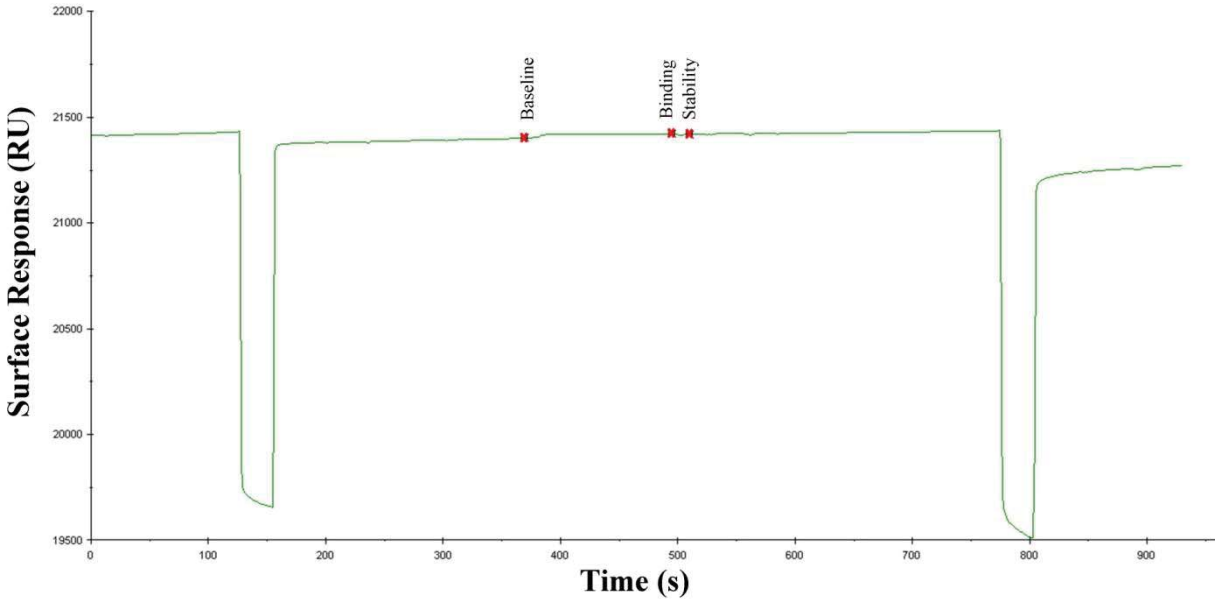

Figure 4.34 After the first injection of ZZPhaC beads (1 ng/mL) at 5 µL/min for 24 s on FC2, there appeared to be no binding on the Au surface.

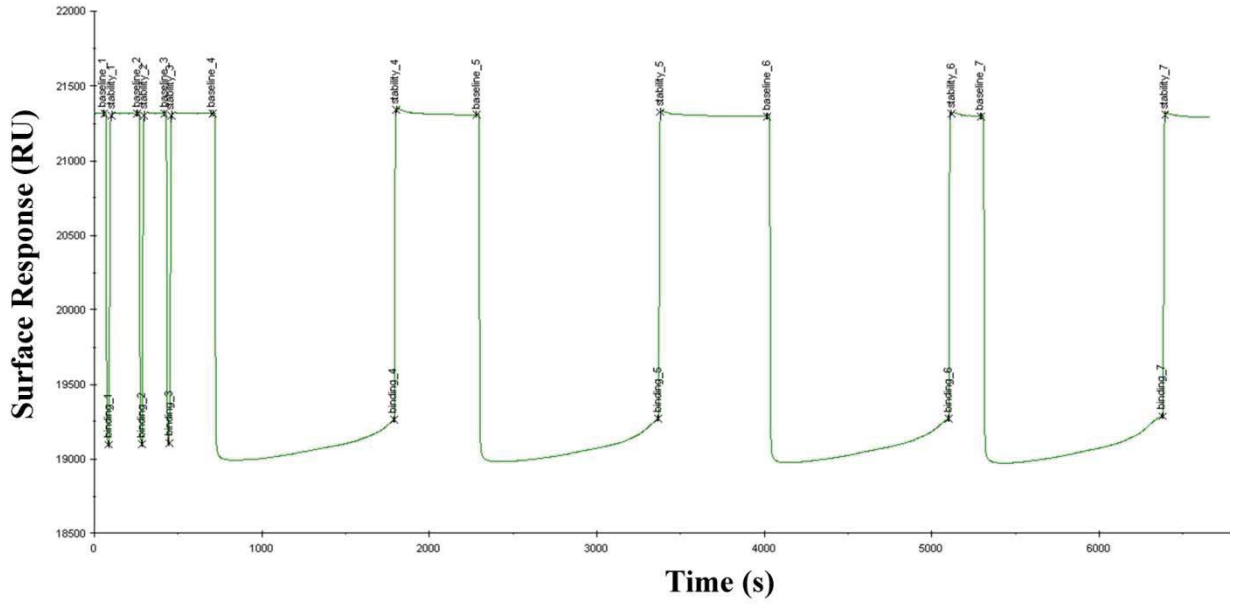

Figure 4.35 The short pulse injections of ZZPhaC (1 ng/mL) at 5 µL/min showed a very low surface response.

The concentration of the ZZPhaC bead solution was increased to 10 ng/mL and injected with a short pulse which resulted in a surface response of -3.3 RU. The surface response indicated that the ZZPhaC beads were not immobilised onto the surface. The injection contact time was increased to 1080 s and the surface response was 522.7 RU. A typical immobilisation level for a protein or protein linked ligand is roughly 5,000 to 10,000 RU and the immobilisation level for most of the small molecules should the approximately 1000 RU.[38]

The molecular weight of PHA granules can be up to 2 x 10^6 kDa with diameters typically around 200 to 500 nm.[21,39] ZZPhaC was known to be approximately 100 to 200 nm.[40] However the molecular weight and the size of the ZZPhaC beads are still relatively larger than a typical protein such as ovalbumin (45 kDa) which is commonly used for surface immobilisation. Thus, the expected immobilisation level of ZZPhaC was approximately 5,000 to 10,000 RU.

The RU after the long injection (1080 s) suggested that the beads have been immobilised onto the Au surface, and it is common to perform short pulse injections after a long injection to check the surface loading. Hence four more short pulse injections were carried out to check the loading of the surface. Each short injection resulted in a decrease in surface response of approximately 10 RU, which indicated that the surface was fully occupied and the immobilisation step was completed (Figure 4.36). It was considered that ZZPhaC beads might require longer contact time to allow the material to interact with the Au surface, and further long injection may increase the surface loading. These initial experiments were set up to probe the possibility of using ZZPhaC beads as a sensor surface binding material, and the results suggested that further loadings of the surface in future experiments may be possible to optimise the uptake.

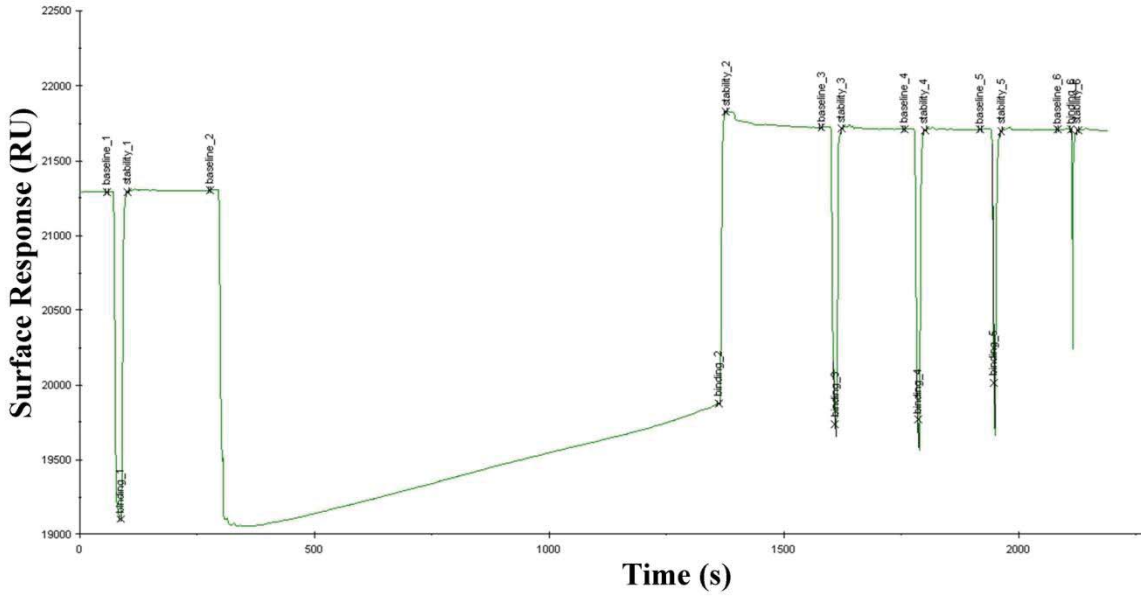

Figure 4.36 The immobilisation concentration of the ZZPhaC beads was increased to 10 ng/mL. The immobilisation step began with a short pulse of injection followed by a long pulse injection. The surface loading was checked by several short pulse injections. The final immobilisation level was 522.7 RU.

4.7.1.4 Binding performance testing with rat Anti-P4 on the Au-ZZPhaC surface

Rat Anti-P4 solutions were injected over the Au-ZZPhaC surface at 5 µL/min and the surface responses were observed (Figure 4.37). The surface was regenerated with NaOH (50 mM) after each injection. The initial runs for the ZZPhaC SPR immobilised surface (FC2) showed very little difference compared with the gold surface (FC1). With a higher concentration of rat Anti-P4 the non-immobilised gold surface generated higher surface responses overall (Table 4.3).

Table 4.3

[Rat Anti-P4] (µg/mL)	FC1 (RU)	FC2 (RU)
1.0	111.4	118.6
2.5	148.9	155.7
5	196.7	192.7
10	269.1	249
20	358.1	318.9

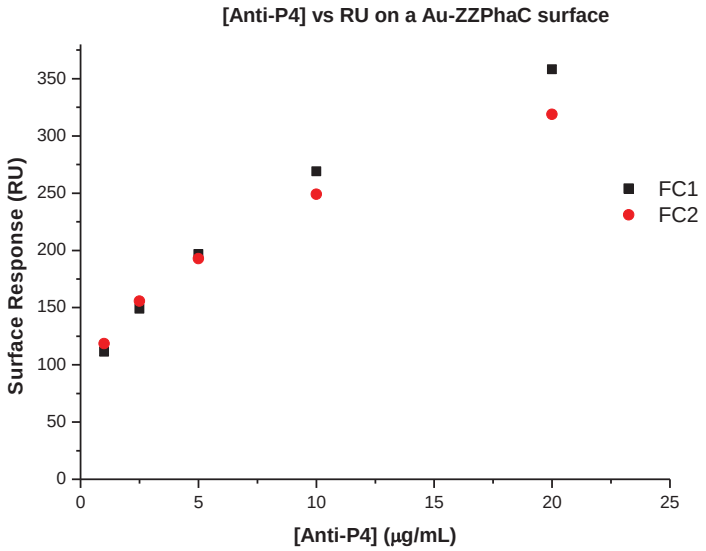

Figure 4.37 Surface response of ZZPhaC beads immobilised on FC2 and bare gold FC1. The binding performance of rat Anti-P4 on both channels was very similar; with a higher concentration of rat Anti-P4 the surface response of FC2 was lower than the FC1 bare gold surface.

The stability of the ZZPhaC beads under a continuous flow was determined by the flow cell system. However, the imitated flow cell system still has some variations compared with the SPR flow cell system. For example, the flow rate of the SPR system is much lower than the constructed flow cell, and the pressure of the SPR system is also greater. Considering such factors, the cursory binding performance testing was carried out without the surface activation and deactivation procedure used for the CM5 sensor surface. Hence the binding performance of the Au-ZZPhaC surface could be affected.

The rat Anti-P4 binding curve was repeated with the same series of concentrations on the Au-ZZPhaC surface (Figure 4.38). The blank solution (HBS-EP$^+$ buffer) was injected and generated 5.6 RU for FC1 and 11.6 RU for FC2. A series of rat Anti-P4 solutions were injected and the surface responses indicated that the ZZPhaC surface interacted with the rat Anti-P4 and resulted in a greater surface response compared with the bare gold surface (Table 4.4).

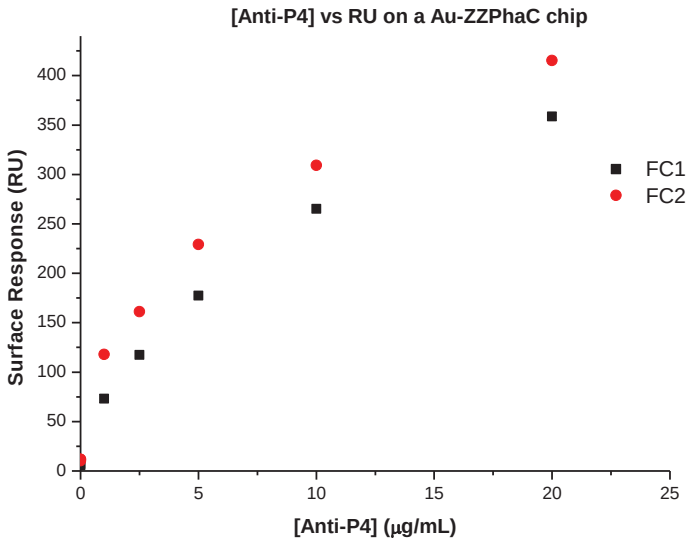

Figure 4.38 The Au-ZZPhaC sensor chip was used to repeat the binding curve of rat Anti-P4, where FC1 contained only bare gold and FC2 was immobilised with ZZPhaC beads.

The rat Anti-P4 interacted with the ZZPhaC surface and the surface response increased as the concentration of rat Anti-P4 increased. At 1.0 μg/mL, the FC2 had a surface response of 118 RU while FC1 was 73 RU.

The rat Anti-P4 appeared to interact with the bare gold surface without the binding partner progesterone. The thioether sulfur and thiol groups on the amino acids can interact with the gold surface. Hence the bare gold surface showed a surface response as rat Anti-P4 was injected.

Table 4.4

[Rat Anti-P4] (μg/mL)	FC1 (RU)	FC2 (RU)	Enhancement of ZZPhaC on Au surface (%)
0	5.6	11.6	51.7
1.0	73	118	38.1
2.5	117.3	161.1	27.2
5	177.3	229.2	22.6
10	265.2	309.3	14.3
20	358.6	415.2	13.6

The ZZPhaC sensor surface (FC2) showed a clear surface enhancement compared with the reference gold surface (FC1) and the surface response increased as the concentration of rat Anti-P4 increased (Table 4.4).

The binding response (RU) was plotted versus the calculated rat Anti-P4 concentration (Figure 4.38), the binding response for both FC1 (bare Au) and FC2 (Au-ZZPhaC surface) were linear. The higher slope of the calibration curve (binding curve) indicated that ZZPhaC could be a potential binding material to substitute the dextran binding layer for SPR sensing.

The Au-ZZPhaC sensor chip was subjected to SEM analysis to assess the binding between the ZZPhaC beads and Au surface after SPR analysis.

The SEM images showed the two channels from the SPR flow cell units (Figure 4.39), and the Au surface was not completely occupied. The surface response from the immobilisation step was 522.7 RU, and for a typical immobilisation the surface response should be approximately 5,000 to 10,000 RU. The immobilisation step ceased at 522.7 RU in this feasibility study, but further studies to optimise the immobilisation level could be explored in the future. The purpose of this investigation was to explore the possibility of substituting the dextran binding layer of the CM5 sensor chip with ZZPhaC beads as a new binding material.

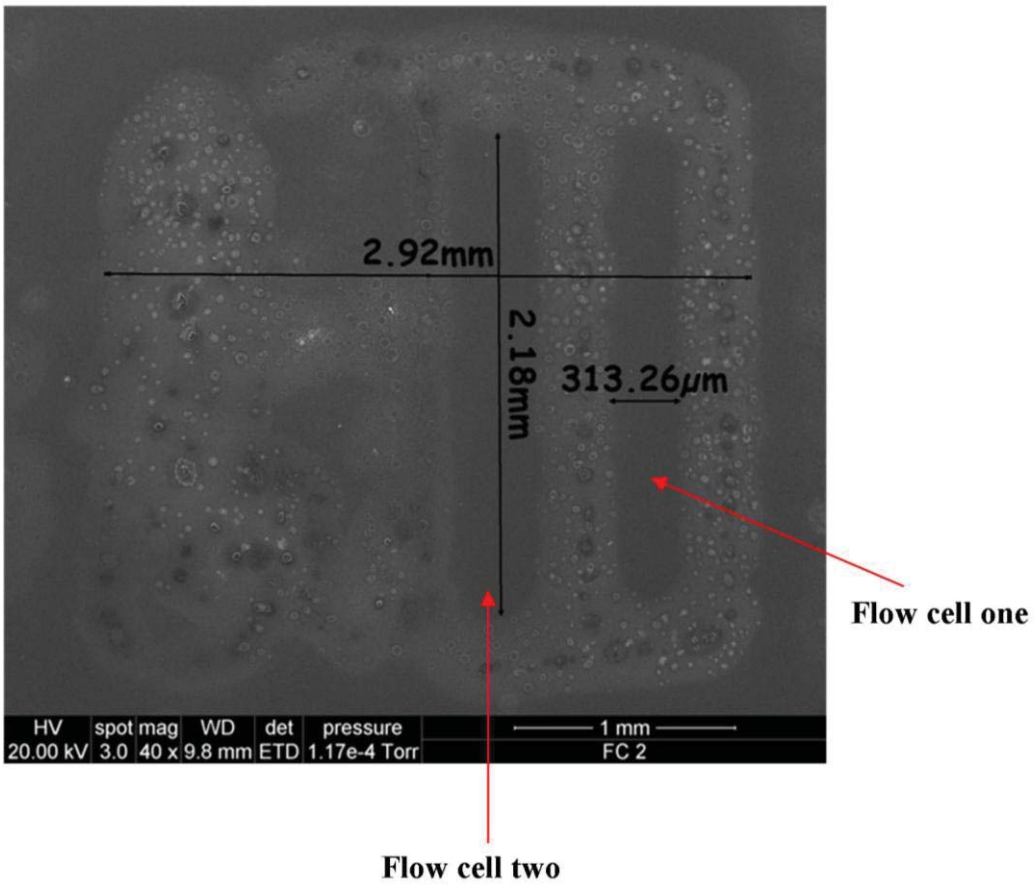

Figure 4.39 The SEM image (40x magnification) of the SPR sensor chip with ZZPhaC beads. FC2 was immobilised with ZZPhaC beads and FC1 was the reference cell without a binding layer (bare gold).

The binding response was low possibly due to the low occupancies of the ZZPhaC on the Au surface. It is clear from the SEM images that the SPR immobilisation did not evenly distribute the ZZPhaC beads onto the Au surface (Figure 4.40). At 10 ng/mL the ZZPhaC beads unevenly dispersed on the surface and did not form a complete monolayer as opposed

to the dextran. Therefore, the binding response was likely hindered due to the limited number of ZZPhaC beads on the surface.

The SPR immobilisation method reduced the aggregation of the beads on the Au surface (Figure 4.40) compared with the outside immobilisation sensor surface (see Figure 4.32 and Figure 4.33). Hence the ZZPhaC surface response from the antibody injections was slightly enhanced compared with the bare Au surface.

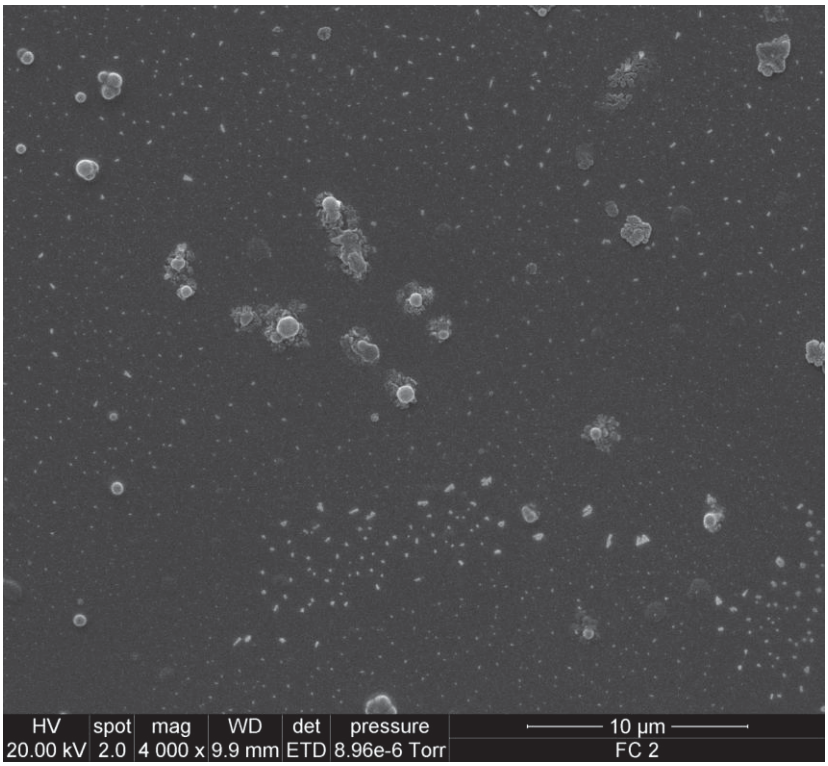

Figure 4.40 The SPR immobilisation method reduced the aggregation of the ZZPhaC beads (4,000x magnification) and allowed rat Anti-P4 binding to occur.

These studies point the way to future experiments in the possible use of beads as dextran layer replacements in the CM5 chips. It is suggested that:

(i) Smaller beads of 3GNZZPhaC may allow it to be used as the binding material.

(ii) A charge surface on the beads would prevent aggregation and allow formation of a uniform monolayer.

4.8 Preliminary LFIA testing

AuNPs are the most commonly used colour indicator of LFIA (see Chapter 3 section 3.2). The AuNPs can be reasonably easy to conjugate with antibodies as a signal generator. Both 3GNZZPhaC and ZZPhaC have the property of binding to AuNPs, as well as binding to antibodies, and being dyed using Nile red. Therefore, it may be possible to use it as a replacement of AuNPs or incorporated with AuNPs as a conjugate in LFIA sensing.

The 3GNZZPhaC and ZZPhaC beads were used in the preliminary LFIA tests (Table 4.5). Each solution well contained 5 μL of test bead solution and buffer (Chase buffer, buffered saline with nonionic detergent and preservative). The total volume of the well solution was 30 μL (Set 1 and Set 2). The test half strip comprised a test line and control line; the steroid-BSA conjugate was used as the test line and polyclonal IgG as control line.

The bead solution for Set 3 was prepared using 50 μL of a stock bead solution (0.1 mg/mL) diluted in 500 μL of PBS buffer then centrifuged for 15 min. The supernatant was discarded and beads were re-suspended in 500 μL of PBS buffer.

Table 4.5

Set No.	Solution well	Sample
1	1	ZZPhaC: 5 μL, 0.1 mg/mL Buffer: 25 μL
1	2	3GNZZPhaC: 5 μL, 0.1 mg/mL Buffer: 25 μL
2	3	ZZPhaC: 5 μL, 0.1 mg/mL AuNPs: 5 μL, pH 7
2	4	3GNZZPhaC: 5μL, 0.1mg/mL AuNPs: 5 μL, pH 7
3	5	ZZPhaC: 5 μL, 100 μg/mL Buffer: 25 μL
3	6	3GNZZPhaC: 5 μL, 100 μg/mL Buffer: 25 μL
Au	7	Buffer: 25 μL AuNPs: 5 μL, pH 7

The strips were scanned 15 min after the assay started using a phosphorimager (FLA-500). The results showed that the majority of the 3GNZZPhaC and ZZPhaC beads aggregated at the bottom of the strips (Figure 4.41). Theoretically both 3GNZZPhaC and ZZPhaC beads

should have bound only to the control which consisted of a polyclonal antibody (IgG) for secondary binding. However, the results from both Set 1 and Set 2 indicated that both beads had non-specific binding as they bound to the test line which consisted of a steroid-BSA conjugate (Figure 4.41). The non-specific binding in Set 2 was not caused by the AuNPs since the reference strip in solution well 7 showed no non-specific binding to both test and control lines.

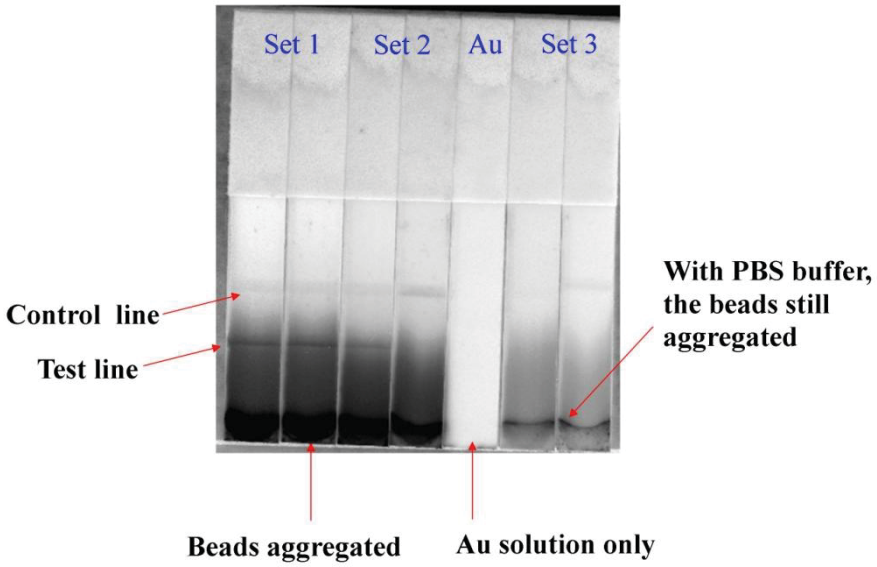

Figure 4.41 A preliminary assay using 3GNZZPhaC beads and ZZPhaC beads as binding material.

In Set 2, the 3GNZZPhaC beads with AuNPs showed less non-specific binding, but the aggregation level was still high. As coordination of the AuNPs to both 3GNZZPhaC and ZZPhaC beads reduced the coagulation level compared with Set 1, we theorised the binding sites were occupied by the AuNPs rather than the beads aggregating.

In Set 2, the ZZPhaC beads had lower non-specific binding level and slightly less aggregation occurred at the bottom of the strip compared with the 3GNZZPhaC beads. It is possible that as the ZZPhaC beads are smaller than the 3GNZZPhaC beads, the coagulation level was reduced.

As the concentrations of the bead solutions used for both Set 1 and Set 2 overloaded the strips, they were reduced in Set 3 (Table 4.5). Sonication and lowering the concentration of both bead solutions slightly reduced the aggregation level and non-specific binding (Set 3). Until the aggregation of the beads can be reduced or prevented, it is unlikely that further investigation with this system would be successful.

4.9 Conclusions

In this chapter:

a) A flow cell for the use of 3GNZZPhaC beads has been designed, constructed, and successfully operated.
b) 3GNZZPhaC beads immobilisation on the Au coated glass slide of the flow cell has been studied.
c) SEM studies of the immobilisation of 3GNZZPhaC and ZZPhaC beads showed the majority of beads coagulated on the Au surface, but single beads have also been observed.
d) Studies on the use of ZZPhaC beads as an alternative SPR sensing material performed.
e) Preliminary binding tests undertaken with ZZPhaC beads using outside immobilisation on a Au surface.
f) Binding studies for ZZPhaC beads immobilised on an Au chip inside of a Biacore X100 have been made.
g) 3GNZZPhaC and ZZPhaC beads were tested as an alternative signal generator in LFIA.

From the surface studies, it is clear that the 3GNZZPhaC beads have gold binding properties and have the potential to become an alternative binding material for SPR sensing. The ZZPhaC beads showed interesting binding properties to the gold surface which was not expected. The flow cell studied indicated that the 3GNZZPhaC beads still bind to the Au surface under constant flow. The SEM images suggested that the 3GNZZPhaC beads can be immobilised under a pressurised SPR system.

The aggregation of the beads hindered their possible application for lateral flow immunoassay, and this would need to be resolved before they could be of potential use.

The size of the binding material is crucial and limited to less than 100 nm due to the sensitivity of SPR signals. In this study the 3GNZZPhaC beads have a diameter up to 500 nm which makes them unsuitable for SPR sensor development because the sensing range is within 300 nm above the sensor surface. However, the ZZPhaC beads with diameters in the range 50-100 nm, along with their unique binding property to the Au surface, were more useful for SPR studies. The binding response of the ZZPhaC bead surfaces indicated that there is a possible application for them as a new SPR binding material for antibody detection, and further studies seem warranted.

References

(1) Hazer, B.; Steinbu¨chel, A. *Applied Microbiology and Biotechnology* **2007**, *74*, 1-12.

(2) Furrer, P.; Panke, S.; Zinn, M. *Journal of Microbiological Methods* **2007**, *69*, 206-213.

(3) Shang, L.; Jiang, M.; Yun, Z. H.; Yan, H. Q.; Chang, H. N. *World Journal Of Microbiology And Biotechnology* **2008**, *24*, 2783-2787.

(4) Bhubalan, K.; Lee, W. H.; Loo, C. Y.; Yamamoto, T.; Tsuge, T.; Doi, Y.; Sudesh, K. *Polymer Degradation and Stability* **2008**, *93*, 17-23.

(5) Albuquerque, M. G. E.; Eiroa, M.; Torres, C.; Nunes, B. R.; Reis, M. A. M. *Journal of Biotechnology* **2007**, *130*, 411-421.

(6) Solaiman, D.; Ashby, R.; Hotchkiss, A.; Foglia, T. *Biotechnology Letters* **2006**, *28*, 57-162.

(7) Chen, C. W.; Don, T. M.; Yen, H. F. *Process Biochemistry (Amsterdam, Netherlands)* **2006**, *41*, 2289-2296.

(8) Haas, R.; Jin, B.; Zepf, F. T. *Bioscience Biotechnology And Biochemistry* **2008**, *72*, 253-256.

(9) Koller, M.; Bona, R.; Chiellini, E.; Fernandes, E. G.; Horvat, P.; Kutschera, C.; Hesse, P.; Braunegg, G. *Bioresource Technology* **2008**, *99*, 4854-4863.

(10) Goff, M.; Ward, P. G.; O'Connor, K. E. *Journal of Biotechnology* **2007**, *132*, 283-286.

(11) Bengtsson, S.; Werker, A.; Christensson, M.; Welander, T. *Bioresource Technology* **2008**, *99*, 509-516.

(12) Salamon, Z.; Macleod, H. A.; Tollin, G. *Biochimica Et Biophysica Acta-Reviews on Biomembranes* **1997**, *1331*, 117-129.

(13) Lemoigne, M. *Bulletin de la Societe de Chimie Biologique* **1926**, *8*, 770-782.

(14) Rehm, B. H. A.; Qi, Q.; Beermann, B. B.; Hinz, H.; Steinbuchel, A. *Biochemical Journal* **2001**, *358*.

(15) Rehm, B. H. A. *Biochemical Journal* **2003**, *376*, 15-33.

(16) Ren, Q.; De Roo, G.; Kessler, B.; Witholt, B. *Biochemical Journal* **2000**, *349*, 599-604.

(17) Liebergesell, M.; Steinbuechel, A. *European Journal of Biochemistry* **1992**, *209*, 135-150.

(18) Liebergesell, M.; Schmidt, B.; Steinbuchel, A. *FEMS microbiology letters* **1992**, *78*, 227-232.

(19) McCool, G. J.; Cannon, M. C. *Journal of Bacteriology* **1999**, *181*, 585-592.

(20) McCool, G. J.; Cannon, M. C. *Journal of Bacteriology* **2001**, *183*, 4235-4243.

(21) Rehm, B. H. A. *Microbial Bionanotechnology: Biological Self-Assembly Systems and Biopolymer-Based Nanostructures*; 1 ed.; Horizon Bioscience: Wymondham, **2006**.

(22) Russell, R. A.; Holden, P. J.; Garvey, C. J.; Wilde, K. L.; Hammerton, K. M.; Foster, L. J. R. *Physica B: Condensed Matter* **2006**, *385-386*, 859-861.

(23) Russell, R. A.; Holden, P. J.; Wilde, K. L.; Hammerton, K. M.; Foster, L. J. R. *Journal of Biotechnology* **2007**, *132*, 303-305.

(24) Jahns, A. C.; Haverkamp, R. G.; Rehm, B. H. A. *Bioconjugate Chemistry* **2008**, *19*, 2072-2080.

(25) Tamerler, C.; Oren, E. E.; Duman, M.; Venkatasubramanian, E.; Sarikaya, M. *Langmuir* **2006**, *22*, 7712-7718.

(26) Peters, V.; Rehm, B. H. A. *Applied and Environmental Microbiology* **2006**, *72*, 1777-1783.

(27) Hezayen, F. F.; Steinbuchel, A.; Rehm, B. H. A. *Archives of Biochemistry and Biophysics* **2002**, *403*, 284-291.

(28) Lassalle, V.; Ferreira, M. L. *Macromolecular Bioscience* **2007**, *7*, 767-783.

(29) Brockelbank, J. A.; Peters, V.; Rehm, B. H. A. *Applied and Environmental Microbiology* **2006**, *72*, 7394-7397.

(30)*Nanotechnology Research Group*; http://seat.massey.ac.nz/research/centres/nano/labs.asp

(31) Ahmad, A.; Ramakrishnan, A.; McLean, M. A.; Breau, A. P. *Biosensors & bioelectronics* **2003**, *18*, 399-404.

(32) *Real-time analysis of biomolecular interactions : applications of BIACORE* Nagata, K.; Handa, H., Eds.; Springer: Tokyo, **2000**.

(33) Pockrand, I.; Swalen, J. D.; Gordon, J. G. I.; Philpott, M. R. *Surface Science* **1978**, *74*, 237-244.

(34) Mustafa, D. E.; Yang, T.; Xuan, Z.; Chen, S.; Tu, H.; Zhang, A. *Plasmonics* **2010**, *5*, 221-231.

(35) Rebe Raz, S.; Leontaridou, M.; Bremer, M. G. E. G.; Peters, R.; Weigel, S. *Analytical and Bioanalytical Chemistry* **2012**, *403*, 2843-2850.

(36) Gillis, E.; Traynor, I.; Gosling, J.; Kane, M. *Journal of AOAC International* **2006**, *89*, 838-842.

(37) Jiang, X. Q.; Waterland, M.; Blackwell, L.; Wu, Y. Q.; Jayasundera, K. P.; Partridge, A. *Steroids* **2009**, *74*, 819-824.

(38) BIACORE; AB ed.; General Electric Healthcare: 2008.

(39) Grage, K.; Jahns, A. C.; Parlane, N.; Palanisamy, R.; Rasiah, I. A.; Atwood, J. A.; Rehm, B. H. A. *Biomacromolecules* **2009**, *10*, 660-669.

(40) Lewis, J. G.; Rehm, B. H. A. *Journal of Immunological Methods* **2009**, *346*, 71-74.

Chapter 5

Conclusions and future work

Conclusions

The objective of this investigation was to develop SPR and LFIA based biosensors for progesterone sensing in bovine serum and milk.

The SPR study focused on three aspects:

(i) comparison of P4 linkers in sensing sensitivity using rat Anti-P4,

(ii) investigation of two monoclonal antibodies (rat Anti-P4 and mouse Anti-P4) on three different P4 sensor surfaces,

(iii) development of the P4 inhibition assay for bovine serum and milk P4 detection.

The binding performance of three P4 sensor surfaces including 4TP-P4-OVA, 4TPH-P4-OVA and P4-PEG-OVA were tested using both rat Anti-P4 and mouse Anti-P4. As the linker length between the P4 molecule and the OVA increased the binding sensitivity increased, and it is an important feature for the SPR based sensor to be able to enhance the binding response. The conjugate linker length can be a potential strategy to enhance the surface sensitivity. The P4-PEG-OVA surface presented the best performance for both rat Anti-P4 and mouse Anti-P4, and it was selected and incorporated with mouse Anti-P4 for bovine serum and milk P4 analyses. The P4-PEG-OVA sensor surface showed a possible application for real serum and milk sample analysis with sample pre-treatment, and the results allowed the detection of the profile of the bovine estrous cycle. The accuracy in detecting the estrous cycle is significant for fertility and pregnancy in cattle since the bovine estrus is known to be a short period of time.

For the LFIA study, a LFIA strip was developed using P4-PEG-OVA due to its high SPR surface response. The half strip was prepared by spraying P4-PEG-OVA as the test line and IgG as the control line. The binding performance of the mouse Anti-P4-Au was carried out and a concentration was selected to perform the inhibition assay.

The established standard curve was used for bovine serum and milk analyses. The serum samples were analysed after sample dilution, and the calculated concentrations were compared with the independently analysed concentrations by ECLIA. The P4 cycle calculated from the LFIA standard curve showed a good P4 fitting profile with overestimation in concentration, but enabled the detection of the bovine estrous cycle. The milk samples required modification in sample pre-treatment, and the inhibition assay was carried out to determine the P4 concentration in each sample. The calculated P4 cycle was compared with the independent ELISA analysed P4 cycle and the result indicated that the LFIA method had the potential to be a quick, easy and cost effective way for semi-quantitative P4 analysis in milk samples.

A model flow cell was designed, constructed and tested with immobilised 3GNZZPhaC beads on the Au coated slide. The results indicated that the 3GNZZPhaC beads may have potential use as a surface sensor. The immobilisation of ZZPhaC beads was performed using a commercially available Au sensor chip in a Biacore X100 system. The binding performance of the beads sensor surface was tested using rat Anti-P4 with a varied flow rate. The results showed the ZZPhaC beads were stable under a pressurised system (the Biacore closed system) and an interaction between the Anti-P4 and Au-ZZPhaC was observed. It was determined that the beads may possibly be used as an alternative SPR sensor surface material.

In summary, SPR and LFIA based immunoassays were developed and tested on bovine serum and milk samples, and they showed to be a useful, rapid, cost effective real world application in the detection of the bovine estrus and potential pregnancy in a cow.

Future work

The SPR sensitivity can potentially be optimised by:

(i) Improving the binding performance by using a range of different antibodies to increase the surface response for P4. The sensitivity of the binding of an antibody towards a particular steroid can be varied.

(ii) Further increasing the length between the P4 molecule and OVA.

(iii) Incorporating the Anti-P4 with AuNPs. The enhancement in surface response may lead to a more sensitive sensor surface.

The LFIA sensitivity can also be further investigated by:

(i) Testing the P4-PEG-OVA sensor strip with different Anti-P4-Au conjugates and with different antibodies.

(ii) Adjusting the flow rate of the P4-PEG-OVA strips by fabricating a membrane material with a lower porosity than the Hi Flow Plus 75 membrane made from nitrocellulose currently used. The sensitivity of the strips is inversely proportional to the membrane porosity, hence the P4-PEG-OVA can be tested using different membranes to optimise the binding between the mouse Anti-P4 and P4-PEG-OVA.

PHA Beads

The aggregation and coagulation problems of PHA granules may be prevented by introducing a charge on the surface of the beads which could be achieved by altering the pH of the solution. Secondly to limit the non-specific binding which could result in coagulation of the beads a blocking agent could be used. The introduction of AuNPs in LFIA tests showed a reduction in the coagulation level, hence they may be a possible blocking agent. The PHA granules displayed some potential as a surface application and possibly a new sensing material for a SPR sensor, but require further work towards resolving the aggregation and coagulation issues.

Appendix: Experimental

A.1 General experimental

A.1.1 Reagents and solvents

All starting materials were obtained from commercial sources and used without purification unless otherwise noted. All reagents and solvents were obtained from commercial sources and used as supplied. Solvents used in the reactions were analytical grade and used directly.

A.1.1.1 Chemicals

Sodium hydroxide, sodium carbonate, sodium bicarbonate, hydrochloric acid, sodium hydroxide, sulphuric acid, hydrogen peroxide, 1,3-dicyclohexylcarbodiimide, dimethylformamide, triethyl amine, tetrahydrofuran, N-hydroxysuccinimide, 1-ethyl-3(-3-dimethylaminopropyl)carbodiimide-HCl, hexane, ethyl acetate, methanol, ethanol, acetonitrile (HPLC grade), potassium chloride, potassium dihydrogen phosphate, sodium chloride, disodium hydrogen phosphate, sodium azide were from the Sigma Aldrich.

Progesterone was from Sigma-Aldrich, P8793-5G, sucrose from SERVA, trehalose from BDH, ovalbumin from Sigma-Aldrich A-5503, Triton X-100 from Lonover scientific supplies Ltd., bovine serum albumin from Invitrogen™, 30036-578, anti-mouse IgG (whole mouse) antibody produced in a rabbit from Sigma, M6024, and mouse anti-progesterone (SE7720) monoclonal antibody was obtained from Abd Serotech (Oxford, UK). A centrifugal filter 0.5 mL 3K (Millipore Amicon Ultra), Hi-Flow plus 75 membrane cards (60 mm x 301 mm) and cellulose fiber sample pads (17 mm x 300 mm) were from Millipore (Massachusetts, USA), PD-10 desalting columns were from GE Healthcare, and a golden silicon cantilever from Ultrasharp, Noncontact NSG II. 0.20 μm cellulose acetate syringe filters were from Advantec®, 0.45 μm syringe filters from Phenomenex® NZ Ltd, 1 mL syringes from NORM-JECT®, 20 μm filter membranes (diameter: 47 mm) from Grace Davidson Discovery Science), Dialysis tubing benzoylated 9 mm flat width from Sigma-Aldrich D2272-5FT, and 40 nm gold nanoparticles from BBInternational, 13259.

Reagents for the SPR work, including the CM5 chip, SIA kit Au, amine coupling kit (0.1 M NHS, 0.4 M EDC and 1 M ethanolamine) and HBS-EP running buffer (0.01 M HEP-ES$^+$ pH 7.4, 0.15 M NaCl, 3 mM EDTA and 0.005 % surfactant P20) were purchased from GE Healthcare (Uppsala, Sweden).

3GNZZPhaC and ZZPhaC beads were obtained from Professor Bernd Rehm's research group and PolyBatics (Palmerston North, New Zealand)

A.1.2 Instruments

A UV-3101PC (SHIMADZU Japan) was used for the antibody titration experiment. An Eppendorf Mini Spin was used for serum and milk sample preparation. The Syringe pump (Cole Parmer®) was used for flow cell setup, and the sputter coater was used to fabricate the Au surface for the SEM studies as well as the flow cell sensor surface. The BIAcore X100 system (GE Healthcare, Uppsala, Sweden) was used for all SPR analyses. A Nanodrop® ND-1000 UV-Vis Spectrophotometer was used for determination of P4 conjugates. A Stereomicroscope Olympus BX51 was used for fluorescence microscopic studies.

A FEI Quanta 200 Environmental Scanning Electron Microscope was used for scanning electron microscopy studies. An IsoFlowTM Reagent Dispenser (Imagenetechnology, Hanover, USA) was used to dispense control and test lines on a nitrocellulose membrane. The strips were cut with an M-70 cutter (advanced Sensor System Ltd, Ambala, India). A HP scanjet 3500c photo scanner and dedicated software were used to obtain images of the strips. An Asylum Research MF-3D instrument was used for preliminary AFM studies.

A.1.3 Software

The intensity of the control and test lines on the strips was quantified with a strip reader system (version 2.00, Simon Brown Ltd, Launceston, Tasmania, Australia). OriginPro 7.0 (OriginLab, Northampton, MA, USA) was used for all curve fitting and data analysis.

A.2 Chapter 2 Experimental

A.2.1 Sample collection (by Zoe Matthews)

The control samples for the identification and measurement of early diagnostic biomarkers in sporidesmin-induced subclinical facial eczema in a cattle trial were collected from 3 control cows (table A.1).

Table A.1 Physical characteristics of the control cows

Cow No.	Tag No.	Age (year)	Weight (kg)	Last Calf
1	152	4	445	16/08/2010
2	22	10	432	26/08/2010
3	384	8	464	27/08/2010
4	239	5	395	13/08/2010

A.2.1.1 Milk samples

Milk samples were collected using herd testing equipment from Dairy 4, Massey University. The herd testing equipment was washed and sterilised between sampling.

The controlled volume of milk was sampled from the milk meter under a continuous milking process, and then stored at -80℃.

A.2.1.2 Serum samples

The blood samples were collected via venipuncture from the tail vein or the jugular vein. Samples were rested at room temperature between 2 to 6 hr to allow the blood to clot. The clot was removed from the sample by spinning at 3000 rpm for 6 min (Heraus Multifuge 1 s). The liquid serum was transferred into a 5 mL polypropylene tube then stored at -80℃.

A.2.2 Synthesis of P4 derivatives

Dr Wayne Campbell and Dr Krishanthi Jayasundera worked in the lab and made the compounds indicated which have been used in this work.

A2.2.1 Progesterone P4 Propyl Linker Synthesis (4TP-P4) by Dr Wayne Campbell

*3-(pregn-4-ene-3,20-dione-4-yl)thiopropanoic acid (**3**)*

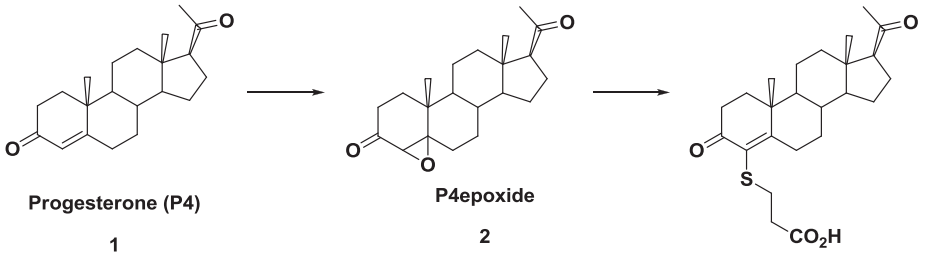

The title compound (**3**) was prepared by first synthesising compound (**2**) This was done according to a literature method.[1,2] P4 (1) (123.5 mg, 0.392 mmol) was dissolved in methanol (8 mL), and a 10% solution of NaOH (0.5 mL). 30% of H_2O_2 (0.5 mL) was added to the mixture and stirred at 0 ℃ for 2 hr. The solution was neutralised using diluted acetic acid and concentrated to 1/3 of the original volume under reduced pressure. Ethyl acetate was added to the white precipitate and extracted with Milli-Q H_2O followed by a saturated aqueous NaCl solution. The organic solvent was concentrated under reduced pressure and the residue (compound **2**) was purified by silica gel chromatography using ethyl acetate/n-hexane (1:1). A white coloured powder of compound **2** was formed with 58% yield.

Compound **3** was synthesised according to a literature[1] procedure. A solution of 3-mercaptopropanoic acid (37.6 mg, 1.06 mmol, 4.9 eq) and 25% of aqueous KOH solution (0.104 mL) was stirred under room temperature for 10 min. 4, 5-Epoxy progesterone (**2**, 70.5 mg, 0.213 mmol, 1 eq) in ethanol (1 mL) was then added to the mixture followed by stirring at room temperature overnight. 3-mercaptopropanoic acid (37.6 mg, 1.06 mmol, 4.9 eq) was added to the mixture and stirred at 80℃ for 5 hr. Additional 3-mercaptopropanoic acid (37.6 mg, 1.06 mmol, 4.9 eq) was added to the mixture and stirred at 80 ℃ overnight. The mixture

was cooled to room temperature, and Milli-Q H_2O was added to the mixture. The pH of the solution was adjusted to 4 using diluted aqueous HCl at 0 ℃, and the solution was extracted with ethyl acetate. The organic layer was washed with Milli-Q H_2O and saturated aqueous NaCl solution, then dried using anhydrous $MgSO_4$. The solvent was then removed under reduced pressure. The residue was purified using silica gel chromatography using ethyl acetate/n-hexane (3:1).

A.2.2.2 Progesterone P4 Propyl Linker OVA Conjugate (4TP-P4-OVA, Figure 2.6)

by Dr Wayne Campbell

DMF (175 μL) was added to a mixture of 4TP-P4 (9.20 mg, 0.022 mmol) and 1,3-dicyclohexylcarbodiimide (DCC) (5.1 mg, 0.025 mmol). The N-hydroxy succinimide (NHS) solution (2.75 μL in 0.895 M DMF gives 0.0246 mmol) was added to the 4TP-P4 mixture and stirred for 3 hr at room temperature in a sealed vial. The ovalbumin (OVA) solution (20.0 mg in 1.75 mL buffer) solution was added to the 4TP-P4 mixture slowly with stirring. The solution was stirred overnight followed by dialysis over 2 days with Milli-Q H_2O (3 changes per day), and the solution was then dialysed with PBS buffer (pH 7.4, one change in the morning, and one in late afternoon). The solution was then purified with a PD100-Desalting column with 2.5 mL of PBS buffer. The eluted sample is known as 4TP-P4-OVA and is stored at -4 ℃.

A.2.2.3 Progesterone P4 Propyl-Hexyl Extended Linker Synthesis (4TPH-P4)

by Dr Wayne Campbell

6-[3-[(pregn-4-ene-3,20-dione-4-yl)thiopropano-yl]amino]hexanoic acid (4TPH-P4)

3-(pregn-4-ene-3,20-dione-4-yl)thiopropanoic acid (**3**) (100 mg, 0.239 mmol) was dissolved in dry DMF (0.75 mL). A solution of 1,3-dicyclohexylcarbodiimide (DCC) (59.2 mg, 0.287 mmol, 1.2 eq) in DMF (0.25 mL) was added, followed by addition of a solution of N-hydroxy succinimide (NHS) (33.0 mg, 0.287 mmol, 1.2 eq) in DMF (0.25 mL). After stirring for 2 1/4 hr in a sealed vial (white precipitate forms), a saturated solution of 6-aminocaproic acid (94.1 mg, 0.717 mmol, 3.0 eq) in Milli-Q water (0.25 mL) was added. The reaction mixture was stirred at room temperature overnight (tan mixture forms). $CHCl_3$ (40 mL) was added and the organic layer washed with H_2O (2 x 50 mL). The organic layer was separated and dried (Na_2SO_4), filtered and the solvent removed under reduced pressure to give an oil (excess DMF present). The excess DMF was removed by azeotroping with MeOH under reduced pressure, then high vacuum to give the crude product as a white solid. The crude product was purified *via* column chromatography (flash Silica gel, 30 mm^{dia} x 140 mm, DCM:MeOH (3%): formic acid (1 drop per 100 mL)) collecting the major middle band. The solvent was removed and the solid redissolved in minimal EtOAc, filtered and the product precipitated with hexane to give a white solid. This was collected by centrifugation (washing with hexane twice) and dried under high vacuum to give the product as a white solid (74.8 mg, 0.141 mmol, 59%, *cf* 43% *via* 2-step). Checked and correct by ^{1}H NMR, ES-MS (+ve & -ve modes).

A.2.2.4 Progesterone P4 Propyl-Hexyl Extended Linker OVA Conjugate (4TPH-P4-OVA, Figure 2.7) by Dr Wayne Campbell

3-(pregn-4-ene-3,20-dione-4-yl)thiopropanoic acid (9.2 mg, 22 µmol) and 1,3-dicyclohexylcarbodiimide (DCC) (5.1 mg, 25 µmol, 1.1 eq) were dissolved in dry DMF (0.175 mL). To this was added a solution of NHS (27.5 µL, 0.895 M, 24.6 µmol, 1.1 eq) in DMF. The mixture was stirred for 3 hr in a sealed vial at room temperature forming a white precipitate. The resulting mixture was added slowly to a solution of OVA (20.0 mg, 0.44 µmol) in PBS buffer (1.75 mL, pH 7.08).

A.2.2.5 Synthesis of *N*-(13-(carbonylamino)-4,7,10-trioxatridecanyl)- 3-(pregn-4-ene-3,20-dione-4-yl)thiopropanamide (P4S$(CH_2)_2$-PEG-COOH)

by Dr Krishanthi Jayasundera

The steps involved in synthesis of the P4-PEG derivative (**6**) are given Scheme 2.1 below. Commercially available progesterone was used as the starting material. Firstly, P4 (**1**) was converted to the P4epoxide (**2**) and then to P4S$(CH_2)_2$COOH (**3**) following literature procedures[1,3,4] and discussed in A.2.2.1. Compound **3** was converted to **4** and then to **5** and finally to **6** and these latter three steps are now given and are outlined in Scheme 2.1.

Compound **2**, **3**, **4**, **5** and **6** have been identified and characterised by NMR and mass spectrometry, and the information will be published by the authors in the upcoming paper.

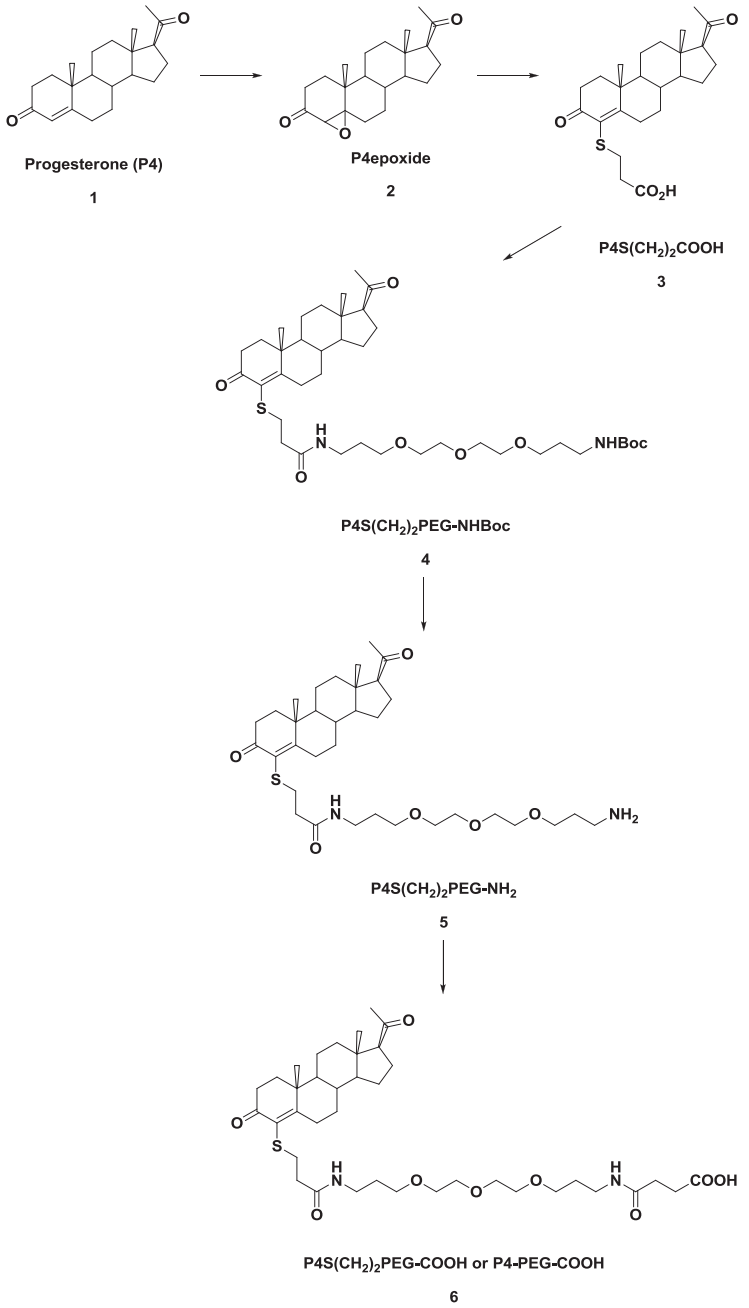

Scheme 2.1 Synthesis of P4S$(CH_2)_2$PEG-COOH

A.2.2.6 Synthesis of P4S$(CH_2)_2$-PEG-NHBoc (4) by Dr Krishanthi Jayasundera

A solution of DCC (134 mg, 0.65 mmol, 1.3 eq), and NHS (74 mg, 0.065 mmol, 1.3 eq) in DMF (1.0 mL) were added dropwise to P4S$(CH_2)_2$COOH (**3,** 209 mg, 0.5 mmol, 1.0 eq, in 2 mL of DMF) at room temperature under an atmosphere of nitrogen.

The mixture was stirred for 12 hr in the absent of light and the resulting white precipitate was filtered and dried. An aqueous solution of the PEG amine derivative (240 mg, 0.75 mmol, 1.5 eq) was added to the active ester in DMF (**3**) followed by triethyl amine (250 μL) and stirred under the absent of light for 12 hr. 50 mL of water was added to the mixture, and extracted with DMC (20 mL x 3) then washed with cold saturated $NaHCO_3$ (20 mL x 2) and water (20 mL x 2), dried with $MgSO_4$. The solvent was evaporated and the residue was purified by column chromatography eluting with DCM/MeOH 15/1 to afford the product as a yellow oil (yield 234 mg, 63%).

A.2.2.7 Synthesis of P4S$(CH_2)_2$-PEG-NH_2 (5) by Dr Krishanthi Jayasundera

The solution of P4-PEG-NHBoc (**4**, 102 mg, 0.14 mmol) was stirred with formic acid (2 mL) for 3 hr at room temperature. The solvent was removed under reduced pressure to give compound **5** as a yellow-orange oil. Compound **4** was used for the next step without further purification.

A.2.2.8 Synthesis of P4S$(CH_2)_2$-PEG-COOH (6) by Dr Krishanthi Jayasundera

Succinic anhydride (17 mg, 0.16 mmol, 1.16 eq) was added to the solution of P4-PEG-NH_2 (**5**, 87 mg, 0.14 mmol, 1 eq) in 5 mL of toluene/methanol (4/1) and the mixture refluxed under nitrogen for 1 hour. The solvent was removed and the resulting oil was purified by silica gel chromatography eluting with DCM/MeOH/HCOOH (10/1/0.1) and product **6** formed as a yellow-orange oil.

A.2.2.9 Conjugation of the P4 derivative to ovalbumin to give P4-PEG-OVA (Figure 2.8)

The P4 derivative (compound **6**, 20 mg) was added to a mixture of DCC (1 M, 30 μL), NHS (1 M, 30 μL) in DMF (60 μL) and stirred at room temperature for 2 hr. The mixture was added to OVA (20 mg, 0.5 μmol in PBS, cold) and stirred at 4℃ overnight. The mixture was then dialysed with Milli-Q H_2O for 2 days (3 changes per day), then with PBS buffer for 1 day (pH 7.4, 3 changes per day) at 4 ℃. The solution was then purified on a PD10 desalting

column at room temperature using PBS buffer as the eluent and the purified conjugate (3.5 mL) was collected.

A.2.3 SPR

A.2.3.1 P4 conjugate immobilisation

A.2.3.1.1 4TP-P4-OVA

A mixture (1:1) of 70 µL of EDC (390 mM, in HBS-EP$^+$) and NHS (100 mM, in HBS-EP$^+$) was injected over a CM5 chip (Biacore, lot 10033548) at 10 µL/min for the surface activation process. 4TP-P4-OVA was diluted in sodium acetate solution (pH 4.0, 10 mM) and filtered through a 0.22 µm syringe filter (Phenomenex). The 4TP-P4-OVA (5.5 mg/mL) was injected and immobilised on FC2, whilst OVA (2 mg/mL) was injected and immobilised on FC1. The injection rate was 5 µL/mL for 20 min and the target immobilisation level was at 10,000 RU. A solution of ethanolamine hydrochloride (1 M, pH 8.5) was injected at 10 µL/min to deactivate the unreacted active ester groups on the CM5 sensor surface. The final immobilisation level for FC1 was 7637.4 RU and FC2 was 6289.9 RU.

A2.3.1.2 4TPH-P4-OVA

The immobilisation process for 4TPH-P4-OVA onto a CM5 sensor surface (Biacore, lot 10033548) was carried out following the steps in section A.2.3.1.1 and resulted in a final immobilisation level of 6762.6 RU for FC1 and 6883.4 RU for FC2.

A.2.3.1.3 P4-PEG-OVA

The immobilisation process for P4-PEG-OVA (6.4 mg/mL) onto a CM5 sensor chip (Biacore, lot 10042916) was carried out following the steps in section A.2.3.1.1. After the activation step, P4-PEG-OVA (100 µL) was diluted in 900 µL (10 mM) sodium acetate buffer. The P4-PEG-OVA solution was injected over FC2 at 5 µL/min for 24 s followed by a 200 s injection. The surface was deactivated by injecting ethanolamine hydrochloride solution (1 M, pH 8.5) at 10 µL/min for 420 s and the final immobilisation level was 6171.3 RU. The immobilisation

level for FC1 was to be as close to FC2 as possible. OVA (5.3 mg/mL, 100 µL) was diluted in sodium acetate buffer (900 µL, 10 mM) and injected over FC1 after the activation process. The OVA solution was injected at 5 µL/min for 60 s, 24 s, 60 s, 60 s, 120 s, 24 s (x7 times), 60 s, 24 s (x4 times) followed by ethanolamine hydrochloride injection at 10 µL/min for 420 s. The final immobilisation level for FC1 was 6251.0 RU.

A.2.3.2 Anti-P4 binding curve

The binding performance of the Anti-P4 was carried out by establishing the binding curve for each antibody (rat and mouse), and then the concentration of Anti-P4 and the best injection time for the appropriate response on the sensor surface were determined.

A.2.3.2.1 Rat Anti-P4 (Sigma P19222)

Rat Anti-P4 stock solution (0.1 mg/mL) was used to make samples of concentrations (1, 3, 5, 7, 9, 11, 20 µg/mL) in HBS-EP$^+$ buffer, then injected over the sensor surface at 30 µL/min for 120 s. The surface was regenerated by injecting duplicates of NaOH (50 mM) at 5 µL/min for 30 s.

A.2.3.2.2 Serotech (SE77201430)

Mouse Anti-P4 stock solution (1 mg/mL) was used to make samples of different concentrations (0.1, 0.2, 0.3, 0.4, 0.5, 0.6, 0.7, 0.8 µg/mL) in HBS-EP$^+$ buffer, then injected over the sensor surface at 30 µL/min for 120 s. The surface was regenerated by injecting duplicates of NaOH (50 mM) at 5 µL/min for 30 s.

A.2.3.3 Inhibition assay

A P4 inhibition assay was used to develop a P4 standard curve. A series of P4 standards (ranging from 0 to 58 ng/mL) was prepared using HBS-EP$^+$ buffer as the diluents. The P4 standards were mixed in a 1:1 volume ratio with mouse Anti-P4 (1.2 µg/mL) and allowed to incubate at room temperature for 15 min. The samples were injected over the sensor surface

at 30 μL/min for 120 s. The regeneration of the surface was performed by two injections of NaOH solution (50 mM) for 30 s at 5 μL/mL.

A.2.3.4 Free serum P4 analysis preparation

Serum samples from cow 1 was used for free P4 analysis. The serum samples were thawed on ice then spun down using a centrifugal filter (Millipore, Amicon Ultra centrifugal filter 0.5mL 3K) at 13,400 rpm for 30 min. The filtrate was store at -4 ℃.

A.2.3.5 Solvent extraction for serum samples

Serum samples from cow 1 were used for solvent extraction. 600 μL of serum was obtained and the pH adjusted to 9.8 using carbonate-bicarbonate buffer (400 μL) and shaken for 24 hr at 200 rpm. 15 mL of hexane was added to the sample solution and mixed for 1 hour at 300 rpm. The samples were dried under vacuum, and reconstituted in methanol and stored at -4 ℃.[5]

A.2.3.6 SPR assay for milk analysis preparation

1 mL of acetonitrile was added to 300 μL of milk sample and mixed thoroughly using a vortex, followed by sonication. The samples were spun down by centrifugation at 13,400 rpm for 10 min. The solvent was removed by freeze drying overnight, and the samples were reconstituted with 300 μL of HBS-EP$^+$ buffer and sonicated for 20 min before performing the SPR assay.

A.2.3.7 SPR Serum analysis

The treated serum samples were mixed with equal volumes of Anti-P4 (1.2 μg/mL) and allowed to incubate at room temperature for 15 min. The samples were injected at 30 μL/min for 120 s over the P4-PEG-OVA sensor surface. The surface was regenerated by 2 injections of NaOH (50 mM). The results were plotted using a standard curve and the P4 concentration in each serum sample was calculated.

A.2.3.8 SPR milk analysis

The treated serum samples were mixed with an equal volume of Anti-P4 (2.5 μg/mL) and allowed to incubate at room temperature for 15 min. The milk samples were injected over the P4-PEG-OVA sensor surface at 30 μL/min for 120 s and regenerated with 2 injections of NaOH at 5 μL/min for 30 s. The analysis was performed in triplicate.

A.3 Chapter 3 Experimental

A.3.1 Preparation of a 10% bovine serum albumin (BSA) solution

10% of BSA (w/v) was dissolved in Milli-Q H_2O, followed by filtration using a 0.45 μm syringe filter and stored at -20℃.

A.3.2 Preparation of PGD solution

1% of BSA (10%, w/v solution), was added to a phosphate buffer (50 mM, 1 mL), followed by addition of a 0.1% of sodium azide, 30 mg of trehalose (BDH), 60 mg of sucrose (SERVA) and 2.5 μL of Triton X100 (Lonover scientific supplies LTD.).

A.3.3 Antibody titration

A 1 mg/mL of P4-Anti (Serotech) stock solution was prepared and the matrix below was set up in 1 mL cuvettes with variation of protein concentrations (Table A.2).

Table A.2

Stock [Anti-P4] (mg/mL)	Anti-P4 (µL)	Buffer (µL)	[Anti-P4] (µg/mL)
0	0	50	0
0.1	7	43	13
0.1	3	17	65
1	6.5	44	130
1	9.75	40	195
1	13	37	260
Stock [Anti-P4] (mg/mL)	Anti-P4 (µL)	Au, NaCl (µL)	Titration[Anti-P4] (µg/mL)
0	50	500, 100	0
13	50	500, 100	1
65	50	500, 100	5
130	50	500, 100	10
195	50	500, 100	15
260	50	500, 100	20

The blank sample contained 100 µL Milli-Q H_2O and was scanned between 300-800 nm. 500 µL of colloidal gold (BBInternational, 40 nm) was added to each cuvette and mixed thoroughly, allowing the mixture to incubate at room temperature for 2 min. 100 µL of NaCl (10%, w/v) was added to each cuvette a minute apart. The spectrum of each sample was recorded from 300-800 nm and the optimal Anti-P4 concentration was determined.

A.3.4 Preparation of P4-PEG-OVA sensor strips

The lateral flow test strip was prepared using the commercially available nitrocellulose membrane card which contained P4-PEG-OVA (6.5 mg/mL) as the test line and rabbit anti-mouse IgG (1 mg/mL) as control line. P4-PEG-OVA (6.4 mg/mL) solution was diluted using 75 µL of PBS buffer (100 mM) and 558 µL of Milli-Q H_2O to give a final concentration of 1 mg/mL. The test and control line were sprayed onto the nitrocellulose membrane at 50 mm/s with a dispensing rate at 1.008 µL/cm. The cards were sprayed at 1.008 µL/cm at a speed of 50 mm/s, and the distance between the test and control line was 50 mm. The sprayed membrane was dried at 40 ℃ for 1 hr, and the membrane was cut into 5 mm strips. The strips were stored in a dry box at room temperature. The bottom of the strips where the conjugate pad was designed to be attached was removed before the assay was performed.

A.3.5 Conjugation of Anti-P4 to gold

The Anti-P4 whose concentration was determined by antibody titration (section 3.3.1) was used for the conjugation of Anti-P4 to Au nanoparticles. 15 µg/mL of Anti-P4 (Serotech) was conjugated to 10 mL of gold nanoparticles (BBInternational, 40 nm, pH 7.4) and the solution was stirred at room temperature for 1 hour. 1 mL of 10% BSA was added and the solution was stirred for a further 1 hour at room temperature. The conjugated Anti-P4-Au particles were then transferred to centrifuge tubes and centrifuged for 1 hour at 8000 g at 4 ℃. The supernatant was carefully removed and the gold pellet was resuspended in 1 mL of PGD mixture. The conjugate was then filtered through 0.45 µm filter and stored at 4 ℃.

A.3.6 Anti-P4-Au binding curve

The binding affinity of the Anti-P4-Au was performed to determine the binding curve. A series of solutions with different Anti-P4-Au concentrations (0.1 µg/mL to 1.2 µg/mL, made up to 75 µL with HBS-EP^+ buffer) was produced and the strips were placed into the solution well vertically. The assay was performed in triplicate. The assay was allowed to develop for 20 min, and the strips were scanned and subjected to quantitative analysis.

A.3.7 P4 standard curve

The assay reagents (Anti-P4-Au, PBS buffer, and P4 standard which gave total volume 75 µL) were directly pipetted into the solution well of a low binding microtiter plate. The P4-PEG-OVA strips were inserted vertically into the solution wells. The assay was allowed to develop for 20 min and the strips were scanned and then subjected to quantitative analysis.

A.3.8 LFIA assay for serum analysis

The developed assay for the P4 standard curve was used for serum analysis. The established P4 standard concentrations were used and spiked with 5 µL of diluted serum sample (0.045 ng/mL) as a blank sample to reduce the matrix effects. The assay for the standard curve consisted of 38 µL of Anti-P4-Au (1:37 dilution with HBS-EP^+ buffer), 5 µL of P4 standard solution, 5 µL of diluted serum (blank) and 27 µL of PBS buffer (10 mM). The serum sample analysis followed the same procedure, the assay contained 38 µL of Anti-P4-Au, 5 µL serum sample (1:10 dilution with PBS buffer), and 32 µL of PBS buffer (10 mM). The assays were allowed to be developed for 20 min, scanned and then subjected to quantitative analysis.

A.3.9 LFIA assay for milk analysis

The milk preparation protocol described in section A.2.3.6 was used to prepare the LFIA milk samples. The freeze dried milk samples were reconstituted in PBS buffer (10 mM), and the assay was performed. The assay consisted of 38 µL of Anti-P4-Au (1:37 dilution with HBS-EP^+), 5 µL of freeze dried milk, and 32 µL of PBS (10 mM). The assay was allowed to be developed for 20 min before the quantitative analysis.

A.3.10 NZVP serum analysis

The immunoassay was used for in vitro quantitative determination of progesterone in serum and plasma. The electrochemiluminescence immunoassay (ECLIA) was performed on a Elecsys and Cobas immunoassay analyzer.

A.3.11 NZVP milk analysis

The OVUCHECK® MILK test was performed on the milk samples. The test is based on the competitive binding of unlabelled progesterone present in the standard or whole milk samples. A fixed quantity of progesterone was labelled with the enzyme alkaline phosphatase (AP, conjugate) to binding sites on a limited amount of specific progesterone antibodies. The sample wells were pre-coated with specific progesterone antibodies, which provided a solid phase for the capture of the progesterone present in the samples. All components in the sample well other than those bound to the wells are washed away. The bound AP-labelled progesterone remaining in the wells is inversely proportional to the concentration of the unlabelled progesterone present in the samples. The bound labelled progesterone was then measured by reacting AP with its substrate. The colour produced by the reaction was measured spectrophotometrically (absorbance at 405 nm) and the concentration of the progesterone in the milk sample was determined from the standard curve.

A.4 Chapter 4 Experimental

A.4.1 Isolation of 3GNZZPhaC and ZZPhaC beads

The polymer beads were isolated by harvesting respective cells using centrifugation for 20 min at 6000 × *g* and 4 °C. The sediment was washed and suspended in 3 volumes of 50 mM phosphate buffer (pH 7.5). Cells were passed through a French Press two times at 16 kpsi. The cell lysate (0.75 mL) was loaded onto a glycerol gradient (88% and 44% (v/v) glycerol in phosphate buffer). After ultracentrifugation for 2.5 hr at 100 000 × *g* and 10 °C, beads could be isolated from a white layer above the 88% glycerol layer. The PHA beads were washed with 10 volumes of phosphate buffer (50 mM, pH 7.5) and centrifuged at 100 000×*g* for 60 min at 10 °C. The sediment containing the PHA beads was suspended in phosphate buffer and stored at 4 °C.

A.4.2 Spin coating

100 µL of 3GNZZPhaC bead solution (0.1 mg/mL) was placed on a clean Au coated microscopic slide (1cm x 1cm). The sample was spun for 2 min 20 s at 1000 rpm and was allowed to dry and subjected to SEM studies.

The spin coating process was repeated with the ZZPhaC bead solution (1 mg/mL).

A.4.3 Dip coating

The dip coating device was built and placed in a cold room (3.5 ℃) for the dip coating process. The stock 3GNZZPhaC bead solution (0.1 mg/mL) was sonicated and diluted using HBS-EP$^+$ buffer to 10 ng/mL. A Au coated mylar chip was cleaned with ethanol/Milli-Q H_2O and then attached to the dip coating device. The dip coating process was carried out with the bead solution under continuous stirring for 1 hour. The bead coated mylar chip was rinsed with Milli-Q H_2O and allowed to dry and subjected to a SEM study. The procedure was repeated with the ZZPhaC bead solution.

A.4.4 SEM sample preparation

The sample slides were taped to the aluminium stub using double sided tape, the sample slides and the stub were then connected using a drop of silver paint (at the edge of the slide and the stub). The sample was then Au sputtered coated for 200 s (BAL-TEC SCD 050), and then was ready for SEM imaging.

A.4.4 Flow cell system

The glass slides were cleaned with methanol and sonicated for 15 min. The sonicated glass slides were cleaned and dried using chemwipe. The slides were Au sputtered coated at 18-20 mA and then they were attached with double-sided tape with pre-cut flow cell channel shape, and stored at room temperature. The reference slides were prepared following the sample process but without the Au coating.

The flow cell system was set up as described in section 4.5; the stock solution of 3GNZZPhaC beads (13 mg/mL) was diluted in HBS-EP^+ buffer. The 1 mL syringe was loaded with the diluted bead solution (10 ng/mL) and the solution injected over the sealed flow cell with reference slide at the rate of 2 mL/hour. The flow cell was injected with 100 µL of Milli-Q H_2O as the regeneration step to remove bead residues in the system. The reference slide was detached from the flow cell setup and subjected to an SEM study.

The flow cell was cleaned with methanol and an air duster. The procedure was repeated for the Au coated slide which had varied volumes of injection of the 3GNZZPhaC beads.

A4.5 SPR

A.4.5.1 Outside immobilisation

The SIA Kit Au (Biacore) was used for ZZPhaC outside immobilisation. The Au chip was cleaned and rinsed with Milli-Q H_2O. 100 µL of ZZPhaC beads (1 ng/mL) were immobilised onto the Au chip and incubated for 10 min, then the excess bead solution removed by rising with Milli-Q H_2O. The binding performance of the ZZPhaC sensor surface was observed by performing the binding affinity study. A series of mouse Anti-P4 solutions were injected over the sensor surface at 5 µL/min for 120 s, the response unit was recorded for each mouse Anti-P4 concentration and the surface was regenerated with NaOH (50 mM).

A.4.5.2 SPR immobilisation

The SIA Kit Au (Biacore) was used for ZZPhaC immobilisation. The ZZPhaC beads were immobilised onto FC2 in the Biacore X100 instrument. The Au sensor surface was cleaned with NaOH (200 mM), and HCl (200 mM) followed by rising with Milli-Q H_2O. The cleaned Au sensor chip was assembled into the cassette and docked into the X100. The ZZPhaC bead solution (1 ng/mL) was injected at 5 µL/min for 24 s, followed by 1080 s, but no binding occurred. The ZZPhaC bead solution concentration was increased to 10 ng/mL with the first injection at 5µL/min for 24 s, followed by a second injection for 1080 s. A further three

injections (24 s each) were performed to ensure the surface was fully immobilised. The final immobilisation level was 522.0 RU. The FC1 was left as a bare Au surface to monitor the non-specific binding. The ZZPhaC immobilised sensor chip (Au-ZZPhaC) was subjected to a binding affinity study.

A.4.6 FT-Raman study

FT-Raman spectra were recorded from solid samples using a Bruker IFS-55 Equinox FTinterferometer bench (Bruker Optik GmbH, Ettlingen, Germany) equipped with a FRA-106 Raman accessory and a D418-T liquid nitrogen cooled Ge detector. A 1064 nm cw Nd:YAG laser (Coherent, Lübech, Germany) was employed; laser power of 120 mW for PhaCZZ Au was used and 250 mW for ZZPhaC. The interrogated area was approximately 1 mm in diameter and a 180º backscattering arrangement was used. OPUS (version 5.5, Bruker Optik GmbH, Ettlingen, Germany) was used to record spectral data. Spectra were 500 (ZZPhaC) or 20 000 (ZZPhaC-Au) accumulated scans, at 4 cm^{-1} resolution, across 250-3400 cm^{-1}. The Blackman-Harris 4 apodisation function, a scan velocity of 5.0 kHz and a zero filling factor of 2 were used.

The spectral resolution of freeze dried ZZPhaC and ZZPhaC-Au samples (Figure A.1) improved significantly compared with solution samples. The spectrum broadened when AuNPs were attached to the surface. It was thought AuNPs would have an enhancement effect, but this was not seen in the ZZPhaC samples. The interaction between the AuNPs and the ZZPhaC surface protein was not resolved.

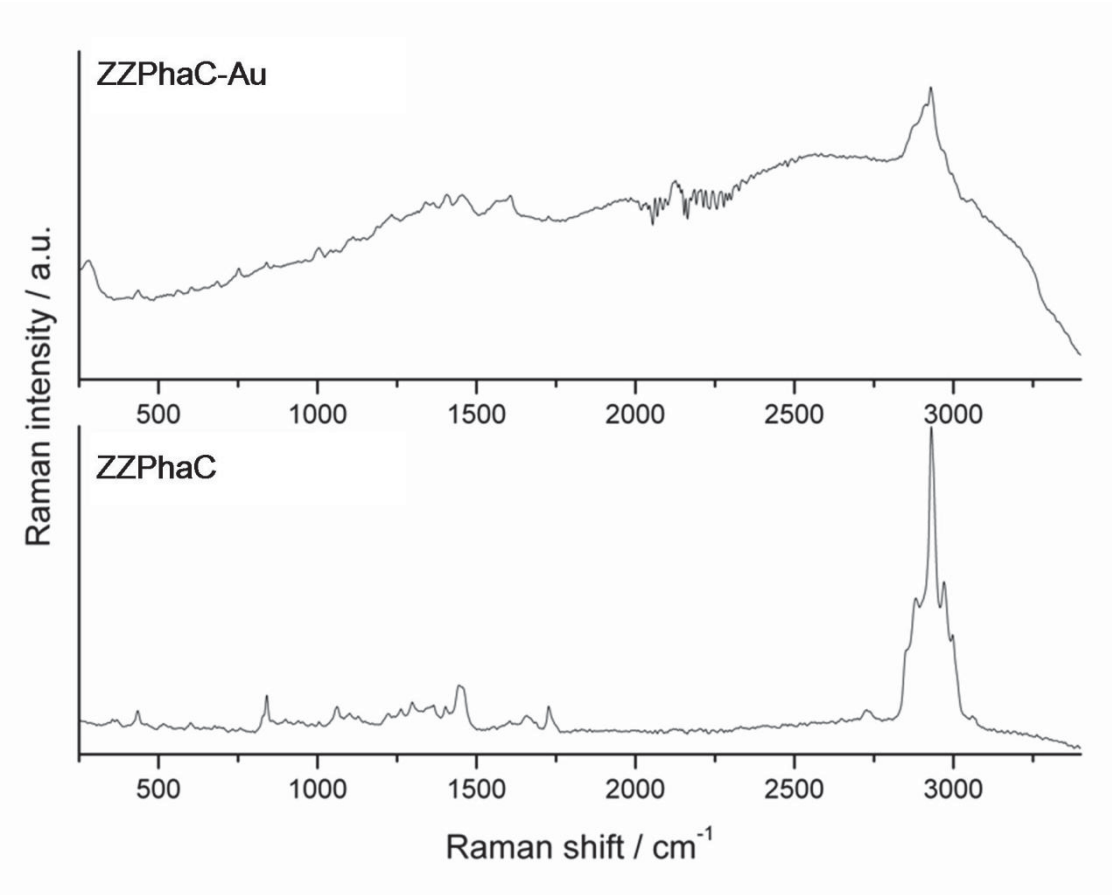

Figure A.1 FT Raman spectra of ZZPhaC and ZZPhaC-Au. The AuNPs did not enhance the sensitivities of the spectrum, but broadened it.

A.4.7 X-ray crystallographic studies

The 3GNZZPhaC samples (including solution and freeze dried samples, both reference and gold nanoparticle samples) were prepared in the capillary tubes and data were collected using the X-ray data collection system (Figure A.2) which included the Rigaku MicroMax-007 microfocus X-ray generator with an Axco P70 Capillary optic to focus and monochromate the X-ray beam. This optic is designed for poorly diffracting crystals and it provides flux intensity of ~8 x 1010 photons/mm^2/sec. 3GNZZPhaC solution (100 ng/mL) was initially prepared in HBS-EP$^+$ buffer (10 mM), the diffraction images were collected with 5 and 20 minutes exposure time. Diffraction images were also collected for freeze dried samples of 3GNZZPhaC beads and 3GNZZPhaC+AuNPs with 20 min exposure time.

The diffraction pattern of solution samples of 3GNNZPhaC and 3GNZZPhaC with Au bound showed very broad peaks which indicated that the biopolyesters had very low degrees of crystallinity (or not crystalline) (Figure A.2, A.3).

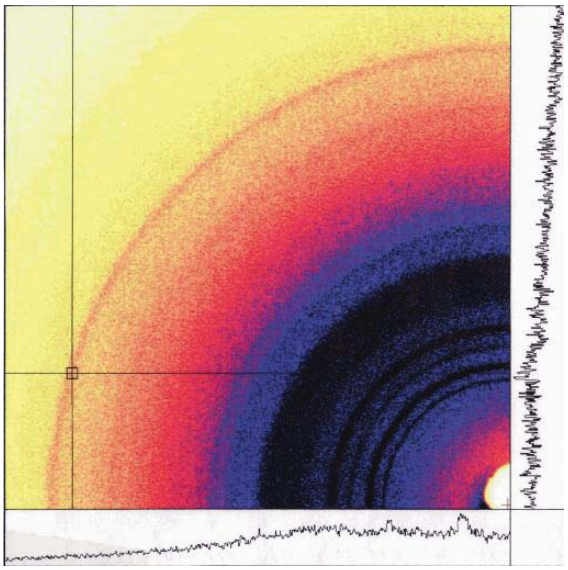

Figure A.2 The diffraction pattern of a 3GNZZPhaC solution.

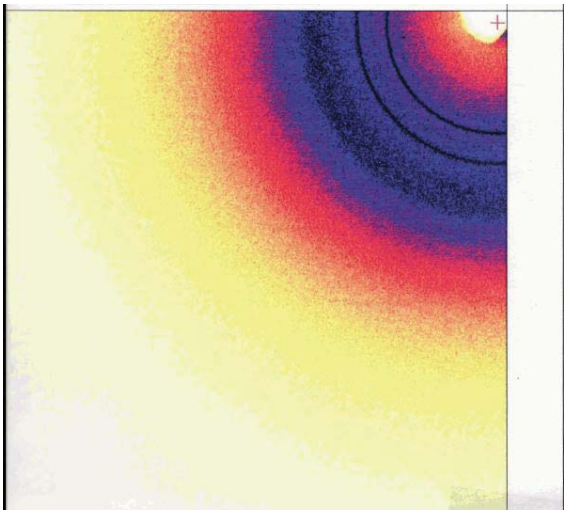

Figure A.3 The diffraction pattern of 3GNZZPhaC+Au solution. The image showed a lack of a defined peak at 2.37 Å in comparison with Figure A.2.

The diffraction pattern was characteristic of organic matter (almost not crystalline).
The results of the solution samples could also be due to the low concentration of the samples, hence data for freeze dried samples were also collected. The image of freeze dried 3GNZZPhaC+Au (Figure A.4) showed defined peaks at 44, 7.36, 6.69, 5.88, 5.30, 4.71-3.84, 3.31, 2.77, 2.62 Å, as well as weakly defined peak at 2.37 Å. However, the weak peak

disappeared in plain freeze dried 3GNZZPhaC sample images, and the image was not improved by increasing the exposure time. It was most likely the signal was caused by the AuNPs bound to the surface. Therefore, the preliminary X-ray powder diffraction images indicated that the freeze dried 3GNZZPhaC and 3GNZZPhaC+Au samples showed more crystallinity (Figure A.4), and it suggested that the core of the polyester beads was crystalline.

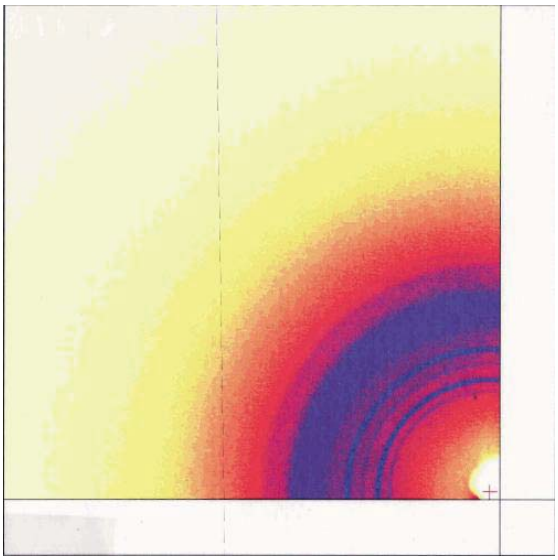

Figure A.4 The X-ray powder diffraction image of freeze dried 3GNZZPhaC+Au showed that it was partially crystalline.

References

(1) Yoshida, H.; Nakai, S.; Nimbari, F.; Yoshimoto, K.; Nishimura, T. *Steroids* **1989**, *53*, 727.

(2) Abul-Hajj, Y. J. *Journal of Medicinal Chemistry* **1986**, *29*, 582.

(3) Hosoda, H.; Miyairi, S.; Nambara, T. *Chemical & Pharmaceutical Bulletin* **1980**, *28*, 1294.

(4) Hosoda, H.; Ushioda, K.; Shioya, H.; Nambara, T. *Chemical & Pharmaceutical Bulletin* **1982**, *30*, 202.

(5) Lee, H.; Chang, J.; Lee, G. *Analytical and Bioanalytical Chemistry* **2010**, *396*, 1713.